CHARACTERIZATION OF VOPQ, A TYPE III SECRETED EFFECTOR PROTEIN FROM *VIBRIO PARAHAEMOLYTICUS*

APPROVED BY SUPERVISORY COMMITTEE

Kim Orth, Ph.D.

Lora Hooper, Ph.D.

Vanessa Sperandio, Ph.D.

Neal Alto, Ph.D.

Hongtao Yu, Ph.D.

Dedication and Acknowledgements

This dissertation would not have been possible without the support of so many people to whom I am especially grateful. First, I would like to thank my mentor, Dr. Kim Orth, for her guidance and mentorship over these last few years. I am most grateful for her persistence and patience throughout graduate school, forgiving my missteps and stupid mistakes. Her scientific exuberance and willingness to tackle any problem will forever be a part of my own approach to science. I would like to thank my committee members, Drs. Lora Hooper, Neal Alto, Hongtao Yu, and Vanessa Sperandio for their guidance and support. Dr. Joachim Seemann performed all the VopQ microinjection experiments and I am grateful for his expertise and insight. In addition, other members of the UT Southwestern community, such as Dr. Stuart Ravnik and Dr. Nicolai van Oers, have provided excellent advice throughout graduate school that cannot go unmentioned.

Thank you to all the members of the Orth lab, past and present, for providing for me an intellectually stimulating environment and teaching me so many things, all while making the lab a fun place to work. In particular, I'd like to acknowledge Melanie Yarbrough, Ph.D. and Michelle Laskowski-

Arce, Ph.D. for their camaraderie, knowledge, support, and most of all, discussions about everything from cats to science.

I would like to acknowledge Dr. Larry Ruben, under whose mentorship I obtained a Master of Science degree in Biological Sciences at Southern Methodist University. I am eternally grateful for your continued friendship and support. It is from your inspiration that I continue to pursue research.

I would like to thank my family. My parents, Patricia and Forbes W. Burdette Jr., have been my biggest allies throughout my life. They have always encouraged me to strive for the best in all that I do. My mother is my biggest cheerleader. I could not have achieved this goal, and others in my life, without her advice and guidance. My father, Forbes Burdette, has provided me with unwavering support and instilled in me work ethic and a sense of curiosity. His attempt at understanding my work has been greatly appreciated. To my brother, F. Willard Burdette III, who has set the example in our family. He has taught me that anything can be achieved in life with a positive attitude and hard work.

To Butler, my best friend and love of my life. Thank you for understanding my commitment and dedication to what I do. I could not have made it through graduate school without your humor, advice and

support. It is for you that this dissertation is written in Helvetica. Thanks are due also to the rest of the Looney family; Cathie, Jim and Elaine, who have provided me a home away from home during my time in Texas.

To my furry friends, Scout and G.D., whose warm bodies and smiling faces greet me everyday. To my other friends, specifically Susanne Richman and Carrie Lee who were there in high school when I first dreamed of becoming a doctor, and have been with me ever since. To Wayne and Kelli Geyer, I am forever thankful for their continued friendship.

CHARACTERIZATION OF VOPQ, A TYPE III SECRETED EFFECTOR PROTEIN FROM *VIBRIO PARAHAEMOLYTICUS*

by

DARA LESLEY BURDETTE

DISSERTATION

Presented to the Faculty of the Graduate School of Biomedical Sciences

The University of Texas Southwestern Medical Center at Dallas

In Partial Fulfillment of the Requirements

For the Degree of

DOCTOR OF PHILOSOPHY

The University of Texas Southwestern Medical Center at Dallas

Dallas, Texas

April, 2009

CHARACTERIZATION OF VOPQ, A TYPE III SECRETED EFFECTOR PROTEIN FROM *VIBRIO PARAHAEMOLYTICUS*

DARA LESLEY BURDETTE

The University of Texas Southwestern Medical Center at Dallas, 2009

Supervising Professor: KIM ORTH, Ph.D.

Vibrio parahaemolyticus is a Gram-negative bacterium responsible for gastroenteritis associated with the consumption of raw or undercooked shellfish. Its most well-characterized virulence factors are hemolysins that cause β-hemolysis on a special blood agar. Mutants lacking these hemolysins are still virulent in animal and tissue culture models of infection. These phenomena can be attributed in part to one of two type III secretion systems; one on chromosome 1 and the other on chromosome

2. We demonstrate that *Vibrio parahaemolyticus* utilizes the type III secretion system on chromosome 1 to induce a temporally regulated series of events that initiates with the induction of autophagy, followed by cellular rounding and finally cellular lysis and death. To the best of our knowledge, no other Gram-negative extracellular bacterium has been shown to induce autophagy during infection.

To understand the mechanism of *Vibrio parahaemolyticus* induced cell death, we focused our analysis on VopQ, a type III secreted effector encoded by the type III locus on chromosome 1. We demonstrate that VopQ contributes to cytotoxicity as *ΔvopQ* strains induce cell lysis less efficiently. In addition, VopQ is necessary and sufficient for the induction of autophagy during infection. VopQ-mediated autophagy occurs independently of phosphatidylinositol 3-kinases and prevents phagocytosis. Additional experiments using *Saccharomyces cerevisiae* demonstrate VopQ induces autophagy and cell death through an evolutionarily conserved mechanism.

Results presented herein delineate a novel virulence mechanism used by *Vibrio parahaemolyticus* to cause disease. This study also highlights the effector VopQ as a novel inducer of autophagy and a key mediator of cytotoxicity during infection.

Table of Contents

List of Publications

Burdette, D.L., Seemann, J., Orth, K. *Vibrio* VopQ induces autophagy and antagonizes phagocytosis. *Mol Microbiol*. (Submitted, March 2009).

Burdette, D.L.*, Yarbrough M.L.*, Orth, K. Not without cause: Vibrio parahaemolyticus induces acute autophagy and cell death. *Autophagy.* (2009) 5(1):100-102. (*These authors contributed equally to this work.)

Burdette, D.L.*, Yarbrough, M.L.*, Orvedahl, A.O., Mueller, L., Gilpin C., and Orth, K. *Vibrio parahaemolyticus* orchestrates host cell death by induction of autophagy, cell rounding and then lysis. *Proc. Natl. Acad Sci USA*. (2008) 105(34):12497-502. (*These authors contributed equally to this work.)

Hao, Y.H., Wang, Y., **Burdette, D.**, Mukherjee, S., Keitany, G., Goldsmith, E., and Orth, K. Structural Requirements for *Yersinia* YopJ Inhibition of MAP Kinase Pathways. *PLoS ONE*. (2008) 3(1):e1375.

Liverman, A.D., Cheng, H.C., Trosky, J.E., Leung, D.W., Yarbrough, M.L., **Burdette, D.L.**, Rosen, M.K., and Orth, K. Arp2/3-independent assembly of actin by the *Vibrio* type-III effector VopL. *Proc. Natl. Acad Sci USA*. (2007) 104, 17117-22.

Rothberg, K.G., **Burdette, D.L.**, Pfannstiel J., Jetton, N., Singh R., and Ruben, L. The RACK1 homologue from *Trypanosoma brucei* is required for the onset and progression of cytokinesis. *J Biol Chem*. (2006) 281, 9781-90.

Trosky, J.E., Mukherjee, S., **Burdette, D.L.**, Roberts, M., McCarter, L., Siegel, R.M., and Orth, K. Inhibition of MAPK Signaling by VopA from *Vibrio parahaemolyticus. J. Biol. Chem*. (2004) 279, 51953-7.

List of Figures

List of Tables

List of Abbreviations
(in alphabetical order)

2xYT – Two times yeast extract and tryptone

3-MA – 3-methyladenine

ASC – apoptosis-associated speck-like protein containing a caspase recruitment domain

AMP – Adenosine monophosphate

AMP - Ampicillin

atg – Autophagy gene

BCG – Bacillus Calmette-Guérin

BEL – Bromoenol lactone

BHA – Butylated hydroxyanisole

BLAST – Basic Local Alignment Search Tool; http://ncbi.nih.gov/BLAST/

βME – Beta-mercaptoethanol

BSA – Bovine serum albumin

BP – 2'2'bipyridyl

cfu – Colony forming units

CIAS1 – cold-induced autoinflammatory syndrome 1

Cm – Chloramphenicol

CVT – Cytoplasm to vacuole

DMEM – Dulbecco's modified eagle's medium

DMSO - Dimethylsuphoxide

DTT – Dithiothreitol

ECL - Electrochemiluminescence

eIF2α – Eukaryotic initiation factor 2 subunit alpha

ER – Endoplasmic reticulum

FACS – Fluorescence assisted cell sorting

GAL – Galactose

GAP – G-protein activating protein

GEF – Guanine nucleotide exchange factor

Gen - Gentamicin

GFP – Green fluorescent protein

GST – Glutathione S-transferase

HBSS – Hank's Balanced Salt Solution

HIS - Histidine

HMGB1 – high mobility group box 1

HRP – Horseradish peroxidase

IL-1β – Interleukin-1β

IP_3 – Inositol phosphate 3

IPTG – Isopropyl-beta-D-thiogalactopyranoside

Kan - Kanamycin

kDa – kilodalton

KP – Kanagawa phenomenon

LB – Luria-Bertani

LC3 – Microtubule-associated protein light chain 3

LDH – Lactate dehydrogenase

Leu – Leucine

LPS – lipopolysaccharide

MAFP – Metylarachidonylfluorophosphonate

MAPKK – Mitogen activated protein kinase kinase (MEK)

Mbp – Megabase pairs

MHC – Major histocompatibility complex

MLB – Marine LB

MMM – Minimal Marine Medium

MOI – Multiplicity of Infection

MyD88 – myeloid differentiation primary response gene (88)

Neo - Neomycin

Ni-NTA - nitriloacetic acid matrix (Qiagen)

NLRP3 – the NOD-like receptor protein 3

NOD – nucleoside oligimerization domain

ORF – Open reading frame

O.D. – Optical density

p70S6K – p70 S6 kinase

PAI-1 – Pathogenicity island 1

PAI-2 – Pathogenicity island 2

PAMP – Pathogen associated molecular pattern

PARP – PolyADP ribopolymerase

PAS – Preautophagosomal structure

PBS – Phosphate-buffered saline

PCR – Polymerase chain reaction

PE – Phosphatidylethanolamine

PI3-kinase – Phosphatidylinositol 3-kinase

PI – Propidium iodide

PI – Protease inhibitors

$cPLA_2$ – Cytosolic calcium-dependent phospholipase A_2

$iPLA_2$ – Calcium independent phospholipase A_2

PMSF – phenylmethylsulphonylfluoride

PS – phosphatidylserine

RhoGTPases – Rho guanosinetriphosphatases

ROS – Reactive oxygen species

SAL – Salubrinal

SDS-PAGE – Sodium dodecyl sulfate polyacrylamide gel electrophoreisis

Sm – Streptomycin

Spc – Spectinomycin

SPI1 – *Salmonella* pathogenicity island 1

SPI2 – *Salmonella* pathogenicity island 2

SFFV – Spleen focus forming virus

T3SS – Type III secretion system

TCA – Trichloroacetic acid

TDH – Thermostable direct hemolysin

Tet – Tetracycline

Tm – Melting temperature

TOR – Target of rapamycin

TLR – Toll-like receptor

TRH – TDH-related hemolysin

TRIF – TIR-domain-containing adapter-inducing interferon-β

TRITC – Tetramethylrhodamine isothiocyanate

TTBS – Tris-buffered saline with tween

Ura – Uracil

Vop – Vibrio outer protein

vps – Vesicle protein sorting

XeC – Xestospongin C

YCD – Yeast complete dropout media with glucose

YCG/R - Yeast complete dropout media with galactose/raffinose

Yop – Yersinia outer protein

YPAD – Yeast peptone adenine dextrose

Ypk – Yersinia protein kinase

Chapter 1

Introduction

Vibrio parahaemolyticus (*V. parahaemolyticus*) is a Gram-negative bacterial pathogen responsible for gastroenteritis associated with the consumption of contaminated shellfish (Daniels et al., 2000). It is a major health concern in Japan and southeast Asia and has also been detected in coastal waters along the eastern and western United States seaboards and on the Gulf Coast (Yeung & Boor, 2004, Nair *et al.*, 2007). The most well studied virulence factor of *V. parahaemolyticus* is the thermostable direct hemolysin (TDH). *Δtdh* strains are, however, still virulent in tissue culture and animal models of infection (Liverman *et al.*, 2007, Park *et al.*, 2004a). In 2003, the genome of *V. parahaemolyticus* was sequenced, identifying two type III secretion systems (T3SS), one on each of the two *V. parahaemolyticus* chromosomes (Makino et al., 2003). Additional studies using a ligated rabbit ileal loop model of fluid accumulation attributed enterotoxicity to the T3SS on chromosome 2. In addition, they demonstrated that the T3SS on chromosome 1 was responsible for cytotoxicity in a tissue culture model of infection (Park et al., 2004b). The

mechanism of T3SS1-mediated cell death was attributed to apoptosis by DNA fragmentation and Annexin V and propidium iodide staining via fluorescence activated cell sorting (FACS) (Ono et al., 2006). In addition, apoptosis was thought to be caused by the action of multiple effectors encoded within T3SS1, including VopQ and VopS (Bhattacharjee *et al.*, 2006, Ono et al., 2006).

This dissertation seeks to first understand the mechanism of T3SS1-mediated cellular cytotoxicity. In the first aim, I show that cell death elicited by T3SS1 proceeds by a tightly controlled series of events that initiates with the induction of autophagy. This event is followed by the collapse of the actin cytoskeleton, leading to cellular rounding and then the eventual demise of the cell. We hypothesize that this T3SS1-mediated process seeks to rapidly kill host cells in order to prevent phagocytosis and immune clearance of the pathogen. This mechanism may also aim to benefit the bacteria by providing pre-degraded cytosolic nutrients during lysis.

In order to fully understand T3SS1-mediated pathogenesis, we sought to identify T3SS effectors directly responsible for the phenomena described above. In the second aim, I focused my attention on VopQ, a type III secreted effector encoded within T3SS1. This effector has no

homology to any protein of known function. Herein, we demonstrate that VopQ is both necessary and sufficient to induce autophagy during infection. The mechanism of VopQ-mediated autophagy proceeds by a novel and, as of yet, unidentified phosphatidylinositol-3-kinase (PI3-kinase) independent pathway. Induction of autophagy serves to prevent phagocytosis because cells infected with a *ΔvopQ* strain have a large number of intracellular bacteria, as shown by electron microscopy. Furthermore, we show that VopQ is a major contributor to T3SS1-induced cellular lysis since *ΔvopQ* strains are severely attenuated in their ability to induce lactate dehydrogenase (LDH) release during infection in tissue culture. Finally, infected cells generate reactive oxygen species that are essential for cell lysis. It is unknown at this time if the generation of reactive oxygen species is the mediator of cell death or if selective degradation of cellular antioxidants prevents induction of a protective response during infection.

This study also utilizes the budding yeast *Saccharomyces cerevisiae* (*S. cerevisiae*) as a genetic model to understand the molecular mechanisms behind VopQ-mediated cytotoxicity and induction of autophagy. In chapter 6 of this dissertation, we observe that VopQ is able to induce both cytotoxicity and autophagy in *S. cerevisiae*. This study

reinforces the dogma for type III secreted effectors in that they mimic or capture endogenous and conserved eukaryotic activities.

Ultimately, a better understanding of the virulence mechanisms used by *V. parahaemolyticus* will aid in a better understanding of its pathogenesis. In addition, characterization of *V. parahaemolyticus* T3SS effectors aims not only to identify the molecular mechanism used by this pathogen but also to use the effector as a tool to understand eukaryotic signaling pathways. Undoubtedly, additional mechanistic insights into the function of VopQ and its role in T3SS1-mediated cell death are essential for delineating *V. parahaemolyticus* pathogenesis.

Chapter 2

Literature Review

Vibrio parahaemolyticus

Vibrio parahaemolyticus is a Gram-negative rod shaped bacterium first discovered in 1950 as the causative agent of a food poisoning outbreak resulting from contaminated sardines in Osaka, Japan (Fujino, 1974). Like its cousin, *Vibrio cholerae* (*V. cholerae*), it belongs to the family *Vibrionaceae*, all of which are facultative anaerobes (Gomez-Gil & Roque, 2006). As a halophillic bacterium, *V. parahaemolyticus* is a common isolate from marine and estuarine environments (Yeung & Boor, 2004). Infection with *V. parahaemolyticus* causes gastroenteritis that is typically associated with the consumption of raw or undercooked seafood. Symptoms can include vomiting, diarrhea, nausea, and fever. In rare cases, *V. parahaemolyticus* can also cause wound infections resulting from direct contact with contaminated seawater. While typically a self-limiting infection, individuals who are immune compromised or suffer pre-existing conditions are at risk for developing serious disease, even death (Morris & Black, 1985, Rodrick *et al.*, 1982)

Since 1950, *V. parahaemolyticus* has emerged as a global health epidemic*. V. parahaemolyticus* predominantly causes disease in Southeast Asia where consumption of seafood is high, however isolates have been detected along both coasts of the United States **(Figure 1)** (DePaola *et al.*, 1990, Nair et al., 2007). Recently, pandemic and antibiotic resistant strains have emerged, underscoring the necessity for understanding *V. parahaemolyticus* pathogenesis (Baker-Austin et al., 2009). *V. parahaemolyticus* can be grouped into 13 O groups and 71 K types (Iguchi et al., 1995). Since 1996, serotype O3:K6 has emerged as an important pandemic strain. First isolated in Calcutta, India, this serotype has been responsible for food borne outbreaks in Southeast Asia and the United States (Vuddhakul et al., 2000)). Despite serotype designations, isolates of *V. parahaemolyticus* can also be divided into two groups: clinical and environmental. Clinical isolates harbor a hemolysin called the TDH and a related family of hemolysins called TDH-related hemolysin (TRH) (Miyamoto *et al.*, 1969, Shirai *et al.*, 1990). Both toxins are reversible amyloid toxins cause β-hemolysis on Wagatsuma agar (Fukui et al., 2005). This phenotype is known as the Kanagawa phenomenon (KP) and strains

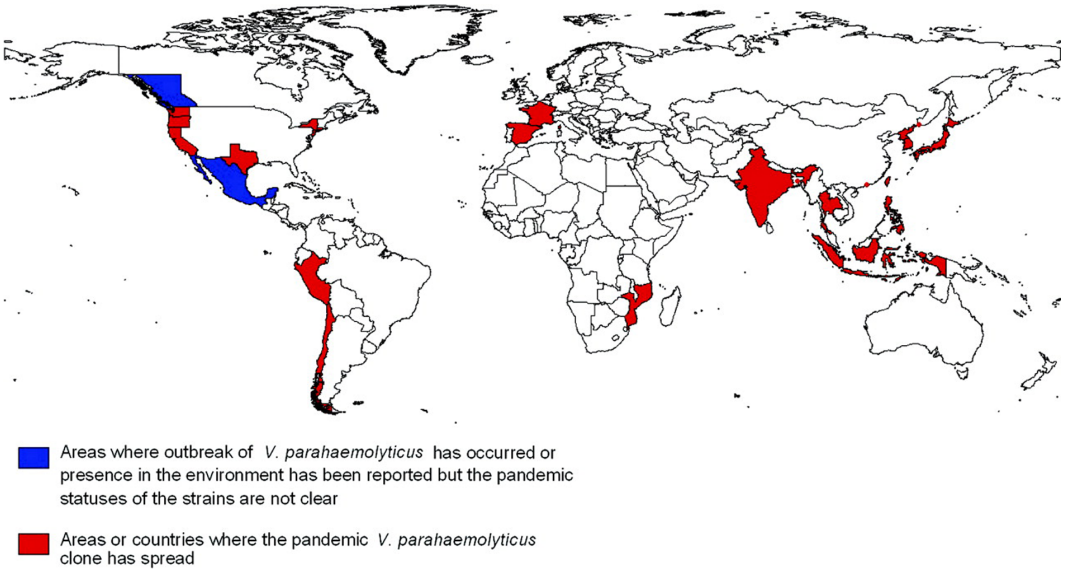

Figure 1. Global distribution of *V. parahaemolyticus* infections (Nair et al., 2007).

possessing this activity are termed KP positive. TDH induces hemolysis due to formation of a 2nm transmembrane pore in the erythrocyte membrane (Honda et al., 1992). In addition to pore formation, TDH can also induce ion permeability, which aids in membrane breakdown. This property contributes to the diarrheal symptoms during *V. parahaemolyticus* infection (Lang *et al.*, 2004, Zhang & Austin, 2005). In addition, all *V. parahaemolyticus* strains harbor a pathogenicity island (PAI-1) on chromosome 1. The presence of a second pathogenicity island on chromosome 2 (PAI-2) varies among clinical isolates (Park et al., 2004b). The majority of clinical isolates (88 – 96%) are KP positive and harbor one, if not both hemolysins, whereas only 1 – 2% of environmental strains produce hemolysins (Makino et al., 2003, Meador *et al.*, 2007, Miyamoto et al., 1969). Interestingly, some recent isolates of pandemic strains have been shown to harbor hemolysins and PAI-1, but not PAI-2 (Makino et al., 2003) (Meador et al., 2007).

In addition to the TDH and TRH toxins, *V. parahaemolyticus* encodes many hallmarks of virulence determination common in Gram-negative bacterial pathogens. *V. parahaemolyticus* is highly motile and has two flagellar systems. The polar flagella apparatus is associated with

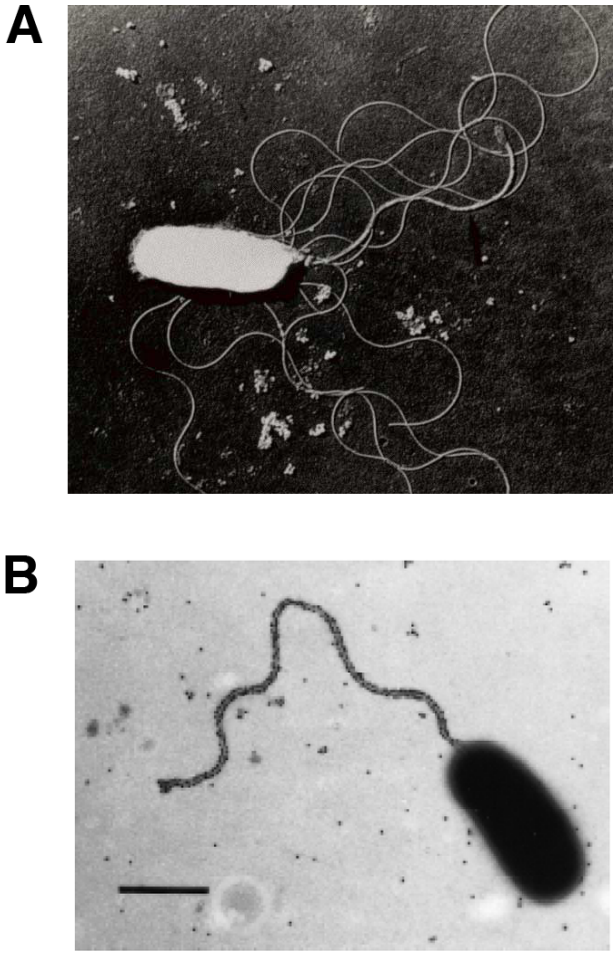

Figure 2. Electron micrographs depicting *V. parahaemolyticus* as a swarmer cell **(A)** and swimmer cell **(B)**. Scale bar in (B) represents 1 μm (McCarter, 1999) (Iida, 2003).

free-living planktonic bacteria (swimmer cell), whereas the lateral flagella system is associated with surface-associated bacteria (swarmer cell) **(Figure 2)** (McCarter, 2004). *V. parahaemolyticus* also exhibits phase variation between opaque and translucent varieties. In both phases, capsular polysaccharide production contributes to biofilm formation (Enos-Berlage et al., 2005). A master regulator belonging to the LuxR family of transcriptional regulators, OpaR, regulates the flagella apparatus, phase variation, and biofilm formation (McCarter, 1998, Guvener & McCarter, 2003). *V. parahaemolyticus* also harbors iron uptake systems and secretes the siderophore vibrioferrin to scavenge iron. Type IV pilli is hypothesized to be essential for colonization of intestinal epithelium (Yamamoto *et al.*, 1999, Nakasone & Iwanaga, 1990, Shime-Hattori *et al.*, 2006). Finally, *V. parahaemolyticus* encodes for two TTSS, one is found on each chromosome (Makino et al., 2003).

Although *V. parahaemolyticus* strains lacking TDH are no longer hemolytic, they are still cytotoxic in tissue culture models of infection. While a *Δtdh* strain may have reduced fluid accumulation, it can still in some cases display enterotoxicity in a ligated rabbit ileal loop model (Makino et al., 2003, Park et al., 2004a). In addition, epithelial tight junction integrity is still compromised during infection with some *Δtdh*

strains (Lynch et al., 2005). Furthermore, tissue culture cells infected with these strains died by apoptosis as shown by FACS analysis and DNA fragmentation (Ono et al., 2006). The T3SSs on each chromosome were evaluated for their contribution to the pathogenicity in the absence of TDH. Δ*T3SS1*/Δ*tdh* mutants are not cytotoxic in a tissue culture model of infection (Bhattacharjee et al., 2006, Ono et al., 2006). Δ*T3SS2*/Δ*tdh* mutants, although cytotoxic in tissue culture, did not cause fluid accumulation in a rabbit ligated ileal loop model (Park et al., 2004b). Ultimately, elements of *V. parahaemolyticus* pathogenicity can be attributed to T3SS1. Therefore, molecular and biochemical characterization of the T3SS1 effectors is required for understanding the virulence mechanisms of this pathogen.

Type III Secretion

The T3SS is a proteinaceous needle-like apparatus that spans both the inner and outer membrane of Gram-negative bacteria **(Figure 3)** (Marlovits et al., 2004). T3SSs are used by bacterial pathogens of both plants and animals to inject proteins directly into the cytosol of host cells. These proteins manipulate the cellular response to infection and allow the

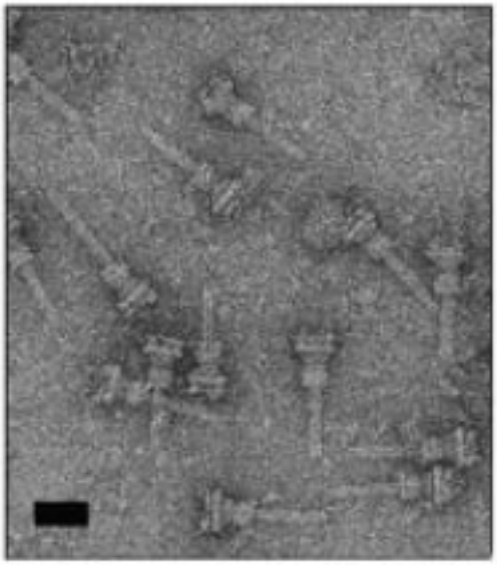

Figure 3. Electron micrograph of the type III apparatus showing its resemblance to a needle-like structure. Scale bar represents 30nm (Marlovits et al., 2004).

pathogen to gain an advantage during infection. T3SSs have been identified and characterized in a variety of Gram-negative bacteria including *Yersinia* spp., *Salmonella* spp., *Shigella*, Enterohaemorrhagic *E. coli* (EHEC), *Pseudomonas aeruginosa*, *Bordetella* spp., and *Burkholderia* spp. (Winstanley et al., 1999) (Parsons et al., 2001) (Rainbow et al., 2002) (Hansen-Wester & Hensel, 2001) (Schroeder & Hilbi, 2008) (Garmendia et al., 2005) (Engel & Balachandran, 2009) (Yuk et al., 1998). Some pathogens have multiple systems that coordinate different temporally regulated events during infection. *Salmonella* spp. and *Yersinia* spp. have two T3SS whereas *Burkholderia pseudomallei* are unique in that they have three T3SSs (Hensel *et al*., 1995, Rainbow et al., 2002) (Pallen et al., 2003). T3SS are not limited to human and animal pathogens. Plant pathogens such as *Erwinia* spp., *Ralstonia* spp., and *Xanthomonas* spp. use T3SSs to induce the hypersensitivity response (HR) (Tang *et al*., 2006, Alfano & Collmer, 2004).

Often found within pathogenicity islands, a typical type III locus encodes for structural genes, genes encoding translocated proteins, and genes required for secretion and translocation such as chaperones and members of the pore complex. The structural genes are highly conserved within the repertoire of Gram-negative bacteria (Hueck, 1998). While the

type III apparatus resembles a needle-like structure, it is most evolutionarily similar to bacterial flagella; both apparatus consist of a basal body that spans both bacterial membranes **(Figure 4)**. The T3SS uses a syringe, reminiscent of the flagella, through which proteins, called effectors, are secreted directly into host cells (Tampakaki et al., 2004) (Blocker et al., 2003). Although not well defined, the signal for secretion is encoded in the secondary structure at the amino terminus of the T3SS effector. These first 50 amino acid residues of the amino terminus are highly disordered and are recognized by components of the secretion system or by chaperones that deliver effectors to the secretion apparatus (Higashide & Zhou, 2006). T3SS chaperones have multiple roles in that they can confer secretion system specificity but also protect the bacterial cell from a toxic effector (Lee & Galan, 2004). Some chaperones do this by maintaining an effector in an unfolded inactive state in the bacteria. During secretion, the effector leaves behind its chaperone and enters the host cell where is can fold into an active conformation and access its substrates or activators. Chaperones can be classified into two groups; chaperones that are devoted to only one effector and chaperones that can assist multiple effectors. Furthermore, there are several T3SS effectors

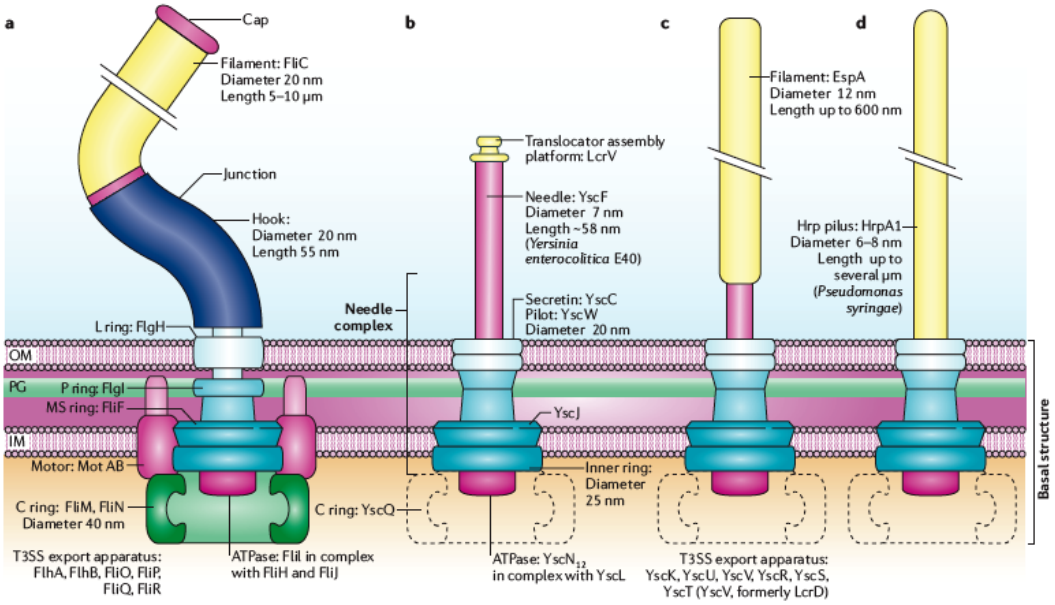

Figure 4. The T3SS spans the inner and outer bacterial membranes and resembles the flagellar apparatus. **(A)** Representative diagram of the flagellum. Injectisome complexes from different bacterial pathogens. **(B)** Ysc complex from *Yersinia* spp. **(C)** EPEC. **(D)** plant pathogens (Cornelis, 2006).

that do not require a chaperone for translocation and secretion (Feldman & Cornelis, 2003).

The mechanism of type III secretion can be divided into two parts: secretion and translocation. Secretion describes the movement of effectors from the bacterial cell cytoplasm through the T3SS apparatus to the outside of the cell, whereas translocation describes movement of the effector from the bacterial cell through the host cell plasma membrane into the cytoplasm of a host cell (Hueck, 1998). The needle structure makes contact with a host cell through a bacterial pore complex on the host cell membrane. The bacterial proteins that make up the pore complex are secreted first through the T3SS and then insert in the host cell membrane. This pore complex acts as a conduit for T3SS effectors to translocate into the host cell (Buttner & Bonas, 2002). Deletion of genes that make up the pore complex renders bacteria unable to translocate effectors into host cells, but the apparatus remains competent to secrete into the extracellular environment (Cornelis, 2002). When effectors are secreted through the T3SS, they are unfolded in an ATP-dependent manner only to refold once inside the eukaryotic cell (Akeda & Galan, 2005) and the entire process occurs very rapidly as seen with YopH, a tyrosine phosphatase from *Y.*

pseudotuberculosis. YopH-dependent dephosphorylation of p130Cas and FAK occurs within 2 minutes of infection (Andersson et al., 1996).

The effectors secreted by the type III apparatus are designated as outer proteins from the bacteria that secrete them. For instance, *Yersinia* spp. secretes Yops (*Yersinia* outer proteins) (Cornelis et al., 1998). The panel of effectors each species of bacteria secrete are uniquely suited to the niches each species occupies. Effectors can be thought of as the bacterial equivalent of a viral oncogene since their function mimics or captures an endogenous eukaryotic activity. Therefore, type III effectors can often be identified by the presence of eukaryotic domains or motifs. Effectors are inactive in the bacteria prior to secretion either because they lack an appropriate substrate or activator, or are held quiescent due to the presence of a chaperone. Once within the host cell cytoplasm, the effector becomes active and can manipulate the cellular response to infection (Trosky et al., 2008).

The T3SS is capable of secreting multiple different effector proteins each with distinct functions. The timing and regulation of the secretion of each effector is a highly coordinated event and deletion of one effector can alter the amount, rate, and timing at which other effectors are secreted though the translocon. In addition, different effectors can have different

decay rates once injected into the host cell. All of these factors can affect results that interpret an effector's contribution to virulence (Kubori & Galan, 2002). Production of the T3SS is an energetically costly event for the bacteria and consequently, its synthesis is a highly regulated event (Gophna et al., 2003). It is no surprise that master regulators of quorum sensing, virulence, and biofilm formation also regulate T3SS production (Falcao et al., 2004). *In vitro*, signals that induce T3SS can be mimicked by chelation of divalent cations (especially calcium) and growth at high temperatures (37°C) (Forsberg et al., 1991) (Lambert de Rouvroit *et al.*, 1992, Cornelis *et al.*, 1989). Furthermore, the movement of effectors into host cells can also be initiated by host cell contact (Pettersson et al., 1996).

The T3SS is a well-established virulence mechanism in Gram-negative bacteria. In *Yersinia* spp., the T3SS acts to suppress the innate immune response by shutting down signaling through the coordinated action of the effectors it secretes. *Yersinia* spp. encodes five effectors found in all species (YpkA/YopO, YopE, YopH, YopJ/YopP, and YopM) that function to disrupt the actin cytoskeleton and alter signaling pathways in the host cell (Navarro *et al.*, 2005, Viboud & Bliska, 2005, Shao, 2008). In *Salmonella* spp., Salmonella pathogenicity island 1 (SPI1) and

Salmonella pathogenicity island 2 (SPI2) are two T3SS that function in different capacities. SPI1 promotes the invasion of non-phagocytic cells in the intestine and induces an inflammatory response (Coombes *et al.*, 2005, Hapfelmeier *et al.*, 2005). Once internalized, SPI2 acts to manipulate the endocytic compartment, preventing fusion of *Salmonella* containing vacuoles (SCV) with the lysosomes (Waterman & Holden, 2003). While elucidating the mechanism of type III effectors is essential for understanding bacterial pathogenicity, the study of type III effectors can also uncover novel eukaryotic signaling pathways involved in the innate immune response.

Type III Secretion Systems of *Vibrio parahaemolyticus*

The genome of *V. parahaemolyticus* is encoded on two circular chromosomes of unequal size. Chromosome 1 is 3.2 Mbp in size and chromosome 2 is smaller at 1.8 Mbp. The approximate GC content for both chromosomes is 45%. In 2003, the genome for the clinical isolate RIMD2210633 was sequenced. Unlike *V. cholerae*, *V. parahaemolyticus* does not harbor genes for cholera toxin production. However, sequencing revealed the presence of two T3SS encoded within pathogenicity islands (Makino et al., 2003). The first T3SS (T3SS1) encoded on pathogenicity

island 1 (PAI-1) on chromosome 1 bears homology to the T3SS of *Yersinia* spp. yet some structural genes are in the opposite orientation **(Figure 5)** (Park et al., 2004b). Several putative type III effectors were identified in this locus using a bioinformatics approach to identify type III associated chaperones in Gram-negative bacteria. Putative type III chaperones identified encode for proteins with a predicted low molecular weight, an isoelectric point of 4, and that belong to the Class I fold of T3SS chaperones. Effectors were then identified in proximal location to these chaperones by the absence of homology to known proteins or homology to proteins with eukaryotic domains or motifs. By this method, the T3SS locus on chromosome 1 is predicted to encode three type III chaperones encoded by *vp1682*, *vp1684*, and *vp1687* (Panina et al., 2005). Each chaperone is predicted to be associated with three T3SS effectors encoded by *vp1680*, *vp1683* and *vp1686*, hereafter referred to as *vopQ*, *vopR*, and *vopS*, respectively (Panina et al., 2005). In addition, using the bioinformatics approach, vpa450 and vpa451 were identified as a putative effector and chaperone pair encoded on chromosome 2, approximately 1 Mbp from T3SS2, and not associated with the T3SS1 locus (Panina et al., 2005). VPA450 was shown to be secreted from T3SS1 despite being encoded on chromosome 2 (Ono et al., 2006).

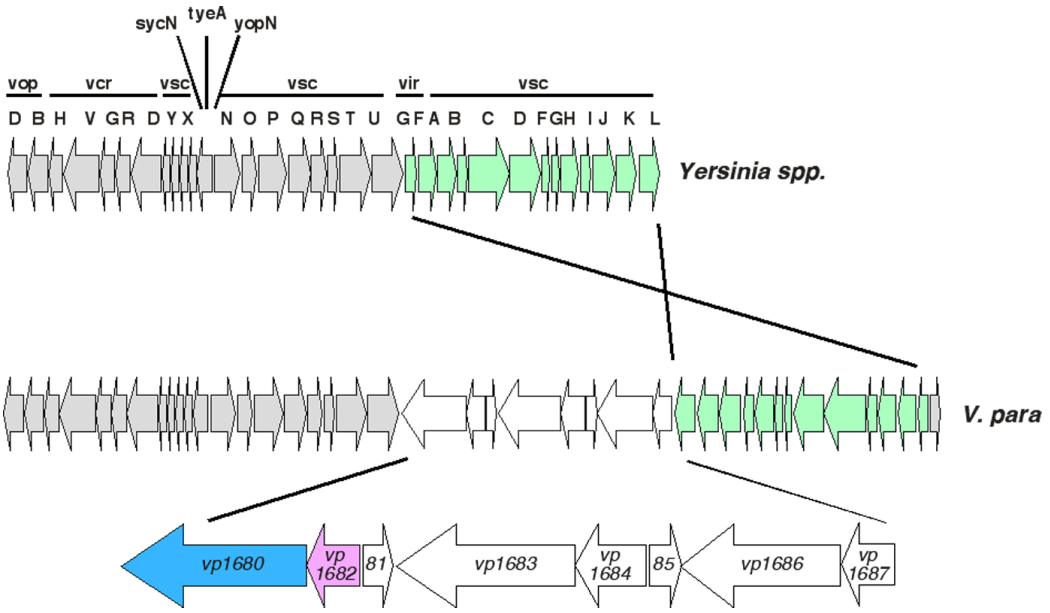

Figure 5. *V. parahaemolyticus* T3SS on chromosome 1. The T3SS locus on chromosome 1 of *V. parahaemolyticus* is homologous in both structure and organization to the T3SS of *Yersinia* spp. (gray), however some structural genes are in the opposite orientation (green). This locus encodes a region of unknown homology that is predicted to encode three type III effector proteins (*vp1680*, *vp1683*, and *vp1686*) and putative cognate chaperones (*vp1682*, *vp1684*, and *vp1687*). VopQ is encoded by *vp1680* (blue) downstream of its chaperone, *vp1682* (pink).

VopQ is 492 amino acids in length and approximately 54kDa. Encoded by *vp1680*, it is immediately downstream and in frame with the open reading frame for *vp1682*, its putative cognate chaperone. It has no homology to proteins of known function in prokaryotes or eukaryotes, however BLAST searches predict orthologues exist in other closely related *Vibrio* species such as *V. alginolyticus*. Interestingly, *V. harveyi* also harbors a *vopQ* orthologues, however BLAST results predict a fusion between the chaperone, *vp1682*, and the effector, *vopQ*, with some amino terminal sequence from *vopQ* lacking in *V. harveyi*. This absent sequence may constitute the secretion signal yet it is unknown if *V. harveyi* secretes this effector. Previous publications suggested this effector is responsible for T3SS1-mediated cytotoxicity and apoptosis as shown by FACS analysis and DNA fragmentation (Ono et al., 2006).

In the aforementioned study, researchers also identified VopS (VP1686), VPA450, and VP1656 (a putative YopD homologue) as being secreted from T3SS1 using two-dimensional sodium dodecyl sulfate polyacrylamide gel electrophoreisis (SDS-PAGE). The putative effector VP1683 (VopR) was not detected in cultured supernatants, yet it is predicted to be a T3SS1-secreted effector (Ono et al., 2006). VopS is 36kDa and was initially as the mediator of apoptosis through binding and

inhibition of NF-κB (Bhattacharjee et al., 2006). Ultimately, VopS was shown to modify Rho-GTPases with an adenosine monophosphate (AMP). This modification, termed AMPylation, occurs on a critical threonine residue in the switch I region of the RhoGTPases, preventing binding to downstream effector molecules (Yarbrough et al., 2009).

Pathogenicity island 2 (PAI-2) on chromosome 2 is approximately 80kb in size and encodes for T3SS2. The GC content of PAI-2 (39.8%) is different from the GC content of the rest of the *V. parahaemolyticus* genome (45.4%) indicating acquisition of this region was the result of a recent lateral transfer event (Park et al., 2004b). Recent evidence suggests this T3SS is shared among other members of the *Vibrio* genus (Okada *et al*., 2009). The locus is bordered on either side by insertion elements, contains two copies of the TDH, and genes homologous to T3SS structural genes from *Yersinia* spp. (Park et al., 2004b). T3SS2 has been shown to secrete four type III effector proteins, VopA, VopC, VopL, and VopT. Neither VopA, VopC, VopL, nor VopT were identified in the screen described above but were predicted to be T3SS effectors based on the presence of eukaryotic domains and homology to known T3SS effectors (Panina et al., 2005). They are not predicted to be associated with or require a chaperone.

VopA is an acetyltransferase, a homologue of the type III effector YopJ of *Yersinia* spp. VopA acetylates the serine and threonine residues on the activation loop of the mitogen activated protein kinase kinase (MAPKK or MEK) superfamily of proteins thus inhibiting activation via phosphorylation. In contrast to the Yersinia homologue YopJ, VopA also acetylates the lysine residue required for ATP binding. Acetylation of these critical residues cripples MAPK signaling during infection inhibiting the innate immune response (Trosky et al., 2007).

VopC is a homologue of cytotoxic necrotizing factor from *E. coli* and although it is toxic when expressed in yeast, there have been no additional mechanistic studies (Kodama et al., 2007). VopL contains regions of homology to Wiskott homology 2 (WH2) domains and proline rich domains (PRM). These eukaryotic domains are found in proteins involved in actin polymerization. VopL is capable of *de novo* actin assembly and this results in modulation of the actin cytoskeleton leading to stress fiber formation during infection and therefore, VopL-mediated disruption of the actin cytoskeleton in gut epithelial cells contributes to T3SS2-mediated enterotoxicity (Liverman et al., 2007). VopT is an ADP-ribosyltransferase (ADPRT) with homology to ExoT and ExoS of *P. aeruginosa*. VopT ADP-ribosylates the G-protein Ras potentially inhibiting nucleotide exchange. *V.*

parahaemolyticus ΔvopT mutants are less cytotoxic *in vitro* than wild type *V. parahaemolyticus* strains but it is not understood how the ADPRT function contributes to this phenomenon (Kodama et al., 2007).

Eukaryotic Cell Death Mechanisms: Apoptosis and so much more

Cellular death is an essential component of multi-cellular organisms. There are many subcellular pathways that culminate in the demise of a cell and these death processes are essential for regulating growth, differentiation, development and immunity. The death process is not stochastic, but a highly regulated and coordinated event (Fink & Cookson, 2005). Apoptosis, or type I programmed cell death, is the most well characterized of the cellular death pathways and is initiated by either a signal at the membrane through death receptors or stress related signals within the cell. These signals initiate a signaling cascade whereby proteases, called initiator caspases, are activated via proteolysis. These initiator caspases then go on to cleave their substrates, which can be other caspases or other protein targets in the cell. The final caspases, termed executioner or effector caspases, function to dismantle the cell in an orderly fashion. Caspase 3 is the quintessential effector caspase and its activation is considered a requirement of apoptosis (Fan et al., 2005).

Other physiological hallmarks of apoptosis include DNA fragmentation, chromatin condensation and membrane blebbing (Saraste & Pulkki, 2000). Apoptotic cells are able to signal through phosphatidylserine exposure to other cells, such as phagocytes, that they are dying. This results in phagocytosis and quiet elimination of the dying cell. Consequently, apoptosis is not a pro-inflammatory event (Hart et al., 2008).

Apoptosis can be monitored by a variety of different techniques. Annexin V and propidium iodide staining selectively stains membrane lipids, specifically phosphatidylserine (PS), which is normally on the inner leaflet of the plasma membrane. During the early stages of apoptosis, flipases catalyze the movement of phospholipids with phosphatidylserine head groups from the inner leaflet to the outer leaflet. This event can now be detected by Annexin V staining, which binds PS. However, PS can also appear on the outer leaflet of necrotic dying cells. Annexin V is used in conjunction with Propidium iodide (PI), a DNA intercalating agent that is excluded from viable cells. Therefore Annexin V positive, PI negative cells are considered apoptotic since the cells are still alive but dying by an autonomously regulated process (van Engeland et al., 1997).

A variety of inhibitors exist that target caspases. The most well known inhibitor is zVAD-FMK which acts as a suicide substrate (Slee et

al., 1996). In addition, poly-ADP ribopolymerase (PARP) is a direct target of caspase 3. During apoptosis, caspase 3 cleaves 116kDa PARP generating an 89kDa species easily detected by western blot. PARP normally functions to target damaged DNA molecules but is unable to do so following caspase cleavage (Scovassi & Poirier, 1999). Thus apoptosis not only dismantles the cell but inhibits cellular repair mechanisms as well.

While caspases 3, 7 and 9 are predominantly associated with apoptosis, some caspases are activated in other death processes distinct from apoptosis. Caspase 1 has been implicated in a highly inflammatory cell death process termed pyroptosis that is still not well understood. Upon activation, caspase 1 associates with other protein components forming the inflammasome. Hallmarks of caspase-1 dependent cell death include DNA damage, caspase 1 activation, and interleukin 1β (IL-1β) release. Unlike apoptosis, caspase-1 dependent cell death is highly inflammatory. This cell death has been termed pyroptosis and can be distinguished from classical apoptosis in that there is no caspase 3 activation. In contrast, caspase 1 is activated, leading to IL-1β release from the cell, and a release of cellular contents as measured by LDH release. Furthermore, like zVAD-FMK, yVAD-FMK functions in a similar manner to inhibit proteases but is specific for caspase 1. Therefore, classical apoptosis is

insensitive to yVAD-FMK inhibition, but caspase 1 dependent cell death is sensitive to both yVAD-FMK and zVAD-FMK inhibition (Bergsbaken et al., 2009).

Other cell death mechanisms leading to a pro-inflammatory release of cell contents are far less well characterized **(Figure 6)**. Oncosis is very similar to pyroptosis except that it involves cell and organelle swelling (Majno & Joris, 1995). Finally, necrosis is considered, in contrast to the mechanisms described above, to be an unregulated process characterized by loss of membrane integrity (Fink & Cookson, 2005). Finally, autophagy (discussed below) is historically considered to be a cell survival pathway. However, deregulation can lead to pathological situations and thus autophagy has been referred to as type II programmed cell death (Lockshin & Zakeri, 2004). To complicate matters, the lines drawn between these death processes tend to blur. Ultimately, multiple techniques must be used to positively determine the mechanism of cell death for any given situation.

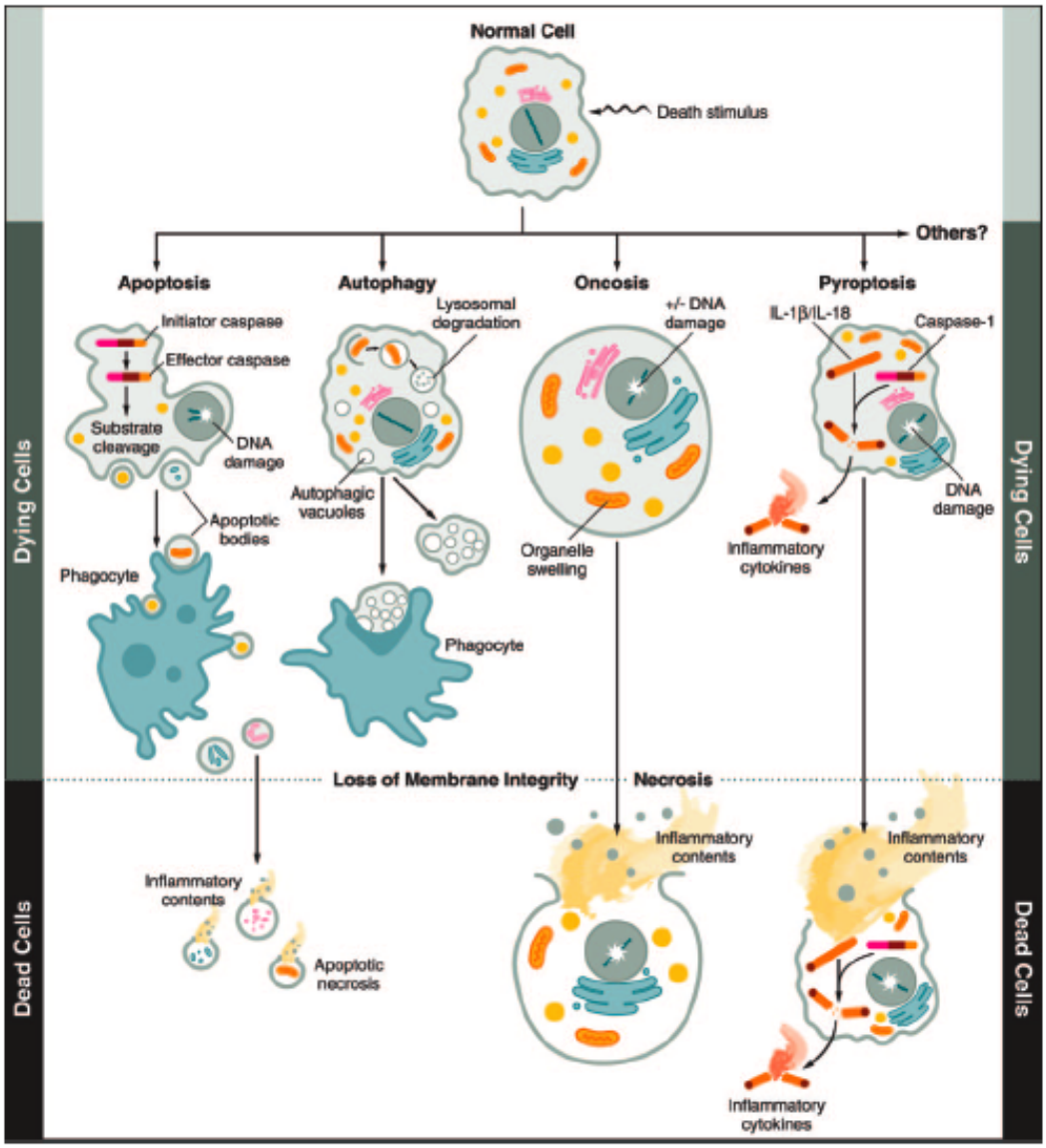

Figure 6. Eukaryotic cell death mechanisms. Different pathways that lead to cell death and the molecular hallmarks that differentiate them (Fink & Cookson, 2005).

Autophagy

Eukaryotic cells use two main pathways to degrade cytosolic proteins – the proteasome:ubiquitin system and a lysosomal dependent pathway. The proteasome:ubiqutiin system is responsible for rapid protein turnover whereas the lysosomal dependent pathway, or autophagy, is responsible for bulk degradation of long-lived proteins or organelles (Murata et al., 2009). Autophagy is induced in response to nutrient starvation or growth factor deprivation and functions to provide the cell with essential metabolites **(Figure 7)**. During autophagy, cellular membranes or phagopores engulf bulk cytoplasmic contents and organelles forming autophagosomes. These autophagosomes traffic to and fuse with the lysosomes, now the autophagolysosome or autolysosome, where resident lysosomal hydrolases degrade these materials. Ultimately, degradation products are reused, thus fending off starvation. There are specific types of autophagy that include microautophagy (engulfment of cytoplasm from the lysosomal vacuole surface), mitophagy (specific engulfment of the mitochondria), pexophagy (specific engulfment of the peroxisome), and xenophagy (autophagy of invading bacteria or viruses) (Yu et al., 2008).

Model organisms such as *C. elegans*, *D. melanogaster*, and *S. cerevisiae* have been useful for the study of autophagy (Kourtis & Tavernarakis, 2009, Melendez & Neufeld, 2008). The autophagy pathway was initially described in the yeast *S. cerevisiae* and remains the best model system to study autophagy (Abeliovich & Klionsky, 2001). To date, over 30 autophagy genes (atg) regulate and are required for autophagy and many mammalian orthologues have been characterized **(Table 1)**. In yeast, the process of autophagy overlaps with the cytoplasm-to-vacuole targeting (CVT) pathway. Distinct from autophagy, this pathway is specific for delivering lysosomal hydrolases to the lysosomes, however many genes required for the CVT pathway overlap with those require for autophagy (Khalfan & Klionsky, 2002).

There are a number of factors that can lead to the induction of autophagy and among them are cellular amino acid and ATP levels, target of rapamycin (TOR) signaling, PI3-kinase signaling, calcium, endoplasmic reticulum (ER) stress and innate immune signaling. These upstream signals converge onto the same autophagic machinery through unknown intermediates. For instance, pathogen recognition receptors such as Toll-like receptors (TLR) 3, 4, 7 and 8 signal to activate autophagy in response

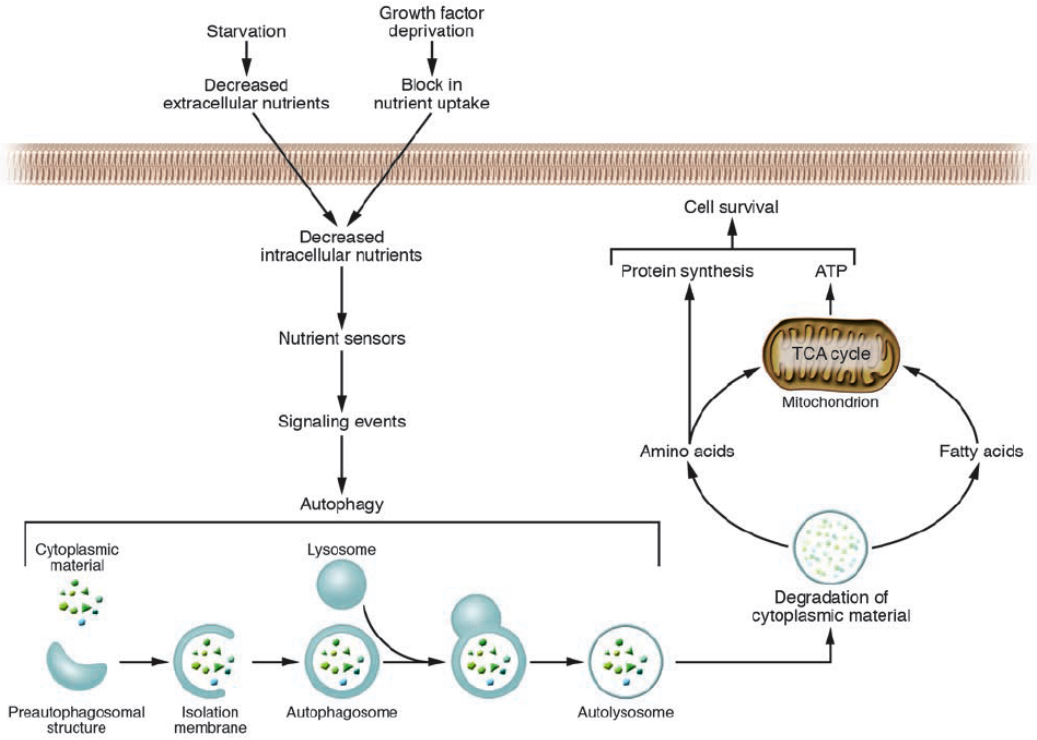

Figure 7. Overview of the autophagy pathway induced in response to nutrient or growth factor deprivation (Levine & Yuan, 2005).

to pathogen associated molecular patterns (PAMPs). This is believed to be part of the innate immune response to invading pathogens. In the case of TLR4, which signals in response to lipopolysaccharide (LPS), the induction of autophagy requires TIR-domain-containing adapter-inducing interferon-β (TRIF), but not myeloid differentiation primary response gene (88) (MyD88). In contrast, TLR7 signaling in response to *M. bovis* bacillus Calmette-Guérin (BCG) requires MyD88. Clearly, understanding the intermediate signals that integrate upstream signals with the autophagic machinery is essential.

The process of autophagy has been well characterized in eukaryotes and can be more specifically summarized into eight steps. A signal transduction event induces dephosphorylation of Atg13, permitting association with the kinase Atg1 (1). This event leads to the formation of the preautophagosomal structure (PAS). This phagopore forms a double-membrane vesicle that envelopes portions of the cytoplasm, including organelles (2). Atg11 and Atg8 assist in the packaging of cargo into these forming autophagosome. PI3-kinase complex I includes Atg6/beclin1, Atg14, Atg9, vacuole protein sorting 34 (Vps34) and Vps15 and regulates vesicle nucleation (3 and 4). The fully formed vesicle is called the autophagosome, which expands with the help of two ubiquitin-like

Table 1: Genes Involved in Autophagy

Yeast Gene	Mammalian homologue	Function	Reference
Atg1	ULK1	Serine/threonine kinase; autophagy induction	(Matsuura et al., 1997)
Atg2	Atg2	Associated with Atg9 and Atg18	(Obara et al., 2008)
Atg3	Atg3	E2 carrier protein for Atg8/LC3 conjugation system	(Tanida et al., 2002)
Atg4	Atg4	Cysteine protease and de-ubiquitinating protein; targets Atg8/LC3	(Tanida *et al.*, 2004, Yoshimura *et al.*, 2006)
Atg5	Atg5	E3 for Atg8/LC3 conjugation system in combination with Atg12	(Hanada et al., 2007)
Atg6	Beclin 1	Bcl-2 binding protein. Tumor suppressor. Member of Class III PI3-kinase complex.	(Liang et al., 2001)
Atg7	Atg7	E1 ligase for the Atg5-Atg12 and Atg8/LC3 conjugation system	(Tanida et al., 2001)
Atg8	LC3	Ubiquitin-like protein, LC3 in mammals	(Kabeya et al., 2000)
Atg9	Atg9	Transmembrane protein associated with Atg2 and Atg18	Tooze, S.
Atg10	Atg10	E2 carrier protein for the Atg5-Atg12 conjugation system	(Phillips *et al.*, 2008, Mizushima *et al.*, 2002)
Atg11	No	Interacts with Atg17 and Atg20; links vesicle forming machinery with CVT pathway	(Monastyrska et al., 2006)
Atg12	Atg12	Ubiquitin-like protein conjugated to Atg5. IN conjunction with Atg5, functions as an E3 for the Atg8/LC3 conjugation system, directs proper Atg8/LC3-PE localization with Atg16L	(Hanada et al., 2007)
Atg13	Atg13	Modulator of Atg1 activity	Tooze, S.
Atg14	Atg14	Associated with PI3-kinase complex	(Itakura et al., 2008)
Atg15	No	Lipase, disintegrates membranes of autophagic bodies, involved in life-span extension	(Tang et al., 2008)
Atg16	Atg16L	Associates with the Atg12-Atg5 conjugation system, potential Rab33 effector, coiled-coil protein; directs proper Atg8/LC3-PE localization in concert with Atg5-Atg12	(Fukuda & Itoh, 2008, Mizushima *et al.*, 2003)
Atg17	No	Activation of Atg1; interacts with Atg29 and Atg31	(Jeffries *et al.*, 2004, Kabeya *et al.*, 2005, Cheong *et al.*, 2005)
Atg18	WIPI1 (WIPI49)	Interacts with Atg9	Jeffries, et al., 2004
Atg19	No	Unclear; Receptor for CVT pathway but interacts with LC3	(Scott *et al.*, 2001, Shintani *et al.*, 2002)
Atg20	No	Interacts with Atg11	(Yorimitsu & Klionsky, 2005)
Atg21	WIPI2	Required for the lipidation and localization of Atg8, phosphatidylinositol binding protein	(Stromhaug et al., 2004)
Atg22	No	Recycles amino acids by vacuolar efflux, links degradation to autophagy	(Yang et al., 2006)

Atg23	No	Required for CVT pathway but not autophagy and maturation of preaminopeptidase I	(Tucker *et al.*, 2003, Meiling-Wesse *et al.*, 2004)
Atg24	No	Inhibits yeast filamentous growth	(Ma et al., 2007)
Atg25	No	Coiled coil protein required for pexophagy in *Hansenula polymorpha*	(Monastyrska et al., 2005)
Atg26	No	Sterol glycosyltransferase required for micro and macrpexophagy	(Cao & Klionsky, 2007)
Atg27	No	A transmembrane efflux protein required for cycling of Atg9	(Yen et al., 2007)
Atg28	No	Coiled coil protein required for pexophagy in *Pichia pastoris*	(Stasyk et al., 2006)
Atg29	No	Required for localization to the preautophagosomal structure	(Kawamata et al., 2005)
Atg30	No	Required for pexophagy in *Pichia pastoris*	(Farre et al., 2008)
Atg31	No	Null mutant is similar to *Datg17*, binds to Atg17	(Kabeya et al., 2007)

conjugation systems (5). Atg5 is conjugated to Atg12 through the actions of Atg7, Atg10 and Atg16. This complex acts as an E3 ligase that conjugates phosphatidylethanolamine (PE) to Atg8 with the help of Atg4 and Atg3. Atg8 is the only protein that remains on the autophagosomal surface for the duration of autophagy. Following fusion with the lysosome (6), the cargo is degraded (7) and its components are released into the cytoplasm through efflux and active permeases (8). The vesicle can be recycled with the help of Atg9, Atg2 and Atg18 or degraded by Atg15 (Levine & Klionsky, 2004) (Klionsky et al., 2007).

One can follow markers of autophagy to monitor its induction, cargo packaging and completion. Upon induction of autophagy, microtubule-associated protein light chain 3 (Atg8 or LC3) is modified in a ubiquitin-like conjugation system with a PE moiety. The unmodified LC3 (LC3-I) is normally cytoplasmic and modification with PE specifically targets LC3 to the forming autophagosomal membrane. The modified (LC3-II) and unmodified (LC3-I) forms migrate differently on SDS-PAGE gels and thus, the process of autophagy can be monitored by following LC3 conjugation (Kabeya et al., 2000). We can also follow LC3 by microscopy using a green fluorescent protein (GFP) tagged form that forms punctate dots during autophagy. Furthermore, electron microscopy is used to identify

double membrane structures corresponding to autophagosomes. Long-lived protein degradation can be monitored for a more quantitative analysis of autophagy. Finally, these assays can be adapted for use in *S. cerevisiae* (Klionsky et al., 2007).

Autophagy in conventional cellular homeostasis is to be appreciated, however autophagy has also been shown to play a roles in cellular differentiation and disease (Cecconi & Levine, 2008). In plants, autophagy delays leaf senescence (Chae *et al.*, 2004, Hanaoka *et al.*, 2002). Autophagy mutants of the social amoebae *Dictyostelium* are defective in sporulation and fruiting body formation respectively. (Schlumpberger *et al.*, 1997, Otto *et al.*, 2003). In higher eukaryotes, autophagy deficient *Drosophila* embryos show defects in pupae formation and in *C. elegans*, autophagy is required for dauer formation (Scott et al., 2004) (Melendez et al., 2003). Finally, in humans, autophagy was first described as being responsible for the erythroid maturation process but has since been shown to be involved in the development of mammary epithelial cells and embryonic development during the early neonatal starvation period (Takano-Ohmuro *et al.*, 2000, Levine & Yuan, 2005, Penaloza *et al.*, 2006, Kuma *et al.*, 2004).

Some diseases result from the misregulation of autophagy. Autophagy in failing cardiomyocytes has been shown to contribute to cardiac hypertrophy and heart failure (Hein *et al.*, 2003, Kostin *et al.*, 2003). The tumor suppressor, Beclin 1, is essential for autophagy and 40 – 70% of breast cancer patients are monoallelic for this gene implying a role for autophagy in tumorigenesis (Liang et al., 1999). In addition, autophagy contributes to a variety of neurodegenerative diseases such as Parkinson's, Alzheimer's and Huntingtin's diseases (Anglade et al., 1997) (Nixon *et al.*, 2000, Qin *et al.*, 2003). While excessive autophagy contributes to disease pathogenesis in these cases, it has been shown to counteract the effects of ageing by eliminating damaged organelles and clearing misfolded proteins (Bergamini *et al.*, 2003, Ravikumar *et al.*, 2002).

Autophagy functions as a means for the cell to degrade undesirable contents such as intracellular bacterial and viral pathogens. Thus, autophagy plays a role in the activation of the immune system in that TLR ligands are delivered to activate the innate immune response and antigens are shuttled to Class II major histocompatibility complex (MHC) compartments for signaling to the adaptive immune system (Delgado *et al.*, 2008, Dengjel *et al.*, 2005). Autophagy targets intracellular bacterial

pathogens such as Group A *Streptococcus*, *Shigella flexneri*, *Listeria monocytogenes*, *Burkholderia pseudomallei*, *Coxiella burnetii*, *Francisella tularensis*, *Salmonella enterica*, and *Mycobacterium bovis* BCG for degradation. However, many have developed virulence mechanisms that enable them to subvert or manipulate the autophagic machinery. Intracellular pathogens such as *Shigella* use the type III effector IscB to escape from the autophagosome, promoting intracellular survival (Ogawa et al., 2005). *Coxiella* persists in large intracellular vacuoles. This bacterium induces autophagy, only to subsequently inhibit autophagosomal maturation and fusion with the lysosomes, creating an intracellular replicative niche (Romano et al., 2007).

While these examples support autophagy in a protective role, during bacterial infection the induction of autophagy is coincident with cell death. For instance, the *Salmonella* type III effector SipB induces macrophage cell death by triggering mitochondrial fusion with the lysosome via autophagy (Hernandez et al., 2003). Despite many examples of the use of autophagy as an innate immune clearance mechanism, signals that lead to the induction of autophagic machinery in response to bacterial invasion downstream of TLRs is not well characterized. However, some potential candidates include disruption of intracellular bacterial

compartments such as phagosomes, intracellular pattern recognition receptors, toxins, or secreted proteins (Orvedahl & Levine, 2009).

Viruses have also evolved mechanisms to subvert autophagy as an immune defense mechanism. In these cases, the protective role of autophagy is clearer. In plants, autophagy limits cell death via a beclin 1 orthologue due to the hypersensitive response (Liu et al., 2005). Autophagy defends against invading viruses that target the nervous system such as Sindbis virus and Herpes Simplex Virus type I (Liang *et al.*, 1998, Orvedahl *et al.*, 2007). Many other viruses encode for mechanisms or evasion or hijacking of host autophagy genes. Finally, eukaryotic organisms such as *Entamoeba invadens*, *Leishmania* spp., *Toxoplasma gondii*, and *Trypansoma cruzi* not only subvert host autophagy defenses but also encode orthologues of autophagy genes. This is also true for pathogenic yeast such as *Candida albicans* and *Cryptococcus neoformans* (Orvedahl & Levine, 2009). The great number of pathogens that target autophagy underscores the need for further research into understanding its precise mechanisms.

Chapter 3

Materials and Methods

Building the Tools

Bacterial Strains and Media: Strains used in this study are described in Table 2. *E. coli* DH5α, K12, and BL21-DE3 strains were maintained on Luria-Bertani (LB) agar plates (1% tryptone, 0.5% yeast extract, 1% NaCl, 1.5% Bacto agar). Liquid cultures were propagated in 2xYT (1.6% tryptone, 1% yeast extract, 0.5% NaCl). All *E. coli* strains were grown at 37°C. *V. parahaemolyticus* strains were maintained on minimal marine medium (MMM) agar plates (5 mM K_2SO_4, 77 mM K_2HPO_4, 35 mM KH_2PO_4, 20 mM NH_4Cl, 5 mM $MgSO_4 \cdot 7H_2O$, 2% NaCl, 0.4% galactose, and 1.5% Bacto agar) at 30°C. Complemented (POR3*ΔvopQ* + vopQ) strains were maintained with tetracycline (20μg/mL). Following growth, *V. parahaemolyticus* isolates on plates were stored in a drawer at room temperature. All other strains were stored at 4°C. Liquid cultures were propagated in marine LB (MLB, 1% tryptone, 0.5% yeast extract, 3% NaCl) at 30°C unless otherwise indicated. *Y. pseudotuberculosis* strains

were propagated on LB agar plates and cultured in LB liquid media at 26°C unless otherwise indicated.

Mammalian Cell Lines: HeLa cells and HEK293 cells were maintained in DMEM supplemented with 10% fetal bovine serum (Sigma), 2 mM L-glutamine, 100 μg/ml streptomycin, 100 U/ml penicillin, 0.1mM non-essential amino acids, and 1mM sodium pyruvate (Invitrogen) at 37˚C with 5% CO_2. The GFP-LC3–stable HeLa cell line was a generous gift from Anthony Orvedahl and Beth Levine. Briefly, the GFP-LC3–stable HeLa cell line was generated by inserting GFP-LC3 from GFP-LC3–expressing plasmid, pEGFP-C1 (Kabeya et al., 2000), between the NheI and EcoRI sites in the pIRESneo3 vector (Clontech) and selecting for stably expressing colonies with G418 (100 μg/ml). The GFP-LC3 HeLa cell lines were maintained as described above for standard HeLa cells but with 100 μg/ml G418. RAW 264.7 macrophages were cultured in DMEM with 10% FBS (Sigma), non-essential amino acids (Invitrogen) and 2mM L-glutamine (Invitrogen). Immortalized B6 macrophages and caspase 1-/- macrophages were a generous gift from Russell Vance (University of California, Berkeley) and maintained in RPMI (Invitrogen) supplemented

with 10% FBS (Sigma), 2 mM L-glutamine, 100 μg/ml streptomycin, 100 U/ml penicillin (Invitrogen).

Polymerase Chain Reaction (PCR): PCR was carried out using VENT polymerase in 1X Thermopol reaction buffer (NEB, New England Biolabs). Approximately 100-300ng of template DNA was used in a total reaction volume of 50μL containing 200ng of each 5' and 3' primers listed in Table 3 with 200μM nucleotide mix (Roche). Product was amplified by denaturing the template DNA at 94° for 2 minutes followed by 30 cycles of 94°C for 30 seconds, 58°C (Tm, °C) for 30 seconds and 72°C for 1 minute, then a 4-minute extension at 72°C followed by a hold at 4°C. The melting temperature (Tm) was adjusted depending on the primers used and is indicated in Table 3. Following PCR, the entire product was separated by agarose gel electrophoreisis, purified by gel extraction (Qiagen), and eluted in 50μL of distilled H_2O.

Cloning: Constructs generated in this dissertation are listed in Table 4. In each case, 10μL of PCR product and 2-5μg of plasmid DNA were digested with 1μL of each indicated restriction enzyme (NEB) in a 30μL volume with 10X bovine serum albumin (BSA) and corresponding 10X restriction buffer

(NEB) for 1 hour at 37°C. Following digestion, DNA was separated by agarose gel electrophoreisis, purified by gel extraction (Qiagen), and eluted in 50μL of distilled H_2O. In all cases, approximately 1μL of digested and purified vector was ligated with 7.5 times the amount of insert with 0.5μL of T4 DNA ligase in 1X ligase buffer (New England Biolabs) in a 10μL volume at 16°C for 13 hours followed by 65°C for 10 minutes. Ligations were transformed into chemically supercompetent DH5α *E. coli* (Invitrogen). Bacteria were incubated with DNA for 30 minutes on ice, then heat shocked in a 42°C water bath for 45 seconds followed by 5 minutes on ice. Bacteria were recovered in 200μL 2xYT for 1 hour at 37°C and then plated on selective media.

Sodium Dodecyl Sulfate Polyacrylamide Gel Electrophoreisis (SDS-PAGE): Samples were diluted into 5X SDS-PAGE sample buffer (250 mM Tris pH 6.8, 50% glycerol, 10% SDS, 0.5% bromophenol blue, 500mM β-ME). SDS-PAGE gels were made according to instructions detailed in Molecular Cloning (Russell & Sambrook). Proteins were separated in SDS-PAGE electrophoreisis buffer (250mM Tris base, 2M glycine, 0.1% SDS) for 20 minutes at 200 volts, followed by 150 volts for 60 minutes. Following SDS-PAGE, gels were transferred to Immobilon-P PVDF

membranes (Millipore) in transfer buffer (125mM Tris base, 100mM glycine, 20% methanol) at 100 volts for 80 minutes.

Western Blotting: After transfer, blots were incubated in 5% nonfat dry milk in TTBS (200mM Tris pH 7.6, 150mM NaCl, 0.1% Tween) for 10 minutes. The blot was incubated in primary antibody diluted in TTBS plus 5% nonfat dry milk for 1 hour at room temperature unless otherwise indicated. Primary antibody was removed and the blot was rapidly rinsed three times in TTBS followed by three 5-minute washes in TTBS. The blot was incubated in horse-radish peroxidase (HRP) conjugated anti-mouse IgG or anti-rabbit IgG secondary antibodies (GE Healthcare) at a 1:2000 dilution in TTBS + 5% nonfat dry milk with gentle agitation for 30 minutes at room temperature. The membrane was developed using ECL plus (Amersham) and exposed to X-Omat blue XB-1 film (Kodak).

Antibodies: All antibodies used for Western blotting and immunofluorescence are listed in alphabetical order with the dilutions used and origin of purchase. Mouse anti-βactin (1:2000, Sigma). Goat anti-aldolase (1:500, Santa Cruz). Rabbit anti-Apg8p (1:2000 overnight at 4°C, Rockland). Mouse anti-calnexin (1:4000, Abcam). Mouse anti-FLAG

(1:5000, Sigma). Mouse anti-GFP (1:1000, JL-8 BD Biosciences). Mouse anti-golgin97 (1:100, Molecular Probes). Mouse anti-Lamin (1:1000, Zymed). Rabbit anti-LC3 (1:300, Novus). Rabbit anti-PARP (1:1000 overnight at 4°C, Cell Signaling. Mouse anti-porin (1:1000, Molecular Probes). Rabbit anti-phospho p70 S6 kinase Thr412 (1:2000, Upstate). Mouse anti-tubulin (1:2000, Sigma). Rabbit anti-phospho-mTOR Ser2448 (1:1000 in 5% BSA overnight at 4°C, Cell Signaling). Rabbit anti-VopQ antibodies against two VopQ peptide sequences (amino acids 130 – 154 and 196 – 663) were generated by Dr. Wayne Lai at the Antibody Core Facility at UT Southwestern Medical Center. Rabbit anti-VopQ was used at a 1:1000 dilution for 1 hour at room temperature.

Generation of *vopQ* Knockout Strains: The *vopQ* ORF and 1kb of flanking upstream and downstream genomic regions was cloned into pLafR to yield pLafR.*vopQ* (Boles & McCarter, 2000). Primers harboring 50 nucleotides of homologous sequences to the regions flanking VopQ were used to amplify the chloramphenicol cassette from pKD3, which was subsequently used for lambda red recombination (Datsenko & Wanner, 2000). The resultant pLafR.*vopQ::cm*^{R} was conjugated into *V. parahaemolyticus* via tri-parental mating and transconjugants were

selected on MMM with tetracycline (20μg/mL). Following selection on tetracycline, bacteria were passaged on heart infusion with chloramphenicol (10μg/mL) to select for recombination of the cassette. To resolve merodiploids, the plasmid pPH1JI (gentamicin^R) was used to kickout the knockout plasmid via incompatibility through selection on MMM + gentamicin (100μg/mL). The resulting clones were verified for sensitivity to tetracycline, and resistance to chloramphenicol and gentamicin. Disruption of *vopQ* was verified by polymerase chain reaction and sequencing using chloramphenicol sequencing primers and *vopQ* sequencing primers listed in Table 3. Absence of VopQ secretion was verified by *in vitro* secretion assays as described. The pPH1JI plasmid was cured by passaging *V. parahaemolyticus ΔvopQ* strains on MLB agar at 37°C three times for three days. Complemented strains were obtained by conjugating the pLafR.*vopQ* plasmid via tri-parental mating and selecting for tetracycline resistance.

Purification of Recombinant VopQ: The coding region corresponding to *vopQ* was cloned into pET15b at the NdeI and BamHI restriction sites to generate pET15b.*vopQ*. This construct was transformed into chemically competent *E. coli* BL21-DE3 and cultures were grown to an O.D.$_{600}$ of 0.6

– 0.8 at 37°C and induced with 0.4mM isopropyl-beta-D-thiogalactopyranoside (IPTG) for 4 hours at 25°C. Bacterial pellets were lysed in phosphate buffered saline with 1% Triton X-100 and VopQ was purified by nickel nitriloacetic acid matrix (Ni^{2+}-NTA) affinity chromatography (Qiagen).

Methods for Understanding *V. parahaemolyticus* Pathogenesis and the Role of the T3SS Effector VopQ

T3SS-Inducing Conditions. T3SS of *V. parahaemolyticus* was induced by growing cultures in MLB overnight, then diluting the cultures 1:15 into fresh MLB plus 10mM Na-oxalate and 10mM $MgCl_2$. Cultures were grown at 37°C for 3 hours before infection. To induce the T3SS of *Y. pseudotuberculosis*, overnight cultures were diluted 1:15 in fresh LB containing 20mM Na-oxalate and 20mM $MgCl_2$ and grown at 26°C for one hour, then shifted to 37°C for two hours.

***In vitro* Secretion Assays:** Bacteria were grown as described above to induce secretion. Following induction, 1 O.D.@600nm of bacteria were harvested via centrifugation. The pellet was resuspended in SDS sample buffer and boiled for 10 minutes. The supernatant was filtered with a 0.2μm syringe filter and trichloroacetic acid (TCA) was added to a final volume of 20% and incubated at 4°C overnight. BSA (6μg) was added as a TCA precipitation control. TCA-precipitated supernatants were centrifuged at 20,000 x *g* for 10 minutes at 4°C and washed with ice-cold

acetone. Dried pellets were resuspended in SDS sample buffer and boiled for 10 minutes.

Infections: HeLa cells or RAW 264.7 macrophages were seeded at a density of 0.15 x 10^6 or 0.5 x 10^6 cells/ml, respectively. For microscopy, cells were plated onto sterile glass coverslips. After 18 – 24 hours, *V. parahaemolyticus* and *Y. pseudotuberculosis* were added to the cells at a multiplicity of infection (MOI) of 10 and 100, respectively. Cell monolayers and bacteria were centrifuged at 200 x *g* for 5 min at the onset of each infection. Cells were harvested for analysis via Western blot by the addition of 200μl of SDS sample buffer to each well unless otherwise specified.

Measurement of Apoptosis in Infected Cells: Raw 264.7 macrophages were left untreated, infected with POR3 or YP126 as described, or treated with 1μM staurosporine for 4 hours. Cells were lysed and normalized for protein content. Caspase 3/7 activity of 40 μg of protein was measured by the Caspase-Glo assay (Promega). Results are expressed as relative luciferase units. For analysis of PARP cleavage, RAW 264.7 macrophages were treated as described and lysed at the indicated time points in PARP

sample buffer (62.5 mM Tris-HCl, pH 6.8, 6 M urea, 2% SDS, 5% β-mercaptoethanol, 10% glycerol, 0.00125% bromophenol blue). Samples were sonicated for 15 s, separated by SDS-PAGE, and immunoblotted with anti-PARP antibody and anti-aldolase antibody to confirm equal loading.

Measurement of LDH Release During Infection: HeLa cells or RAW264.7 macrophages were seeded at a density 0.15 x 10^6 cells/mL or 0.5 x 10^6 cells/ml respectively in a 24 well plate and infected as described in DMEM without serum. At the indicated time points, 200μL of culture supernatant was removed in triplicate from each well into a 96-well plate. This plate was spun at 200 x *g* for 5 minutes at room temperature and 100μL of supernatant was transferred to a new 96-well plate. LDH release was measured with a Cytotoxicity Detection kit (Takara). Results are expressed as cytotoxicity calculated as percent of total lysis of cells lysed in 1% Triton X-100. To measure pore formation, cells were infected in the presence of 5mM and 10mM glycine. Endoplasmic stress inhibitors xestospongin C (XeC, Calbiochem) and salubrinal (SAL, Calbiochem) were used at 1μM and 20μM respectively. Phospholipase inhibitors methylarachidonylfluorphosphonate (MAFP, Sigma) and bromoenol

lactone (BEL, Sigma) were used at 25μM and 50μM respectively. The reactive oxygen species inhibitor butylated hydroxyanisole (BHA, Sigma) was used at 100μM.

Methods for Monitoring Autophagy: To induce autophagy, GFP-LC3 HeLa cells were starved in Hank's Balanced Salt Solution (HBSS, Invitrogen) with protease inhibitors pepstatin A (10μg/mL, Sigma) and E64-d (10μg/mL, Sigma) for four hours. Cells were harvested in SDS sample buffer, boiled for 5 minutes and samples were either immediately processed for Western blotting or frozen at -20°C. GFP-LC3-I and GFP-LC3-II were detected using an anti-GFP antibody. Identical samples were probed with an anti-βactin antibody to confirm equal loading. Relative LC3-II accumulation was determined by quantitating band intensity using ImageJ software and calculating the ratio of LC3-II to LC3-I. The PI3-kinase inhibitor wortmannin (Sigma) was used at 10μM. Brefeldin A (Sigma) was used at 5μg/mL. Nocodazole (Sigma) was used at 10μg/mL.

Preparation of Slides for Confocal Microscopy: Cells were fixed in 3.2% paraformaldehyde in phosphate buffered saline (PBS) for 10 minutes at room temperature and permeabilized in 0.1% Triton X-100 in PBS for 5

minutes at room temperature. Cells were stained with rhodamine-phalloidin (1:40, Molecular Probes) and Hoechst 33342 (1:10000, Sigma) in PBS plus 0.1% BSA for 20 minutes at room temperature. Following 2 washes in PBS, slides were mounted with 10% glycerol containing n-propyl galate and sealed with clear nail polish. Samples were visualized with a Zeiss LSM 510 scanning confocal microscope. Images were converted using ImageJ software and Adobe Photoshop.

Preparation of Samples for Electron Microscopy: Samples were prepared with the assistance of Laurie Mueller at the Molecular and Cellular Imaging Core Facility at the University of Texas Southwestern Medical Center. Cultured cells were fixed in 2.5% glutaraldehyde in 0.1M sodium cacodylate buffer, followed by 1% osmium tetroxide in 0.1M sodium cacodylate buffer. After solvent dehydration, centrifuged pellets of cells were embedded in epoxy resin (EMBED 812, Electron Microscopy Sciences) and polymerized at 60°C. Ultrathin sections were cut at a nominal thickness of 80 nm, picked up on copper grids, and stained with uranyl acetate and lead citrate. Sections were examined at 120 kV with a Tecnai G^2 Spirit transmission electron microscope (FEI Company), and images were acquired with a Soft Imaging System Morada camera. Cells

were counted for the presence of intracellular bacteria. For every 100 cells counted, cells were scored for the presence of intracellular bacteria. Cells were counted 3 times for each sample. The diameter of each circle on the map corresponds to the number of cells harboring 0, 1, 2, 3 or ≥4 bacteria per cell. An asterisk represents >90% of cells counted had that many intracellular bacteria.

Microinjection of Recombinant Purified VopQ: Microinjection experiments were performed by Joachim Seemann (Cell Biology, University of Texas Southwestern Medical Center). Microinjection was performed with a Transjector 5246 and a Micromanipulator 5171 (Eppendorf) as described previously (Bartz et al., 2008). HeLa cells stably expressing GFP-LC3 were grown overnight on glass coverslips and injected into the cytoplasm with 0.5 mg/ml VopQ or 0.5 mg/ml GST as a control. Prior to injection, the proteins were dialyzed against 25 mM HEPES-KOH pH 7.4, 50 mM KAc and mixed with 2 mg/ml lysine fixable 70 kDa Texas-Red dextran (Invitrogen) as a injection marker. After the injections, the cells were incubated for 30 min at 37˚C and then fixed. For inhibitor experiments with VopQ, cells were pretreated for 45 minutes with 10μM wortmannin or 10mM 3-methyladenine (3-MA, Sigma). For the

rapamycin experiment, cells were pretreated for 30 minutes with 10μM wortmannin or 10mM 3-MA and then treated with 1μg/ml rapamycin (Sigma) for 4 hours. All inhibitors were present throughout the duration of all experiments. The cells were fixed for 15 min in 3.7% formaldehyde in PBS and permeabilized for 10 min in methanol at -20˚C. DNA was then stained with Hoechst 33342 (Invitrogen) and the cells were mounted in Mowiol 4-88 (Calbiochem). Fluorescence analysis was performed with an Axiovert 200M microscope (Zeiss) and a LD Plan-Neofluar 40x/1.3 DIC objective (Zeiss). Images were captured with an Orca-285 camera (Hamamatsu Photonics) and the software package Openlab 4.02 (Improvision).

Labeling of Subcellular Organelles: HeLa cells were seeded at a density of 0.15 x 10^6 cells/mL. The following day, cells were transfected with 2μg of either pSFFV-GFP or pSFFV VopQ-GFP using Fugene HD (Roche) according to the manufacturer's instructions. Cells were incubated with 1μM ER Tracker Red with 1:10,000 Hoechst 33342 in HBSS for 30 minutes at 37°C to stain the endoplasmic reticulum. To stain the lysosome and mitochondria, cells were incubated with 75nM Lyso Tracker Red and 250nm Mito Tracker Red respectively in DMEM with 1:10,000 Hoechst

33342 for 30 minutes at 37°C. Following live cell staining, cells were fixed with 3.2% paraformaldehyde, mounted on glass slides and sealed with clear nail polish. Samples were visualized with a Zeiss LSM 510 scanning confocal microscope. Images were converted using ImageJ software and Adobe Photoshop.

Nitrogen Cavitation: HEK293 cells were plated at 0.6 x 10^6 cells per mL in 100mM dishes. The following day, cells were transfected with pSFFV and pSFFV VopQ-FLAG using Lipofectamine (Invitrogen). Cells were harvested and lysed in lysis buffer (20mM HEPES pH 7.6, 150mM NaCl, 2mM $MgCl_2$, 2mM EDTA, 10mM KCl, 0.5mM Na_3VO_4, 0.5mM EGTA, 20mM NaF, 20mM bisglycerophosphate, 1mM dithiothreitol (DTT)). Lysate was placed under 500 psi of N_2 gas for 30 minutes at 4°C. Following lysis under hypoxic conditions, cells were centrifuged at 500 x *g* for 10 minutes at 4°C to isolate nuclei (P1), followed by centrifugation at 10,000 x *g* for 10 minutes at 4°C to isolate subcellular organelles (P10), followed by centrifugation at 100,000 x *g* for 60 minutes at 4°C to isolate the plasma membrane (P100). The supernatant at this step contained the cytosolic fraction (S100). Lysates were separated by SDS-PAGE, transferred to

membranes for Western blotting and probed with anti-VopQ, anti-Lamin, anti-aldolase, and anti-calnexin antibodies.

Immunofluorescence: For staining of the Golgi apparatus using anti-golgin97 antibodies, cells were fixed and permeabilized as described. For microtubule staining using anti-tubulin antibodies, cells were fixed in cold 100% methanol overnight at -80°C, rehydrated for 10 minutes in PBS, and permeabilized as described. Following fixation and permeabilization for both Golgi and microtubules, cells were blocked in blocking buffer (3% BSA, 10% heat-inactivated calf serum in TTBS, 0.2μm filter sterilized) for 30 minutes at room temperature with gentle agitation. Slides were incubated in primary antibody diluted in blocking buffer at 4°C overnight and washed 3 times in TTBS. Slides were incubated in secondary antibodies goat anti-mouse 680 (Golgi) or goat anti-mouse tetramethylrhodamine isothiocyanate (TRITC, microtubules) in blocking buffer for 30 minutes at room temperature in the dark followed by 3 washes in TTBS. Slides were mounted on glass coverslips and sealed with nail polish. Samples were visualized with a Zeiss LSM 510 scanning confocal microscope. Images were converted using ImageJ software and Adobe Photoshop.

Nutrient Release Assay: HeLa cells were plated as described in 24-well dishes and labeled with 0.2μM of L-[^{14}C]-valine for 24 hours. Cells were rinsed 3 times with PBS and chased for 1 hour in the presence of cold 10mM valine to allow degradation of short-lived proteins. Cells were either mock infected, starved with HBSS or infected with POR3. At the indicated time points, the supernatant was removed from each well and centrifuged to isolate the bacteria. To the supernatant, TCA was added to a final volume of 10% and incubated at 4°C for 1 hour and then centrifuged for 10,000 x *g* for 10 minutes at 4°C. The supernatant was added to scintillation fluid and counted as the acid-soluble radioactivity. The HeLa cells were washed 3 times with PBS and these washes were added to the bacteria isolated above. All the bacteria isolated were added to scintillation fluid and counted as radioactivity associated with bacteria. The HeLa cells were lysed in 0.2M NaOH and added to scintillation fluid and counted as the cellular radioactivity. The total radioactivity was the sum of the cellular radioactivity, acid-soluble radioactivity, and radioactivity associated with the bacteria. The % acid-soluble radioactivity and radioactivity associated with bacteria were both calculated as percent of total radioactivity.

Iron Chelation: Overnight cultures of *V. parahaemolyticus* POR3 and *E. coli* K12 were diluted to 0.05 $O.D._{600}$/mL in fresh media alone or fresh media containing 100μM, 250μM and 500μM 2'2'bipyridyl (BP, Sigma). Bacteria were monitored for growth over time by measuring $O.D._{600}$ to determine the optimal 2'2'bipyridyl concentration that effectively chelates iron but does not kill the bacteria. To demonstrate iron chelation is specific, POR3 overnight cultures were diluted to 0.05 $O.D._{600}$/mL in 125μM 2'2'bipyridyl and monitored for growth over time by measuring $O.D._{600}$. At 7 hours, 1mM $Fe(NH_4)SO_4$ was added back to the culture media and bacteria were monitored for growth over time by measuring $O.D._{600}$.

Iron Growth Assay: HeLa cells were plated as described. Prior to infection, HeLa cells were rinsed with 125μM 2'2'bipyridyl in PBS. Cells were then infected with overnight cultures of POR3 and ΔT3SS1/ΔT3SS2 strains grown in MLB or MLB + 125μM 2'2'bipyridyl at an MOI of 10 as described. At the indicated time points, media was removed, serially diluted, and plated onto MMM + 0.1% sodium pyruvate in triplicate. Individual colonies were counted and expressed as colony forming units per mL (cfu/mL).

Yeast Materials and Methods

Yeast strains and media: List of yeast strains used in this study can be found in Table 2. Yeast were maintained without selection on YPAD (1% yeast extract, 2% Bacto-peptone, 2% glucose, and 0.01% adenine). Yeast were maintained with selection on yeast complete dropout media with glucose (YCD) at 30°C. Each liter of yeast complete dropout media contains 1.2g yeast nitrogen base without amino acids and ammonium sulfate (Difco), 5g ammonium sulfate, 10g succinic acid, 6g sodium hydroxide, and 0.75g yeast amino acids except tryptophan, histidine, uracil, leucine, and lysine (-WHULK). 2% glucose (D) or 2% galactose/1% raffinose (G/R) is added as the carbon source. 20g of Bacto agar is added per liter for solid media. Amino acids are added back to the media depending on the strain and plasmid auxotrophies (tryptophan 0.1g/L, histidine 0.05g/L, uracil 0.1g/L, leucine 0.1g/mL, and lysine 0.1g/mL).

Yeast transformation: Yeast were mixed with 7 μL of 1X TE (10mM Tris-HCl pH 7.5, 1mM EDTA) and 5μL of plasmid DNA (200-500ng) to which 80μL of transformation mix is added (100mM DTT, 2M LiOAc in 10X TE, 60% PEG 3350). Yeast were incubated for 1-3 hours at 45°C and plated

on selective media.

Yeast growth curve: Yeast overnight cultures were measured by optical density ($O.D._{600}$) at 600nm. Equivalent $O.D._{600}$ were washed three times in PBS and diluted into YCG/R at a density of 0.1 $O.D._{600}$/mL. At the indicated timepoints, culture density was measured by $O.D._{600}$. In addition, 1.5 $O.D._{600}$ equivalents were harvested for protein extraction and Western blot analysis. For alpha factor synchronization, overnight cultures were resuspended in media containing 10μM alpha factor (Sigma) and incubated for 2.5 hours at 30°C. After 2.5 hours, the culture was centrifuged and washed 3 times with distilled water. Yeast were diluted to 0.2 $O.D._{600}$/mL and returned to growth at 30°C. At 20 minute intervals, 1 $O.D._{600}$ equivalent was removed and fixed in 3.2% paraformaldehyde in 150mM NaCl for 10 minutes. Yeast were then spun and resuspended in 95% ethanol with 1:1000 Hoechst 33342 (Sigma). Cells were washed with 70% ethanol, followed by 35% ethanol and then twice in distilled water. Yeast were transferred to a microscope slide, covered with a glass coverslip and sealed with nail polish. Yeast were viewed using epifluorescence microscopy and photographed with a Zeiss AxioCam and OpenLab 3.1.7 software.

Yeast Dilution Plating: Yeast overnight cultures were measured by $O.D._{600}$. Equivalent $O.D._{600}$ were washed three times in PBS and diluted into PBS at a density of 0.1 $O.D._{600}$/mL. Six serial 1:5 dilutions were made in PBS and 5μL of each dilution was plated onto selective media.

Yeast Protein Extraction: 1.5 $O.D._{600}$ equivalents of yeast culture were harvested by centrifugation at 6000 rpm for 2 minutes. Samples were resuspended in 500μL of distilled water and precipitated with TCA in the presence of NaOH and β-ME for 10 minutes on ice. Samples were centrifuged at 6000 rpm for 2 minutes and washed briefly in 1M Tris. Samples were boiled for 5 minutes prior to separation on SDS-PAGE.

Yeast Deletion Library: The yeast deletion library was transformed with pRS413 VopQ-FLAG using a multiwell yeast transformation protocol designed by Yong Wang (Orth Lab, UT Southwestern). Briefly, 7uL of a DNA mixture (100mM LiAc, 10mg/mL single stranded DNA, 0.3 – 1ug plasmid DNA) was added to each well of a 96-well plate. A 96-well pinner was then used to transfer fresh yeast from YPAD agar plate grid to the 96-well plate containing the DNA mix. Following the addition of the PEG mix

(50% PEG, 1M LiAc) the plates were incubated at room temperature for 30 minutes. 4μL of DMSO (dimethylsuphoxide) was added to each well and the plate was sealed with foil, wrapped in parafilm, and floated in a 45°C water bath for 30 minutes. 4μL of each transformation was plated onto selective media using a multichannel pippettor. Plates were incubated for 5 days at 30°C after which a 94% transformation efficiency was achieved. Following transformation, yeast were grown in liquid selective media in a 96-well format and spotted into YCD-His and YCG/R-His. All positives were scored and a new matrix was made by pulling the positive clones from the original YPAD plates. These yeast were transformed with pRS413 and pRS413 VopQ-FLAG, plated onto selective media, then transferred to YCD-His and YCG/R-His to eliminate false positives. The remaining 89 yeast capable of growing in the presence of VopQ were pulled from the glycerol stocks and transformed again with pRS413 VopQ-FLAG. Transformants were plated on selective media and each strain harboring VopQ was streaked onto YCD-His and YCG/R-His and scored for a fitness level corresponding to the degree of growth in the presence of VopQ. Yeast that grew well in the presence of VopQ scored a 3, whereas yeast that did not grow well scored a 0. From this screen, we obtained 16 positives. The yeast strains corresponding to these 16

positives were pulled from the glycerol stocks again and restransformed with pRS413 and pRS413 VopQ-FLAG. Transformants were plated on selective media and streaked onto YCD-His and YCG/R-His. From this, only 3 yeast strains grew well in the presence of VopQ. These strains were YML063W (*Δrps1b*), YML021C (*Δung1*), and YOR360C (*Δpde2*). Of these three genes, only *Δpde2* was confirmed by PCR sequencing.

Alkaline phosphatase assay: Alkaline phosphatase activity was measured as described (Klionsky, 2007). Yeast were pelleted at 6000 rpm for 2 minutes at 4°C and washed once in ice-cold water with 2mM PMSF (phenylmethanesuofonyl fluoride) and pelleted again. Yeast were resuspended in lysis buffer (20mM PIPES pH 7.0, 0.5% Triton X-100, 50mM KCl, 100mM potassium acetate, 10mM $MgSO_4$, 10μM $ZnSO_4$, 1mM PMSF) to which glass beads were added at half the volume. Yeast were vortexed for 4 minutes and incubated on ice for 4 minutes and then centrifuged at 6000 rpm for 5 minutes at 4°C. Lysate was incubated in a 500μL final volume of reaction buffer (250mM Tris-HCl pH 8.5, 0.4% Triton X-100, 10mM $MgSO_4$, 1.25mM nitrophenyl phosphate) at 37°C in the dark. The reaction was terminated by the addition of an equal volume of stop buffer (2M glycine/KOH pH 11) and the absorbance was measured at

410nm. The nmoles of p-nitrophenol generated was determined from a standard curve and the specific activity was calculated as nmoles p-nitrophenol/minute/mg of protein.

Table 2: Strains

E. coli		
Strain	**Description**	**Ref.**
DH5α	Used for general cloning F- *ϕ80lacZΔM15* Δ(*lacZYA*-argF)U169 *recA1 endA1 hsdR17*(rk-, mk+) *phoA supE44 thi-1 gyrA96 relA1* λ-	Invitrogen
K12	Wild-type *E. coli*	A gift from V. Sperandio
BW25113	Used for λred recombination *lacI*^{q} *rrnB*$_{T14}$ *lacZ*$_{WJ16}$ *hsdR514 araBAD*$_{AH33}$ *rhaBAD*$_{LD78}$, harbors pKD46	A gift from L. McCarter (Datsenko & Wanner, 2000)
BL21-DE3	Used for recombinant protein expression F- *omp*T *hsd*SB(rB–, mB–) *gal dcm* (DE3)	Novagen

V. parahaemolyticus		
Strain	**Description**	**Ref.**
POR1	RIMD2210633 *ΔtdhA ΔtdhS*; Amp^{R}, Kan^{R}	A gift from T. Honda (Park et al., 2004a)
POR2	POR1 *Δvp1662*; Amp^{R}, Kan^{R}	A gift from T. Honda (Park et al., 2004b)
POR3	POR1 *Δvpa1355*; Amp^{R}, Kan^{R}	A gift from T. Honda (Park et al., 2004b)
POR1*ΔvopQ*	POR1 *Δvp1680*; Amp^{R}, Kan^{R}, Cm^{R}	This study
POR2*ΔvopQ*	POR2 *Δvp1680*; Amp^{R}, Kan^{R}, Cm^{R}	This study
POR3*ΔvopQ*	POR3 *Δvp1680*; Amp^{R}, Kan^{R}, Cm^{R}	This study
POR3*ΔvopQ* + VopQ	POR3 *Δvp1680* + pLafR.VopQ; Amp^{R}, Kan^{R}, Cm^{R}, Tet^{R}	This study
POR3*ΔvopS*	POR3 *Δvp1686*; Amp^{R}, Kan^{R}, Cm^{R}	(Yarbrough et al., 2009)

Y. pseudotuberculosis		
Strain	**Description**	**Ref.**
YP126	wild-type, YPIII (pYV+)	A gift from J. Bliska (Bolin et al., 1982)

YP27	*ΔyopEHJ*; YP126 deleted for Yops H, E, and J; Kan^R, Cm^R	A gift from J. Bliska (Palmer et al., 1999)
YP37	*ΔyopEHJOMK*; YP126 deleted for Yops H, E, J, O, M, and YpkA; Kan^R, Cm^R	A gift from J. Bliska (Viboud et al., 2003)
YP44	Translocation mutant. *ΔyopEHJOMKB*; YP37 *ΔyopB4*; Kan^R, Cm^R	A gift from J. Bliska (Ryndak et al., 2005)
YP71	Secretion mutant. YP126 *ysc::Tn5* Kan^R	A gift from J. Bliska (Bolin & Wolf-Watz, 1984)
YP27 + pMMB67HE VopQ-FLAG	YP27 harboring pMMB67HE VopQ-FLAG; Kan^R, Cm^R, Amp^R	This study
YP37 + pMMB67HE VopQ-FLAG	YP37 harboring pMMB67HE VopQ-FLAG; Kan^R, Cm^R, Amp^R	This study
YP44 + pMMB67HE VopQ-FLAG	YP44 harboring pMMB67HE VopQ-FLAG; Kan^R, Cm^R, Amp^R	This study
YP71 + pMMB67HE VopQ-FLAG	YP71 harboring pMMB67HE VopQ-FLAG; Kan^R, Amp^R	This study
YP27 + pMMB67HE VP1682-VopQ-FLAG	YP27 harboring pMMB67HE VP1682-VopQ-FLAG; Kan^R, Cm^R, Amp^R	This study
YP37 + pMMB67HE VP1682-VopQ-FLAG	YP37 harboring pMMB67HE VP1682-VopQ-FLAG; Kan^R, Cm^R, Amp^R	This study
YP44 + pMMB67HE VP1682-VopQ-FLAG	YP44 harboring pMMB67HE VP1682-VopQ-FLAG; Kan^R, Cm^R, Amp^R	This study
YP71 + pMMB67HE VP1682-VopQ-FLAG	YP71 harboring pMMB67HE VP1682-VopQ-FLAG; Kan^R, Amp^R	This study

S. cerevisiae		
Strain	**Description**	**Ref.**
BY4741	*Mat**a** his3Δ1 leu2Δ0 met15Δ0 ura3Δ0*	Research Genetics
BY4741 + vector	BY4741 with pRS413, *HIS3*	This study
BY4741 + VopQ	BY4714 with pRS413 VopQ-FLAG, *HIS3*	This study
SEY6210	*Matα leu2-3,112 ura3-52 his3-Δ200 trp1-Δ901 lys2-801 suc2-Δ9 GAL*	A gift from B. Levine (Robinson et

		al., 1988)
Δatg1	SEY6210 *atg1Δ::HIS3*	A gift from B. Levine
Δatg3	SEY6210 *atg3Δ::HIS3*	A gift from B. Levine
Δatg5	SEY6210 *atg5Δ::LEU2*	A gift from B. Levine
Δatg6	SEY6210 *atg6Δ::HIS3*	A gift from B. Levine
Δatg7	SEY6210 *atg7Δ::LEU2*	A gift from B. Levine
Δatg8	SEY6210 *atg8Δ::LEU2*	A gift from B. Levine
Δatg11	SEY6210 *atg11Δ::HIS3*	A gift from B. Levine
Δatg17	SEY6210 *atg17Δ::HIS3*	A gift from B. Levine
Δvps15	YBR097W; BY4741 *Δvps15::G418*	A gift from A. Shilatifard, Research Genetics
Δvps34	YLR240W; BY4741 *Δvps34::G418*	A gift from A. Shilatifard, Research Genetics
SEY6210 + vector	*Matα leu2-3,112 ura3-52 his3-Δ200 trp1-Δ901 lys2-801 suc2-Δ9 GAL*	This study
Δatg1 + vector	SEY6210 *atg1Δ::HIS3* + pRS416	This study
Δatg3 + vector	SEY6210 *atg3Δ::HIS3* + pRS416	This study
Δatg5 + vector	SEY6210 *atg5Δ::LEU2* + pRS416	This study
Δatg6 + vector	SEY6210 *atg6Δ::HIS3* + pRS416	This study
Δatg7 + vector	SEY6210 *atg7Δ::LEU2* + pRS416	This study
Δatg8 + vector	SEY6210 *atg8Δ::LEU2* + pRS416	This study
Δatg11 + vector	SEY6210 *atg11Δ::HIS3* + pRS416	This study
Δatg17 + vector	SEY6210 *atg17Δ::HIS3* + pRS416	This study
Δvps15 + vector	YBR097W; BY4741 *Δvps15::G418* + pRS416	This study
Δvps34 + vector	YLR240W; BY4741 *Δvps34::G4188* + pRS416	This study
SEY6210 + VopQ	*Matα leu2-3,112 ura3-52 his3-Δ200 trp1-Δ901 lys2-801 suc2-Δ9 GAL* + pRS416	This study

	VopQ-FLAG	
Δatg1 + VopQ	SEY6210 *atg1Δ::HIS3* + pRS416 VopQ-FLAG	This study
Δatg3 + VopQ	SEY6210 *atg3Δ::HIS3* + pRS416 VopQ-FLAG	This study
Δatg5 + VopQ	SEY6210 *atg5Δ::LEU2* + pRS416 VopQ-FLAG	This study
Δatg6 + VopQ	SEY6210 *atg6Δ::HIS3* + pRS416 VopQ-FLAG	This study
Δatg7 + VopQ	SEY6210 *atg7Δ::LEU2* + pRS416 VopQ-FLAG	This study
Δatg8 + VopQ	SEY6210 *atg8Δ::LEU2* + pRS416 VopQ-FLAG	This study
Δatg11 + VopQ	SEY6210 *atg11Δ::HIS3* + pRS416 VopQ-FLAG	This study
Δatg17 + VopQ	SEY6210 *atg17Δ::HIS3* + pRS416 VopQ-FLAG	This study
Δvps15 + VopQ	YBR097W; BY4741 *Δvps15::G418* + pRS416 VopQ-FLAG	This study
Δvps34 + VopQ	YLR240W; BY4741 *Δvps34::G418* + pRS416 VopQ-FLAG	This study
TN124	*Mat**a** leu2-3,112 trp1 ura3-52 pho8::pho8Δ60 pho13Δ::LEU2*	A gift from D. Klionsky, (Noda et al., 1995)
TN124 + vector	TN124 with pR3416	This study
TN124 + VopQ	TN124 with pR3416 VopQ-FLAG	This study

Table 3: Primers

Code	Name	Site[a]	Tag, etc[b]	Sequence[c]	Tm (°C)
200/I	VP1680Hind 3F	HindIII		cagaaagcttatggtgaatacaacgcaa aaaatc	64
203/I V	VP1680FLA GXbaIR	XbaI	FLAG stop	atactctagattacttgtcatcgtcgtccttgt agtcaatccagccttcggctaagta	62
206/A	PRS413GAL VP1680Bam HI	Bam HI		atcggatccatggtgaatacaacgcaa aaaatc	64
207/2 08/B	PRS413GAL VP1680EcoR I	EcoR I	FLAG stop	atcggaattcttacttgtcatcgtcgtccttgt agtcaatccagccttcggctaagtac	66
213/G	PcDNA3VP1 680-HC-HindIII	HindIII		atcgaagcttatgcaacaaacgttagcca ttg	62
219/M	VP1680NdeI 5P	NdeI		atcgatcgcatatgatggtgaatacaacg caaaaaatg	64
220/N	VP1680Bam HI3P	Bam HI	Stop	atcggatccttaaatccagccttcggcta ag	64
224/R	VP1680-N-3PXbaIFLAG	XbaI	FLAG stop	atcgtctagattacttgtcatcgtcgtccttgt agtctggcatcgataagcgctgatc	64
225/2 26/S	VP1680-NH-3PXbaIFLAG	XbaI	FLAG stop	atcgtctagattacttgtcatcgtcgtccttgt agtcatacgccccagcttggcc	60
227/2 28/T	1680KOBam HI5P	Bam HI		atcggatccacatttgctttcgctgccg	58
229/U	1680KOBam HI3P	Bam HI		atcggatccttaactcaaccagtgatga cc	60
232/X	VP1680NotIn ostop3P	Not I		cagatcaggcggccgcaatccagccttc ggctaag	58
247/2 48	VP1682HindI II5P	HindIII		Atcgaagcttatgaacacgattcaaccac tgc	64
230/V	1680P1For-KAN	tcaaatcatgaacaaagtcatgttcaaccactgcgtgtgtaggag ggagttgtgtaggctggagctgcttcg64			58
230/ W	1680P2Rev-KAN	Ctgtaagcgtcgatgcaataagcaaaaagggagcgaatgctc ccttttcttcatatgaatatcctccttag			54

Mutagenesis Primers		
Code	**Name**	**Sequence[d]**
287	VP1680 S288A 5’	gctttaaccactggcataatcgccggcgggggctttgttgctggc
288	VP1680 S288A 3’	Gccagcaacaaagccccgccggcgattatgccagtggttaaag

		c
289	VP1680 D433A 5’	atgcctgctgtccgagcaatggctaaaggtgaagcgggcaaaatc
290	VP1680 D433A 3’	gattttgcccgcttcacctttagccattgctcggacagcaggcat

Sequencing Primers			
Code	**Name**	**Sequence**	**Tm (°C)**
C1	Cat pKD3 C1 REV	gttttcaccatgggcaaatat	58
C2	Cat pKD3 C2 FOR	atcttccgtcacaggtagg	58
C3	Cat 5P REV	atggagaaaaaaatcactggat	58
C4	Cat 3P FOR	tcatcgcagtactgttgtatt	58
235	VP1680SEQ1R	aaacgtatttttgagctgctg	58
236	VP1680SEQ4F	ttagcatgcaggagccgg	58
237	VP1680SEQ2F	aagagaagctgaaaggctcg	62
238	VP1680SEQ3R	atttaagccatacgccccagc	64
239	VP1682SEQ1F	ttagaaaaatcgggagagttg	58
240	VP1682SEQ2R	gagttaagatgctcggtag	56
	VP1680BSEQ5R	Attgtttaactcgttcaatag	54

[a]Blue corresponds to restriction enzyme sequence.
[b]Red corresponds to stop codon.
[c]All primers are listed 5’ to 3’.
[d]Underline sequence corresponds to mutated codon.

Table 4: Constructs

Mammalian Expression Vectors		
Plasmid	**Description**	**Ref.**
pSFFV	Mammalian expression vector, Amp^R, Neo^R, spleen focus forming virus (SFFV) promoter cloned into $pcDNA_3$ backbone	K. Orth (Palmer et al., 1999)
pSFFV-GFP	Mammalian expression vector, eGFP from Invitrogen's peGFPN1 cloned into Not I and Apa I sites in pSFFV, Amp^R, Neo^R	This study
pSFFV VopQ-FLAG	Mammalian expression vector, VopQ cloned into pSFFV with HindIII and XbaI using primers 1 and 4, Amp^R, Neo^R	This study
pSFFV VopQ-GFP	Mammalian expression vector, VopQ cloned in frame into pSFFV-GFP with Hind III and Not I using primers 1 and X, Amp^R, Neo^R	This study
pSFFV VopQ-GFP S288A	Mammalian expression vector, S288A mutant of pSFFV VopQ-GFP using primers 287 and 288, Amp^R, Neo^R	This study
pSFFV VopQ-GFP D433A	Mammalian expression vector, D433A mutant of pSFFV VopQ-GFP using primers 289 and 290, Amp^R, Neo^R	This study
pSFFV VopQ-FLAG S288A	Mammalian expression vector, S288A mutant of pSFFV VopQ-FLAG using primers 287 and 288, Amp^R, Neo^R	This study
pSFFV VopQ-FLAG D433A	Mammalian expression vector, D433A mutant of pSFFV VopQ-FLAG using primers 289 and 290, Amp^R, Neo^R	This study
pSFFV VopQ-FLAG 1-228	Mammalian expression vector expressing VopQ-FLAG truncation (nts 1-684) generated using primers 1 and R, Amp^R, Neo^R	This study
pSFFV VopQ-FLAG 1-301	Mammalian expression vector expressing VopQ-FLAG truncation (nts 1-903) generated using primers 1 and S, Amp^R, Neo^R	This study
pSFFV VopQ-FLAG 229-492	Mammalian expression vector expressing VopQ-FLAG truncation (nts 685-1476) generated using primers G and N, Amp^R, Neo^R	This study
pSFFV VopQ-FLAG 302-492	Mammalian expression vector expressing VopQ-FLAG truncation (nts 904-1476)	This study

	generated using primers I and 4, Amp^R, Neo^R	

Plasmids for expression in *Y. pseudotuberculosis*		
Plasmid	**Description**	**Ref.**
pMMB67HE	IPTG-inducible expression vector for *Y. pseudotuberculosis*, Amp^R	A gift from J. Bleaks (Furste et al., 1986)
pMMB67HE Vop-FLAG	*vopQ* cloned into pMMB67HE using primers 1 and B	This study
pMMB67HE VP1682-VopQ-FLAG	*vp1682* and *vopQ* cloned into pMMB67HE using primers 247/248 and B	This study

Plasmids for generating *V. parahaemolyticus ΔvopQ* strains		
Plasmid	**Description**	**Ref.**
pLafR	Large cosmic vector for generating knockouts in *V. parahaemolyticus*, Tet^{ra}, Inco	A gift from L. McCarter (Friedman et al., 1982)
pLafR.*vopQ*	*vopQ* with 1kb upstream and downstream flanking genomic DNA cloned into the BamHI site in pLafR using primers T and U, Tet^{ra}, Inco	This study
pKD3	Plasmid harboring chloramphenicol cassette used as a template for generating PCR product P1 FOR and P2 REV primers. Used for λred recombination during knockout generation, Cm^R	A gift from L. McCarter (Datsenko & Wanner, 2000)
pLafR.*vopQ::cm*^{R}	Knockout construct after λred recombination Tet^R, Cm^R, IncP	This study
pPH1JI	Plasmid used to kickout pLafR and resolve merodiploids, IncP, Gen^R, Sm^R, Spc^R, *Tra*$^+$, *mob*	A gift from L. McCarter (Hirsch & Beringer, 1984)
pRK2013	RK2 tra donor for conjugation, Kan^R	A gift from L. McCarter, (Ditta et al.,

		1980)

Plasmids for expression in *S. cerevisiae*		
Plasmid	**Description**	**Ref.**
pRS413 Gal1	Yeast expression vector with galactose inducible promoter, Amp^R, *HIS3*	New England Biolabs
pRS416 Gal1	Yeast expression vector with galactose inducible promoter, Amp^R, *URA3*	New England Biolabs
pRS413 VopQ-FLAG	*vopQ* amplified using primers A and B and cloned into the BamHI and EcoRI sites of pRS413 Gal1, Amp^R, *HIS3*	This study
pRS416 VopQ-FLAG	*vopQ* amplified using primers A and B and cloned into the BamHI and EcoRI sites of pRS416 Gal1, Amp^R, *URA3*	This study

Plasmids for recombinant protein expression		
Plasmid	**Description**	**Ref.**
pET15b H_6VopQ	Plasmid for recombinant protein expression in bacteria. *vopQ* amplified with primers M and N cloned into NdeI and BamHI sites of Novagen's pET15b, Amp^R	This study

Chapter 4

Characterization of T3SS1 in Pathogenesis of *Vibrio parahaemolyticus*

Introduction:

V. parahaemolyticus is a Gram-negative bacterium commonly found in marine and estuarine environments (Daniels et al., 2000). Infection leads to acute gastroenteritis and typically results from consumption of contaminated shellfish. Individuals who are immune-compromised or burdened with pre-existing health conditions are at high risk for severe complications that can result in death (Morris & Black, 1985). This bacterium has become increasingly important because pandemic strains are emerging throughout the world (Daniels et al., 2000, Morris & Black, 1985). *V. parahaemolyticus* has also been found along coastal waters and within fish farms in the United States (Daniels et al., 2000, Morris & Black, 1985). *V. parahaemolyticus* infections in the United States are believed to be largely under diagnosed and may represent a major health risk. Therefore, a better understanding of the virulence mechanisms of *V. parahaemolyticus* is essential for better diagnosis,

treatment, and prevention of infections.

The TDH and the TRH are the most well-characterized virulence factors of this bacterium. TDH and TRH are reversible amyloid toxins that cause β-hemolysis on Wagatsuma agar, known as the "Kanagawa phenomenon". However, infection with *Δtdh* and *Δtrh* strains of *V. parahaemolyticus* results in rapid and acute cell death in a tissue culture model (Park et al., 2004a). This cell death is associated with the presence of two T3SS (Park et al., 2004a). Bacterial T3SSs deliver bacterial effectors into the cytosol of host cells during infection (Ghosh, 2004). The structural components of T3SS are conserved among bacterial pathogens, however the effectors each system secretes vary widely. These effectors, like viral oncoproteins, are potent molecules that mimic or capture an endogenous eukaryotic activity to disrupt the cellular response to infection (Mukherjee *et al.*, 2007, Navarro et al., 2005).

Sequencing of the genome of the RIMD2210633 strain of *V. parahaemolyticus* revealed the presence of two T3SSs, one encoded on chromosome 1 (T3SS1) and the other encoded on chromosome 2 (T3SS2). T3SS2 is found only in clinical isolates of *V. parahaemolyticus* and is associated with enterotoxicity in a rabbit ileal loop model (Park et al., 2004b). We have shown that the effectors VopA and VopL from T3SS2

disrupt innate immunity and the actin cytoskeleton, respectively (Liverman et al., 2007, Trosky et al., 2007). However, mutant strains unable to secrete proteins from T3SS2 are still cytotoxic to cells, suggesting a role for T3SS1 in virulence (Liverman et al., 2007, Park et al., 2004a). Genotyping has shown that all isolates of *V. parahaemolyticus* harbor T3SS1, which resembles the T3SS of *Yersinia* spp. in structure and organization, albeit there is no similarity between their predicted effectors (Makino et al., 2003, Park et al., 2004b). The T3SS1 is correlated with cytotoxicity during infection and previous research from other groups suggests cell death proceeds via apoptosis however, the mechanism of cell death is not well established (Bhattacharjee et al., 2006, Ono et al., 2006).

In this chapter, we describe a mechanism used by *V. parahaemolyticus* to cause cell death. Infection with *V. parahaemolyticus* initiates a series of events that begins with the induction of autophagy, followed by cell rounding, then cellular lysis. Ultimately, these events culminate in a highly proinflammatory cell death that may function to benefit the invading bacteria.

Results:

Infection with *V. parahaemolyticus* Strain POR3 induces rapid cytotoxicity in multiple cell types

To develop a better understanding of the mechanism of *V. parahaemolyticus*-induced cytotoxicity, we infected HeLa and RAW 264.7 macrophage cell lines with the *V. parahaemolyticus* strain POR1 (RIMD2210633 *Δtdh* and *Δtrh*) and two isogenic strains derived from POR1 that are incapable of secreting effectors from either POR2 or POR3 (Park et al., 2004a). POR1 induces cytotoxicity in both RAW 264.7 and HeLa cell lines **(Figure 8; C and D)**. Although the POR2 strain is unable to induce this phenotype, obvious changes in the actin cytoskeleton are observed **(Figure 8; E and F)** (Liverman, AB et al., 2007). Infection of either HeLa or RAW 264.7 macrophage cell lines with the POR3 strain induces a cytotoxic phenotype similar to that seen in POR1 infected cells **(Figure 8; 1, C, D and G, H, respectively)**. T3SS1 systems can be primed by incubating bacteria at increased temperatures and chelating calcium with sodium oxalate, a treatment similar to that used for *Yersinia* spp. (Zhang et al., 2005). By inducing T3SS in *V. parahaemolyticus* POR3, we see an acceleration of

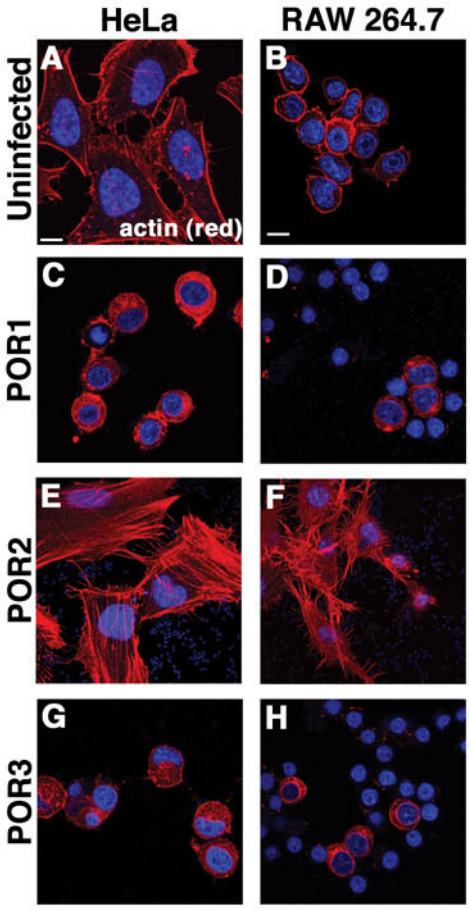

Figure 8. *V. parahaemolyticus*–induced cytotoxicity depends on T3SS1. HeLa cells **(A, C, E, and G)** or RAW 264.7 macrophages **(B, D, F, and H)** were infected with POR1 **(C and D)**, POR2 **(E and F)**, or POR3 **(G and H)** for 3 h and compared with uninfected cells **(A and B)**. Samples were fixed and stained for confocal microscopy. Scale bar represents 10µm.

the T3SS1-dependent cytotoxic phenotype **(Figure 9)**. Cells infected with the induced POR3 strain exhibit cytotoxicity as early as 60 minutes post infection, with only cell fragments observed at 3 hours post infection **(Figure 9; B-E and K-N)**. Infecting with the uninduced POR3 strain slows the death process allowing for observation of the T3SS1-induced cell death for an extended interval **(Figure 9; F-I and O-R)**. These results support the hypothesis that cytotoxicity is mediated by T3SS1 during infection. The remaining experiments described in this study use the POR3 strain to decipher the mechanism used by T3SS1 to induce rapid cytotoxicity.

T3SS1-Induced Cytotoxicity Does Not Depend on Caspase Activation

Cells infected with *V. parahaemolyticus* exhibit morphology consistent with apoptotic death, including cell rounding and nuclear shrinkage **(Figure 10; F-J)** (Thorburn, 2008). This phenotype resembles that seen for cells infected with *Yersinia pseudotuberculosis* (YP126), an extracellular bacterium that induces apoptosis in infected cells **(Figure 10; K-O)** (Monack et al., 1997). To test whether *V. parahaemolyticus* induces cell death by apoptosis, we assayed infected

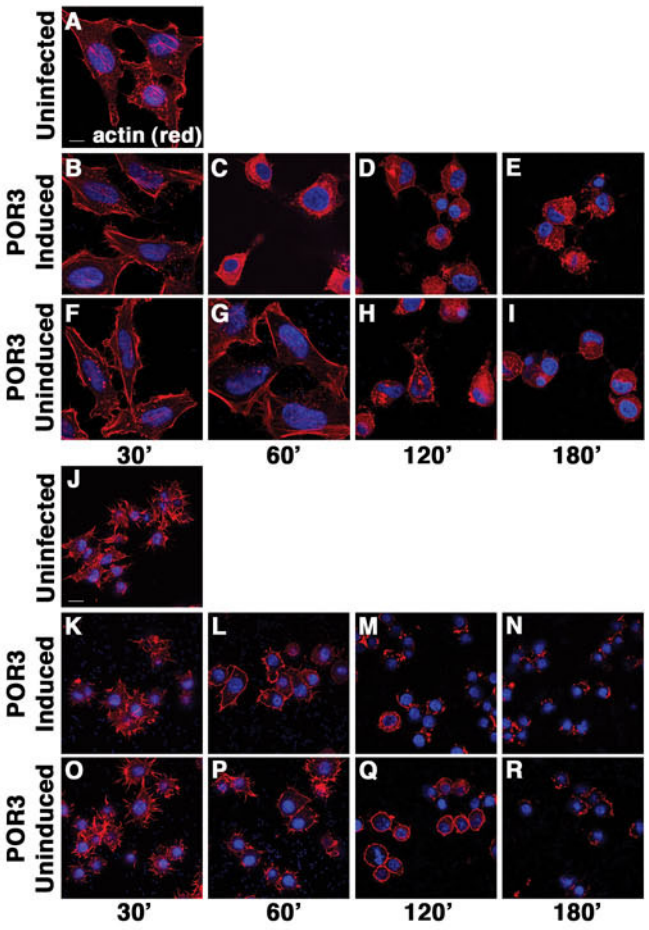

Figure 9. POR3 infection under T3S-inducing conditions accelerates T3SS1-dependent cytotoxicity. **(A–I)** HeLa cells were infected with POR3 grown under T3S-inducing conditions **(B–E)** or with POR3 grown at 30°C overnight **(F–I)** and compared with the uninfected control **(A)**. **(J–R)** RAW 264.7 cells were infected and visualized as described for HeLa cells **(K–R)** and compared with uninfected cells **(J)**. Cells were fixed and stained for confocal microscopy. Scale bar represents 10μm.

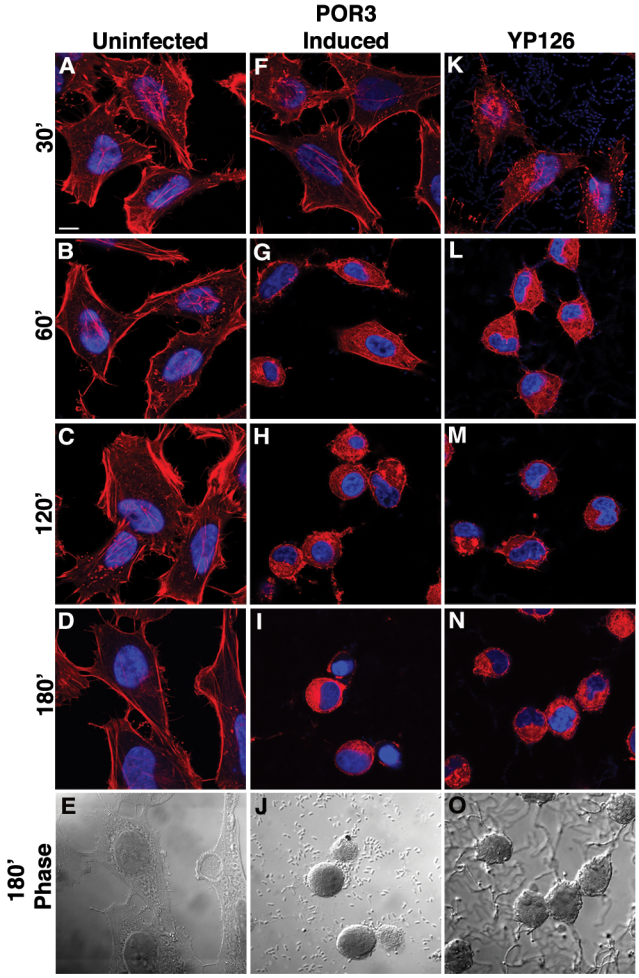

Figure 10. POR3 infection induces rapid cytotoxicity in HeLa cells. POR3 and YP126 grown in T3S-inducing conditions were used to infect HeLa cells. Cells were mock infected **(A-E)**, infected with induced POR3 **(F-J)** or with YP126 **(K-O)**. Cells were visualized using confocal microscopy. Scale bar represents 10µm.

RAW 264.7 macrophages for the activation of caspases. Although caspase activity is elevated in YP126-infected or staurosporine-treated cells, POR3 infected macrophages did not show any evidence of caspase 3/7 activation **(Figure 11A)**. In addition, PARP (poly-ADP ribose polymerase), a downstream target of caspase 3, is cleaved in staurosporine-treated cells or *Yersinia*-infected cells **(Fig 11B; lanes 7-9 and 10-12, respectively)**, but not in POR3-infected cells **(Fig 11B; lanes 4-6)**. Based on these observations, we conclude that POR3-induced cytotoxicity is independent of apoptotic machinery.

POR3-Induced Cytotoxicity Leads to Release of Cellular Contents

Apoptosis causes a non-inflammatory cell death, in contrast to other forms of cell death, such as necrosis, that are highly inflammatory (Festjens et al., 2006). To investigate the mechanism of T3SS1-induced cellular death, we analyzed whether infection by the POR3 strain causes pro-inflammatory cell lysis and release of cellular contents during infection. We observed elevated levels of cytoplasmic LDH release into the media during infection with the POR3 strain, indicating that the integrity of the host cell membrane is being compromised **(Figure 11C)**. As expected,

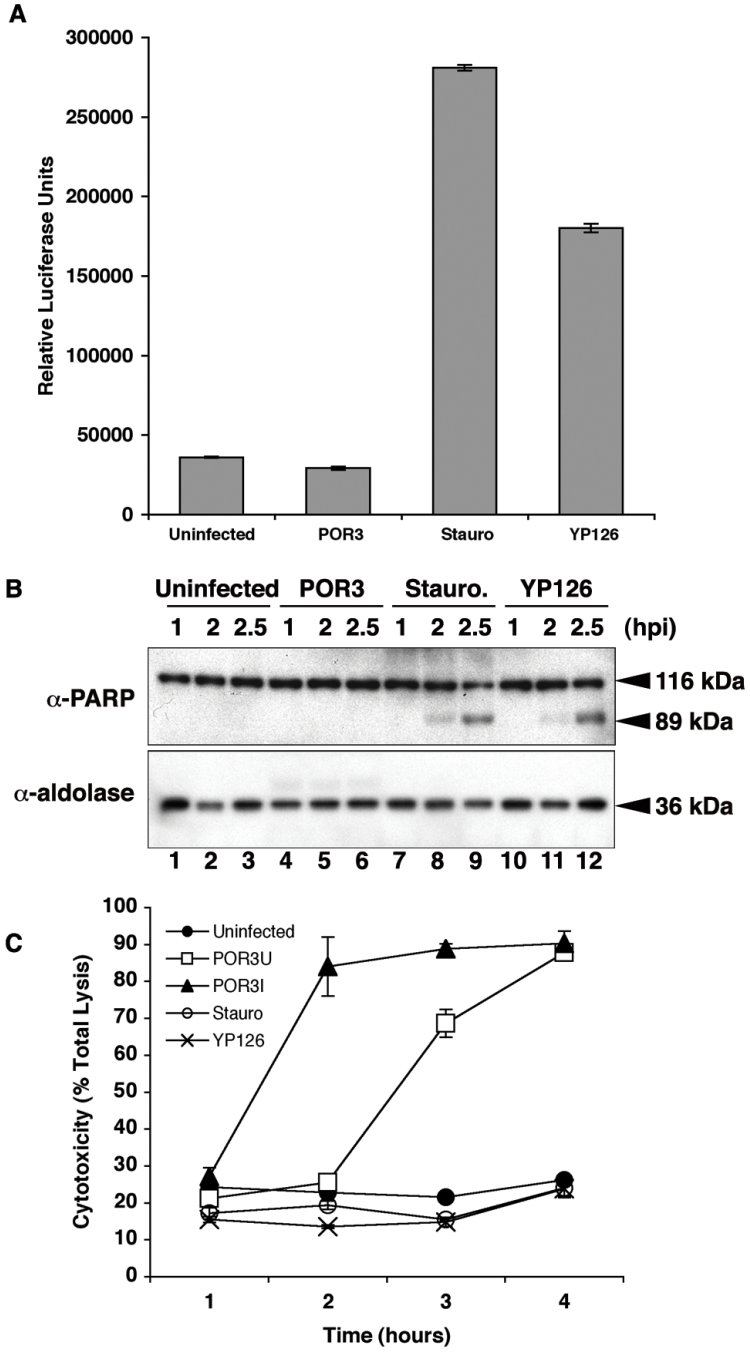
A
300000
250000
200000
150000
100000
50000
0
Relative Luciferase Units
Uninfected
POR3
Stauro
YP126
B
Uninfected
POR3
Stauro.
YP126
1 2 2.5 1 2 2.5 1 2 2.5 1 2 2.5 (hpi)
α-PARP
116 kDa
89 kDa
α-aldolase
36 kDa
1 2 3 4 5 6 7 8 9 10 11 12
C
Uninfected
POR3U
POR3I
Stauro
YP126
Cytotoxicity (% Total Lysis)
100
90
80
70
60
50
40
30
20
10
0
1
2
3
4
Time (hours)

Figure 11. T3SS1-dependent cytotoxicity is not caused by apoptosis. **(A)** Caspase 3/7 activation was examined by the Caspase-Glo assay. RAW 264.7 macrophages were mock infected or infected with POR3 for 2.5 hours. Cells were treated with 1μM staurosporine (staur) or infected with YP126 as positive controls. After infection, cells were lysed and normalized for protein content. Caspase 3/7 activation was measured by luminescence. **(B)** RAW 264.7 macrophage cells were treated identically as above (Mock, lanes 1-3; POR3, lanes 4-6; Stauro., lanes 7-9; or YP126, lanes 10-12). Cells were lysed at the indicated time points in PARP sample buffer, separated by SDS-PAGE, and immunoblotted with anti-PARP antibody or with anti-aldolase antibody to confirm equal loading. **(C)** Cytotoxicity of RAW 264.7 macrophages was measured by LDH release. Cells were infected over a time-course with POR3 grown in T3S-inducing conditions (▲) or in non-inducing conditions (□). Cells were either Mock infected (●), infected with YP126 (×) or treated with 1μM staurosporine (○) as controls. Cytotoxicity was calculated as a percent of total lysis of cells lysed in Triton X-100.

cells induced for apoptotic death with Yersinia infection or staurosporine treatment exhibited no increase in LDH release **(Figure 11C)**. Furthermore, analysis of LDH release in the presence of 5mM glycine did not effect the levels of LDH released from POR3-infected cells, thereby, eliminating necrosis as a possible mechanism for cell death (data not shown) (Brennan & Cookson, 2000, Dong *et al*., 1997, Fink & Cookson, 2006, Festjens et al., 2006). Consistent with our previous findings on cytotoxicity, the induced POR3 strain caused LDH release faster than the uninduced POR3 strain **(2 and 3 h, respectively, Figure 11C)**. In total, these results support the hypothesis that *V. parahaemolyticus* T3SS1-mediated cytotoxicity is not caused by apoptosis and that the infection is proinflammatory due to the release of cellular contents.

Vibrio parahaemolyticus Infection Rapidly Induces T3SS1-Dependent Autophagy

Autophagy is a cellular pathway that has been linked to cell fate and involves the sequestration of cytoplasmic contents in double-membrane autophagosomes that are delivered to lysosomes for degradation (Levine & Yuan, 2005, Thorburn, 2008). To examine the potential role of autophagy in T3SS1-dependent cytotoxicity, we monitored

a marker of autophagic vesicle formation, LC3 (microtubule associated light chain 3), using microscopic and biochemical indicators (Kabeya et al., 2000). Induction of autophagy results in incorporation of LC3 into autophagic vesicles (Kabeya et al., 2000). We generated a stable GFP-LC3 expressing HeLa cell line to assess the formation of autophagic vesicles by fluorescent microscopy (Kabeya et al., 2000). As a positive control, cells were starved in the presence of protease inhibitors to activate autophagy. Over the course of 3h, GFP-LC3 punctae accumulated slowly in starved cells to levels above those in untreated cells **(Figure 12; G-I and A-C, respectively)**. By contrast, the formation of autophagic vesicles in POR3-infected cells was rapid, occurring within one hour after infection and increasing dramatically over the next two hours **(Figure 12; D-F)**. To confirm that cells infected with the POR3 strains were inducing autophagy, the infected cells were analyzed by electron microscopy. The POR3-infected cells contained multiple autophagic vesicles that had engulfed cytoplasm, organelles, membranes, and smaller vesicles **(Figure 12; J-M)**.

To test T3SS1-dependent activation of autophagy further, we used a biochemical indicator for autophagy that monitors a posttranslational

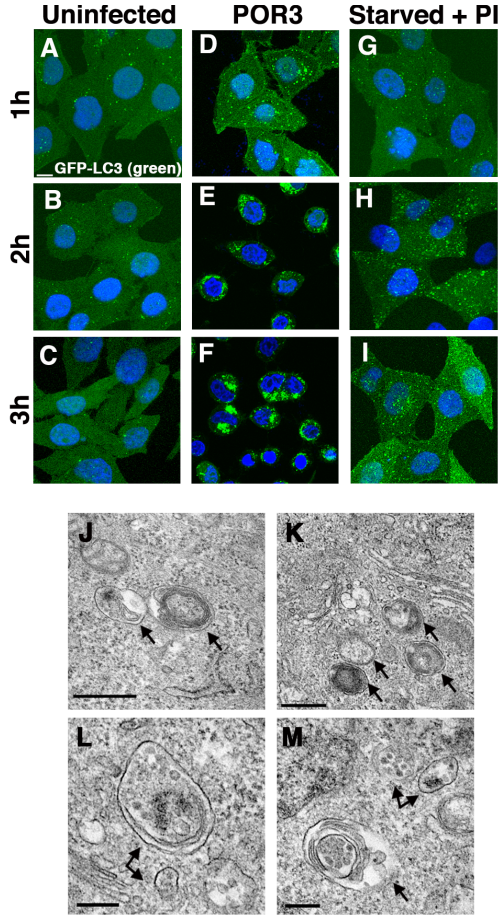
Uninfected
POR3
Starved + PI
1h
2h
3h
A
B
C
D
E
F
G
H
I
GFP-LC3 (green)
J
K
L
M

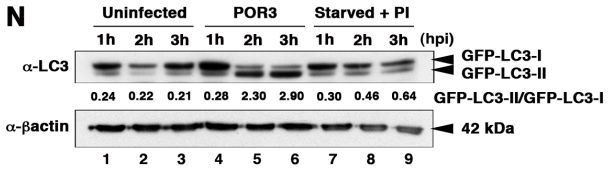
N
Uninfected
POR3
Starved + PI
1h 2h 3h 1h 2h 3h 1h 2h 3h (hpi)
α-LC3
GFP-LC3-I
GFP-LC3-II
0.24 0.22 0.21 0.28 2.30 2.90 0.30 0.46 0.64
GFP-LC3-II/GFP-LC3-I
α-βactin
42 kDa
1 2 3 4 5 6 7 8 9

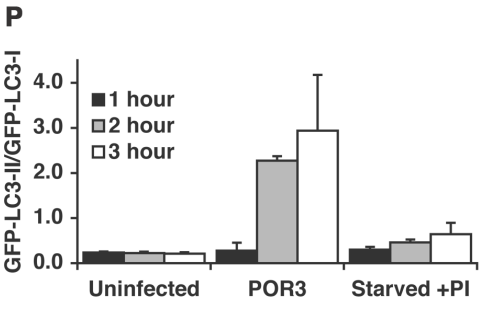
P
GFP-LC3-II/GFP-LC3-I
4.0
3.0
2.0
1.0
0.0
1 hour
2 hour
3 hour
Uninfected
POR3
Starved +PI

Figure 12. *V. parahaemolyticus* induces autophagy. **(A-F)** GFP-LC3 HeLa cells were plated on coverslips and either Mock infected **(A and B)**, POR3 infected for 2 hours **(C and D)** or starved for 4 hours in the presence of protease inhibitors **(E and F)**. Samples were prepared for microscopy. Scale bar represents 10μm. **(G)** POR3 was grown in T3S-inducing conditions and used to infect HeLa cells for 1 hour. Mock and POR3 infected cells were fixed and prepared for electron microscopy. **(H)** HeLa cell lines were stably transfected with pIRESneo3-GFP-LC3 expressing a GFP-LC3 fusion protein and maintained under G418 selection. Cells were either left untreated **(Mock infected, lanes 1-3)**, infected with *V. parahaemolyticus* **POR3 (lanes 4-6)**, or starved with HBSS in the presence of 10μg/mL protease inhibitors **(Starved, lanes 7-9)**, for 1, 2, and 3 hours. Samples were immunoblotted with anti-LC3 antibody and anti-β-actin antibody to confirm equal loading. **(I)** Relative LC3-II accumulation was determined by quantitating band intensity and calculating the ratio of LC3-II to LC3-I. Black, gray, and white bars correspond to 1, 2, and 3 hour timepoints, respectively.

modification of LC3. Cytosolic LC3 (LC3-I) is targeted to newly forming autophagosomes by lipidation with phosphatidylethanolamine via an ubiquitin-like conjugation system, resulting in the formation of membrane-associated LC3-II (Kabeya *et al.*, 2004, Kabeya et al., 2000). In a cell line stably expressing a GFP-tagged LC3, LC3-II accumulates slowly during amino acid starvation in the presence of lysosomal protease inhibitors, as evidenced by the production of the more rapidly migrating LC3-II in SDS/PAGE **(Figure 12; lanes 7–9, and P)**. In cells infected with uninduced POR3 strain, GFP-LC3-II accumulates rapidly within 1 h and continues to be the dominant form throughout infection **(Figure 12; lanes 4–6, and P)**. These studies parallel the timing of our microscopic observations of punctae formation **(Figure 12; A–I)** and autophagic vesicle accumulation **(Figure 12; J–M)**. Consistent with our hypothesis that autophagy depends on T3SS1, only the POR1 and POR3 strains induce conversion of LC3, whereas a T3SS1-negative strain (POR2) does not **(Figure 13)**. Our microscopic and biochemical studies support the hypothesis that infection with *V. parahaemolyticus* induces acute and rapid autophagy before the release of cellular contents, because the accumulation of GFP-LC3 punctae and the conversion of LC3-I to LC3-II

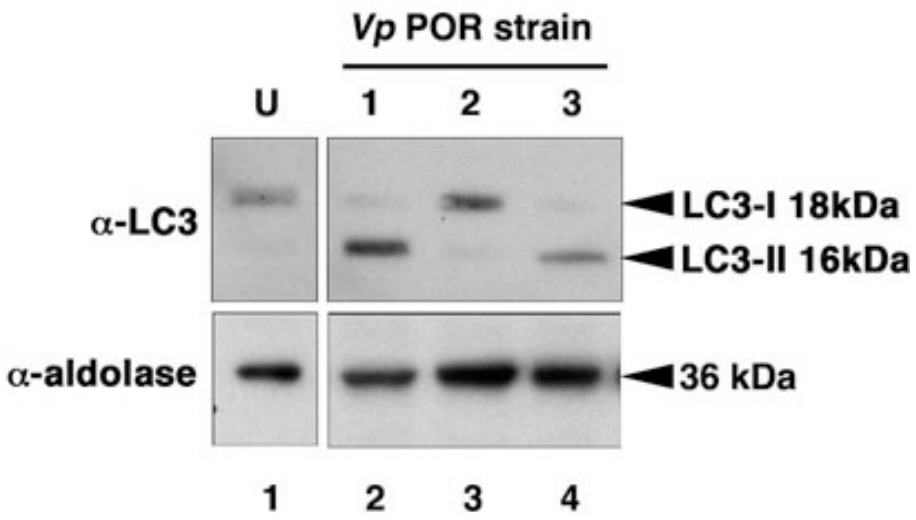

Figure 13. Induction of autophagy depends on T3SS1. HeLa cells were left uninfected **(lane 1)**, or infected with *V. parahaemolyticus* POR1 **(lane 2)**, POR2 **(lane 3)**, or POR3 **(lane 4)** for 2 h. Samples were immunoblotted with anti-LC3 antibody and probed with anti-aldolase antibody to confirm equal loading.

(Figure 12) precede the release of LDH **(Figure 11C)** during infection with the uninduced POR3 strain.

Inhibitors of PI3-Kinase Prevent T3SS1-Induced Autophagy but Not Cell Death.

An early step in the autophagy pathway involves the activation of PI3-kinases, and treatment of starved cells with PI3-kinase inhibitors prevents autophagy (Petiot *et al.*, 2000). We used the PI3-kinase inhibitor wortmannin to test whether *V. parahaemolyticus* induces autophagy using known cellular mechanisms (Powis et al., 1994). Treatment of infected cells with wortmannin inhibits autophagy in *V. parahaemolyticus*–infected cells, as indicated by a dramatic reduction of GFP-LC3 punctae **(Figure 14F)**. Coincident with the decrease in punctae, we observe a decrease in LC3-II accumulation **(Figure 14; G and H; lanes 2 and 5)**. Based on these studies, we predict that acute T3SS1-induced activation of autophagy occurs proximal to, or at the point of, the activation of PI3-kinases. The treatment with this PI3 kinase inhibitor did not rescue the infected cells from death, because the activation of signaling pathways by other T3SS effectors that cause cell rounding and lysis and are not

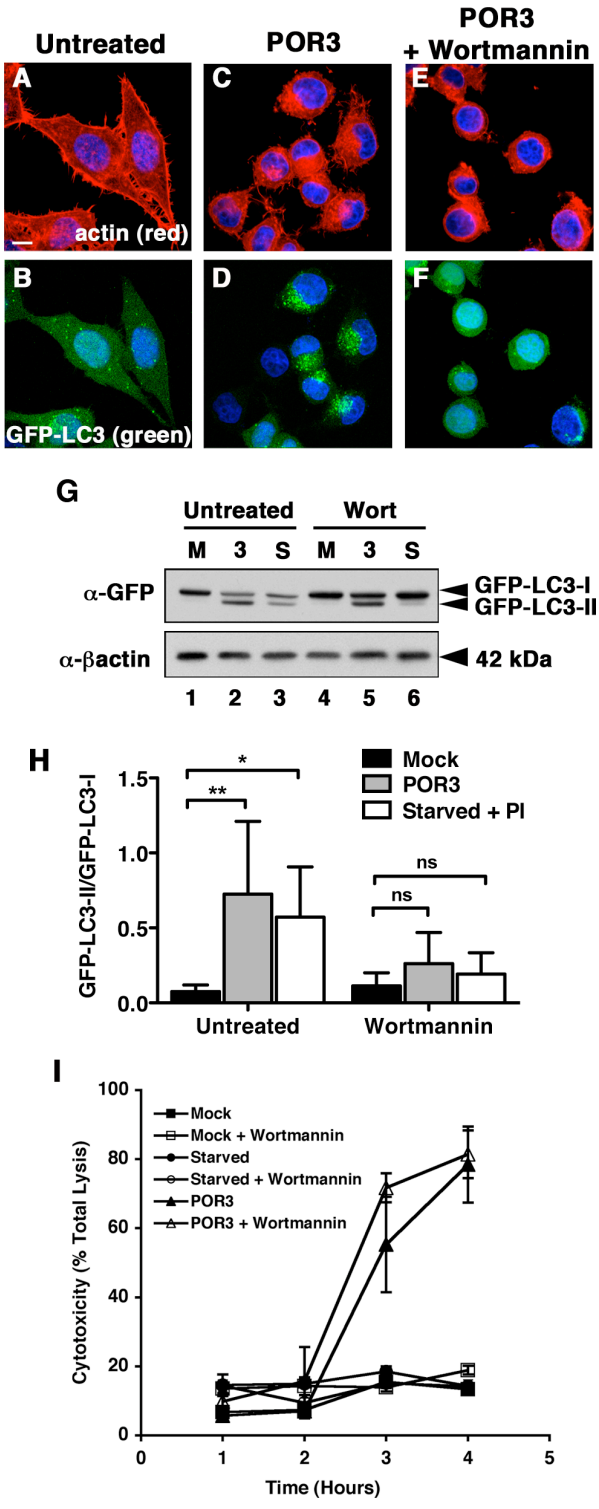
Untreated
POR3
POR3
+ Wortmannin
A
C
E
actin (red)
B
D
F
GFP-LC3 (green)
G
Untreated
Wort
M 3 S M 3 S
α-GFP
GFP-LC3-I
GFP-LC3-II
α-βactin
42 kDa
1 2 3 4 5 6
H
Mock
POR3
Starved + PI
GFP-LC3-II/GFP-LC3-I
1.5
1.0
0.5
0.0
*
**
ns
ns
Untreated
Wortmannin
I
Mock
Mock + Wortmannin
Starved
Starved + Wortmannin
POR3
POR3 + Wortmannin
Cytotoxicity (% Total Lysis)
100
80
60
40
20
0
0 1 2 3 4 5
Time (Hours)

Figure 14. Inhibitors of PI3-kinase prevent *V. parahaemolyticus*-induced autophagy. **(A-F)** GFP-LC3 HeLa cells were Mock infected **(A and B)** or POR3 infected in the absence **(C and D)** or presence of 10μM wortmannin **(E and F)** for 2 hours. Cells were visualized using confocal microscopy. Scale bar represents 10μm. **(G)** HeLa cells were either left untreated **(M, lanes 1 and 4)**, infected with POR3 **(3, lanes 2 and 5)**, or starved in the presence protease inhibitors **(S, lanes 3 and 6)** in the absence **(lanes 1-3)** or presence of 10μM wortmannin **(lanes 4-6)** for 2 hours. Samples were immunoblotted with anti-LC3 antibody and anti-β-actin antibody to confirm equal loading. **(H)** Relative LC3-II accumulation was determined by quantitating band intensity and calculating the ratio of LC3-II to LC3-I. Mock, POR3 infected, and Starved + PI correspond to black, gray, and white bars respectively. **(I)** Cytotoxicity overtime of mock infected (■,□), starved (●, ❍) or POR3 infected (▲,△) HeLa cells in the absence (closed symbols) or presence of 10μM wortmannin (open symbols).

susceptible to this chemical inhibitor **(Figure 14; E and I)**.

Discussion:

Herein, we present a paradigm used by an extracellular pathogen, *V. parahaemolyticus*, to induce cell death methodically and efficiently. This process is independent of classical apoptotic machinery. We observe a multifaceted phenotype in infected cells by which multiple, albeit temporally orchestrated, mechanisms eventually culminate in the efficient death of host cells within hours of infection **(Figure 15)**. Upon infection, we observe the T3SS1-mediated activation of autophagy, both microscopically and biochemically **(Figure 15B)**. We then observe a dramatic rounding of the host cell, undoubtedly caused by changes in the cytoskeleton of the infected cell **(Figure 15C)**. After both of these steps, we observe the release of cellular contents **(Figure 15D)**. We propose that *V. parahaemolyticus* could use T3SS1 to mediate this multifaceted mechanism both to capitalize on the release of these nutrients **(Figure 15E)** and to defend itself against phagocytosis by immune cells responding to proinflammatory signals at the site of infection **(Figure 15F)**. T3SS1 is found in both environmental and pathogenic strains of *V.*

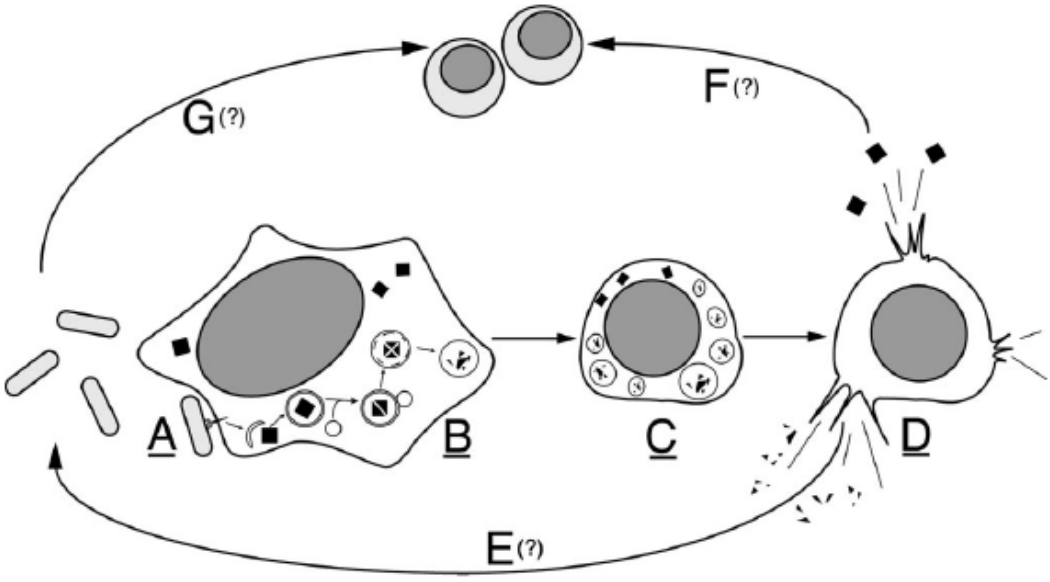

Figure 15. *V. parahaemolyticus* induces a series of events that culminates in the efficient death of host cells. **(A)** *V. parahaemolyticus* uses a T3SS to inject effectors into a host cell during infection. **(B)** Infection results in the rapid induction of autophagy and the formation of autophagosomes. **(C)** Next, we observe rounding and shrinkage of the infected host cell. **(D)** Rounding and shrinking is followed by cell lysis and release of cellular contents. **(E)** We hypothesize that lysis will lead to the release of degraded proteins that can be used by the bacteria for nutrients. **(F)** In addition, the release of inflammatory contents will cause recruitment of innate immune cells, such as macrophages. **(G)** *V. parahaemolyticus* also can target and kill these immune cells, thereby evading an innate immune response. Underlined letters denote mechanisms that have been demonstrated experimentally herein. Letters with question marks denote events that are hypothesized to occur as a result of these mechanisms.

parahaemolyticus (Makino et al., 2003). During infection of an incidental host, such as humans, this type of acute death induced by T3SS1 could work in favor of the pathogen. Similarly, *V. parahaemolyticus*' survival in the environment might be secured by its ability to hijack nutrients from other living cells or, possibly, to evade phagocytosis. A small number of effectors are associated with the T3SS1 (VopQ, VopR, VopS, and VPA450), and these effectors have no homology to any proteins of known function. However, it is predicted that orthologues of some of these effectors will be found in other *Vibrio* species. Thus, it is likely that this mechanism of cell death is an example of a more general mechanism that is used by other bacteria. Autophagy is a pathway used by cells in response to stress, such as nutrient deprivation, to survive (Levine & Yuan, 2005). This pathway also functions in both innate and adaptive immunity (Levine & Deretic, 2007). It has been shown to play a protective role in defense against intracellular pathogens such as *Mycobacterium tuberculosis*, *Shigella spp.*, and many others (Levine & Kroemer, 2008). A host cell can use autophagy to prevent the cytoplasmic replication or invasion of intracellular pathogens by engulfing the pathogens in autophagic vesicles and targeting them to lysosomes (Levine & Deretic, 2007). In addition, recent work has shown that autophagy may provide

defense against a secreted toxin from the noninvasive pathogen *Vibrio cholerae* (Gutierrez et al., 2007). Alternatively, pathogens have evolved ways to usurp this pathway for their own benefit: for example, the intracellular pathogen *Coxiella burnettii* creates a replicative niche within autophagosomes where it can multiply and survive (Kirkegaard et al., 2004). In contrast, *Shigella flexneri* disrupts phagocytosis and escapes into the cytosol. The pathogen then avoids clearance by autophagy through the type III secretion of an effector protein IscB, preventing recruitment of Atg5, a protein necessary for autophagy (Ogawa et al., 2005). In the case of *V. parahaemolyticus*, nutrients released by the infected cell could be used by the pathogen to support its own proliferation. Alternatively, this extracellular pathogen might benefit from inducing autophagy because common intracellular machinery that is used for both autophagy and phagocytosis might be directed away from the host cell membrane, thereby crippling phagocytosis in the infected host cell (Sanjuan et al., 2007). Pathogens use a wide variety of mechanisms to exploit a host cell during infection. Herein, we have described a paradigm whereby an infected cell is directed by a T3SS to induce autophagy and cause cell rounding and release of its cellular contents. We observe that inhibition of autophagy does not prevent the eventual death

of the infected cell. This result in not surprising in light of what is known about the redundant mechanisms used by T3SSs. For example, *Yersinia spp.* disables the actin cytoskeleton in the host cell by using at least four different mechanisms (Navarro et al., 2005). We have observed that in the *V. parahaemolyticus* T3SS1 multiple mechanisms are used to compromise cell integrity, thereby ensuring the demise of the infected host cells. Future studies of the molecular targets that are hijacked by the effectors secreted by *V. parahaemolyticus* T3SS1 will provide further insight into this orchestrated host-cell death.

Chapter 5

Vibrio VopQ Induces PI3-Kinase Independent Autophagy and Antagonizes Phagocytosis

Introduction:

V. parahaemolyticus is a halophillic bacterium commonly found in marine and estuarine environments (Daniels et al., 2000). Infections with *V. parahaemolyticus* arise from the consumption of raw or undercooked shellfish and typically result in gastroenteritis. Wound infections can result from handling contaminated products. In rare cases, when the infection becomes systemic, it can be life threatening to individuals with pre-existing health conditions or to those that are immune-compromised (Morris, 2003, Daniels et al., 2000, Nair et al., 2007). *V. parahaemolyticus* is endemic to Southeast Asia where consumption of seafood is high. However, this bacterium has become an increasing health concern as isolates have been detected along the western and eastern U.S. seaboards as well as the Gulf Coast (Daniels et al., 2000, Morris, 2003). *V. parahaemolyticus* proliferates in warmer temperature waters and consequently, shellfish harbor high bacterial titers in summer months (Kaneko & Colwell, 1975,

Colwell, 1973, Kaysner *et al.*, 1990, DePaola et al., 1990). As global warming causes ocean temperatures to rise, *V. parahaemolyticus* gains access to marine and estuarine environments previously inaccessible due to colder temperatures, thus creating new niches for habitation and colonization (Shope, 1991, McLaughlin *et al.*, 2005).

The most well studied virulence factors of *V. parahaemolyticus* are the TDH and the TRH (Park et al., 2004b, Miyamoto et al., 1969, Fukui et al., 2005). However, strains in which the TDH and TRH are deleted are still cytotoxic in tissue culture models of infection (Park et al., 2004b, Liverman et al., 2007). Sequencing of the *V. parahaemolyticus* genome revealed the presence of two T3SS, one on chromosome I (T3SS1), and the other on chromosome II (T3SS2). T3SS1 is required for cytotoxicity in a tissue culture model of infection whereas T3SS2 has been associated with enterotoxicity in the rabbit ileal loop model of infection (Park et al., 2004b). Recent results from our lab demonstrate that T3SS1-mediated cytotoxicity is caspase independent and involves induction of autophagy followed by cell rounding and subsequent cell lysis (Burdette et al., 2008). This form of cell death is the first example of the induction and usurpation of autophagy by an extracellular pathogen and therefore research into

understanding this mechanism is valuable for understanding *V. parahaemolyticus* pathogenesis as a whole.

T3SS1 resembles the T3SS of *Yersinia* spp. in structure and organization except for a region of unknown homology (Park et al., 2004b). This region harbors genes (*vp1680*, *vp1683*, and *vp1686*) that encode for type-III effectors (VopQ, VopR, and VopS, respectively) and predicted cognate chaperones (Ono et al., 2006, Panina et al., 2005). Previous studies from our lab identified autophagy, cell rounding, and lysis as the mechanism of T3SS1-mediated cell death (Burdette et al., 2008). The cellular rounding induced has been correlated with the presence of VopS, this effector was shown to posttranslationally modify Rho-family GTPases with AMP. This modification, termed AMPylation, prevents the interaction of Rho-family GTPases with downstream signaling molecules impairing actin assembly and resulting in cell rounding (Yarbrough et al., 2009).

V. parahaemolyticus strains lacking VopS are still cytotoxic and able to induce autophagy indicating that another T3SS1-encoded effector is be responsible for mediating these effects during infection (Yarbrough et al., 2009). Herein, we analyze the role of VopQ in T3SS1-mediated cell death and show that this protein is necessary and sufficient for T3SS1-

mediated autophagy. VopQ induces autophagy during infection in a PI3-kinase-independent manner. Finally, electron microscopic analysis shows that POR3*ΔvopQ* infected cells have a high number of intracellular bacteria supporting our hypothesis that the induction of autophagy is affecting the ability of the cell to induce phagocytic machinery. To our knowledge, VopQ is the first bacterial type III effector identified to induce autophagy. We aim to not only understand the molecular mechanism of VopQ in the context of *V. parahaemolyticus* pathogenesis but also to use it as a tool to further our understanding of autophagy during infection.

Results:

VopQ is a Type III Secreted Effector Essential for T3SS1-mediated Cytotoxicity

To understand the role of VopQ during *V. parahaemolyticus* infection and in T3SS1-mediated cytotoxicity, we generated isogenic mutants of the *V. parahaemolyticus* T3SS1-encoded putative effector *vopQ*. Using antibodies against VopQ, secreted VopQ is detected in the POR3 strain and the complemented POR3*ΔvopQ* strain (POR3*ΔvopQ* + VopQ) **(Figure 16; lanes 1 and 3)** but is absent in the *ΔvopQ* strain

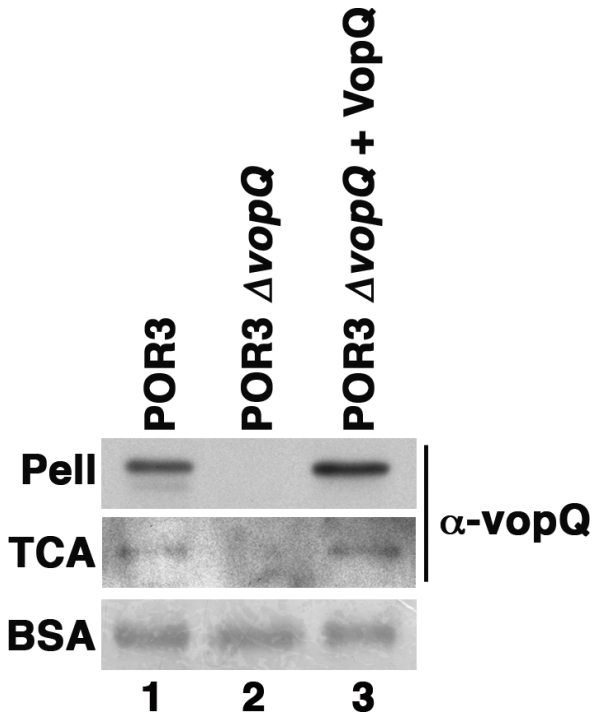

Figure 16. VopQ is a T3SS secreted effector protein. Overnight cultures of *V. parahaemolyticus* POR3 **(lane 1)**, POR3*ΔvopQ* **(lane 1)**, and POR3*ΔvopQ* + VopQ **(lane 3)** strains were diluted back into secretion inducing media and grown for 3 hours at 37°C. Anti-VopQ antibody was used to probe bacterial pellets and TCA-precipitated culture supernatants for the production **(PelI)** and secretion **(TCA)** of VopQ, respectively. The membrane of TCA-precipitated supernatants was stained with coomassie blue for BSA as a control for secretion **(BSA)**.

(POR3*ΔvopQ*) **(Figure 16; lane 2)**. Infection of HeLa cells with *V. parahaemolyticus* strains capable of secreting only from T3SS1 (POR3) results in cellular rounding by 2 hours and ultimate lysis by 3 hours compared to mock infected cells. However, HeLa cells infected with a POR3*ΔvopQ* strain show a delay in cell rounding **(Figure 17)**.

These phenotypic observations implicate VopQ in the induction of cytotoxicity. To test this, we used an LDH release assay to measure the ability of the POR3, POR3*ΔvopQ*, and POR3*ΔvopQ* + VopQ strains to induce cellular lysis over an 8 hour time course. Consistent with previous results, POR3 induced rapid cellular lysis, peaking at 4 hours post infection **(Figure 18; squares)**. However, the POR3*ΔvopQ* strain is severely attenuated in its ability to induce this lysis. The POR3*ΔvopQ* infected cells do ultimately release cellular contents, albeit at much later time points **(Figure 18; triangles)**. The complemented strain (POR3*ΔvopQ* + VopQ) is identical to POR3 in its ability to induce cytotoxicity **(Figure 18; diamonds)**. These results demonstrate that VopQ is a type III secreted effector that contributes to T3SS1-mediated cytotoxicity in a tissue culture model of infection.

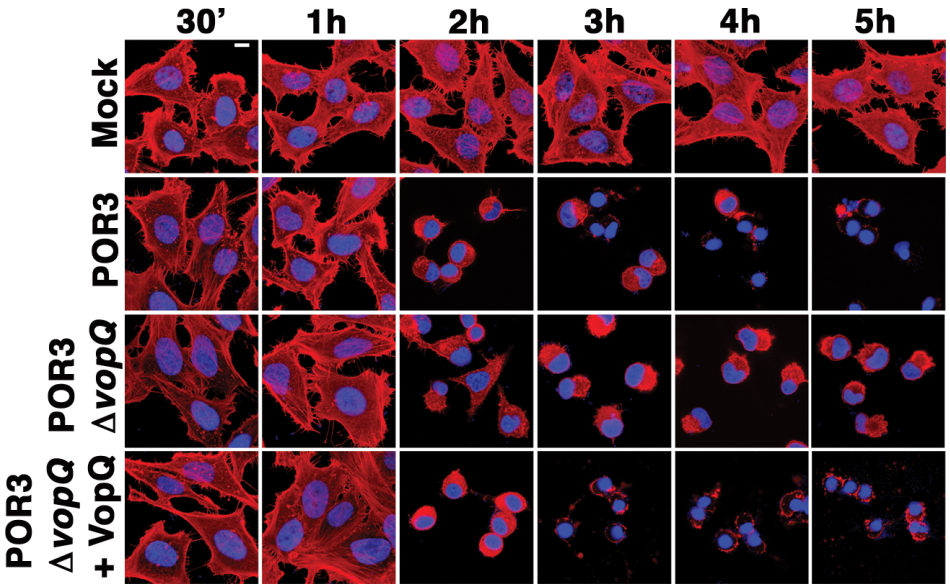

Figure 17. VopQ is a T3SS secreted effector protein required for cytotoxicity. HeLa cells were infected with *V. parahaemolyticus* strains POR3, POR3*ΔvopQ*, and POR3*ΔvopQ* + VopQ. At the indicated timepoints, cells were fixed and processed for confocal microscopy with rhodamine phalloidin to stain for actin (red) and Hoechst for nuclei (blue). Scale bar represents 10μm.

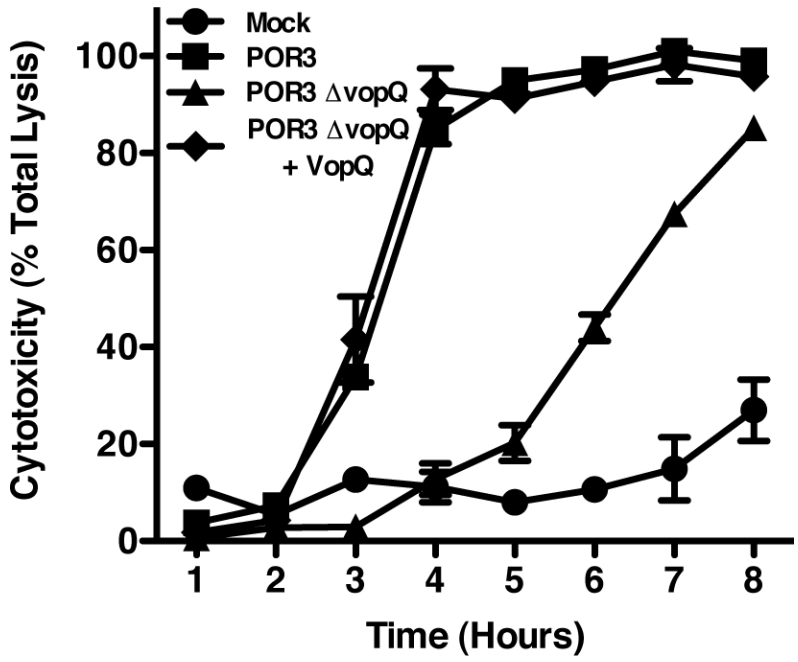

Figure 18. VopQ is a T3SS secreted effector protein required for cytotoxicity. HeLa cells were infected as described in Figure 17. At the indicated timepoints, culture supernatants were evaluated for the release of LDH as a measure of cytotoxicity and reflected as percent of total cellular lysis. Mock (●), POR3 (■), POR3 *ΔvopQ* (▲), and POR3 *ΔvopQ* + VopQ (◆).

VopQ is Necessary and Sufficient to Induce Autophagy

Autophagy is the process by which cells undergo bulk degradation of cytosolic contents under starvation conditions for the purpose of providing the cell with nutrients. Membranes form around cytosolic contents, including subcellular organelles, forming autophagosomes. These autophagosomes are targeted to, and ultimately fuse with, lysosomes where resident proteases digest the contents. Nutrients are recycled back into the cell to fend off starvation (Mizushima et al., 2008). This highly regulated process can be monitored both by biochemistry and microscopy (Klionsky et al., 2007). Microtubule-associated protein light chain 3 (LC3) is a marker of autophagy that, under normal conditions, resides in the cytosol (LC3-I). Upon induction of autophagy, LC3-I is processed and conjugated to PE forming LC3-II that now associates with forming autophagosomal membranes (Kabeya et al., 2000, Levine & Yuan, 2005). The GFP-tagged PE-conjugated form of LC3 (GFP-LC3-II) appears by fluorescence microscopy as punctate dots corresponding to forming autophagosomes during starvation. Using a HeLa cell line stably expressing GFP-LC3, we can follow induction of autophagy by conversion of GFP-LC3-I to GFP-LC3-II by Western blot analysis and by the formation of GFP-LC3 punctae via fluorescence microscopy (Kabeya et al., 2000).

To elucidate whether VopQ plays a role in the induction of autophagy, we infected GFP-LC3 HeLa cells with various strains of *V. parahaemolyticus*. Consistent with previous observations, we see an increase in LC3-II formation in starved cells or cells infected with POR3 **(Figure 19A; lane 2 and 3, respectively and Figure 19B)** (Burdette et al., 2008). By contrast, infection with the POR3*ΔvopQ* strain did not result in conversion of LC3-I to LC3-II **(Figure 19A; lane 4, and Figure 19B)**. An absence of LC3-II formation correlates to reduced GFP-LC3 punctae in *ΔvopQ* infected cells compared to starved or POR3 infected cells **(Figure 19C)**. GFP-LC3 punctae are absent up to 5 hours post infection in POR3*ΔvopQ* -infected cells **(Figure 20)**. These results show that T3SS1-dependent autophagy requires the type III effector VopQ.

In order to demonstrate VopQ alone is sufficient to induce autophagy, GFP-LC3 HeLa cells were microinjected with recombinant purified VopQ or GST as a control. Texas-Red conjugated dextran was co-injected to identify the injected cells. Following injection, these marked cells were monitored for the appearance of GFP-LC3 positive punctae. In control injected cells, the GFP-LC3 signal remained diffuse and cytoplasmic **(Figure 21A)**. However, VopQ injection showed GFP-LC3-

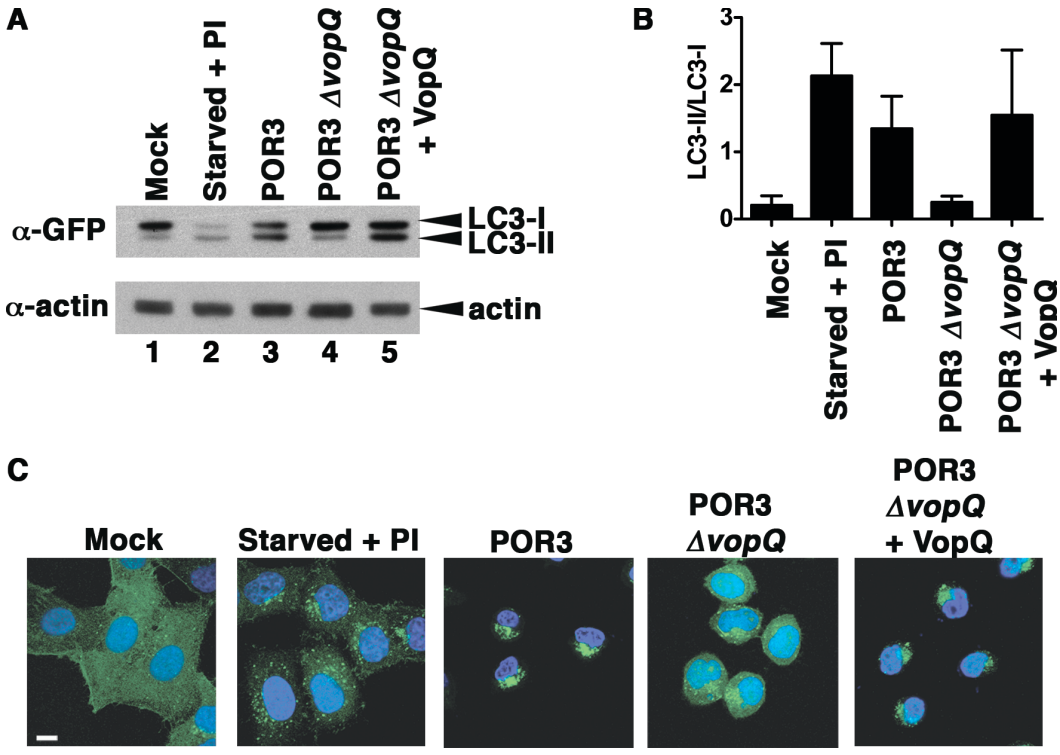

Figure 19. VopQ is necessary for T3SS1-mediated induction of autophagy. **(A)** GFP-LC3 HeLa cells were either mock infected **(lane 1)**, starved with protease inhibitors **(lane 2)**, or infected with POR3, POR3*ΔvopQ*, and POR3*ΔvopQ* + VopQ **(lanes 3, 4, and 5)** and lysates were probed with anti-GFP and anti-bactin antibodies. **(B)** Relative LC3-II accumulation was determined as described in Materials and Methods. The data are the means SD from three independent experiments. **(C)** GFP-LC3 HeLa cells were infected as described in **(A)** and processed for confocal microscopy with staining for Hoechst for nuclei (blue) and visualized for GFP-LC3 punctae formation (green). Scale bar represents 10μm.

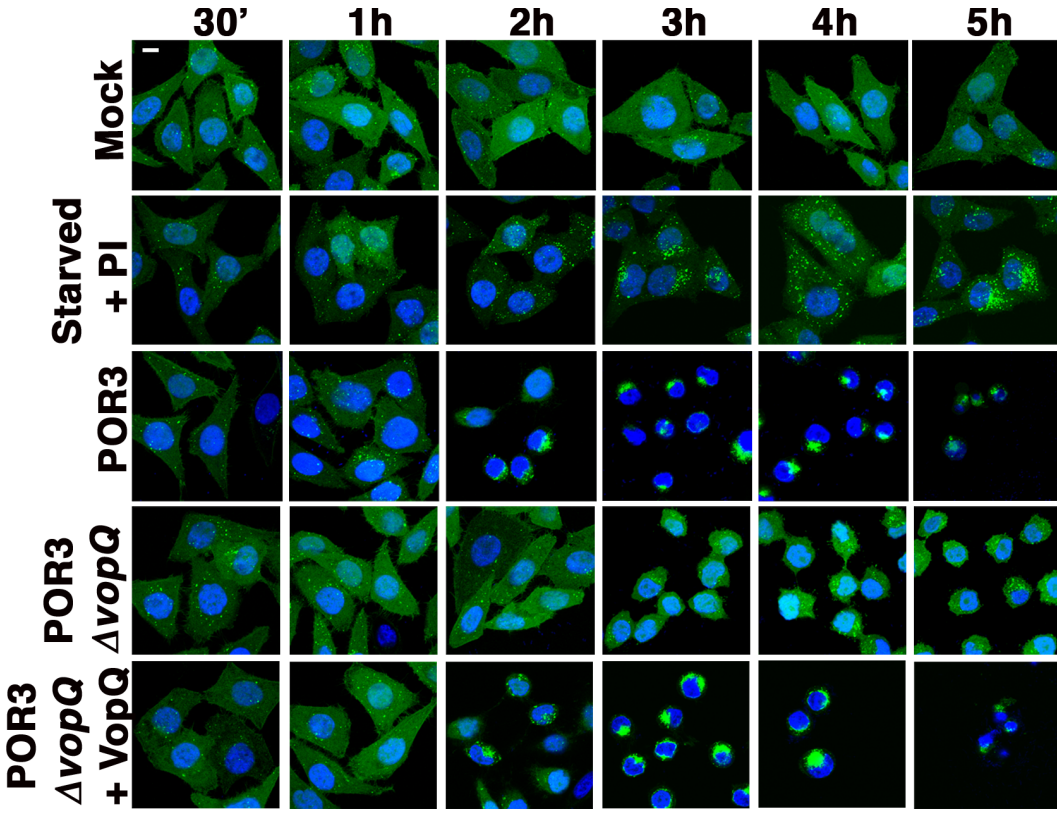

Figure 20. VopQ is essential for T3SS1-mediated induction of autophagy over time. GFP-LC3 HeLa cells were either mock infected, starved in the presence of protease inhibitors, or infected with POR3, POR3*ΔvopQ*, or POR3*ΔvopQ* + VopQ. At the indicated time points, cells were fixed and the nuclei were stained with Hoechst (blue). Slides were imaged using confocal microscopy for the presence of GFP-LC3 punctae (green). Scale bar represents 10μm.

positive punctae after 30 minutes **(Figure 21A)**. To analyze whether these GFP-positive punctae were induced via the classic PI3-kinase dependent autophagy pathway, GFP-LC3 cells were pretreated with the PI3-kinase inhibitors 3-MA or wortmannin. These inhibitors are competent in their ability to inhibit autophagy as seen with, rapamycin, a TOR kinase inhibitor and inducer of autophagy **(Figure 22)**. The VopQ-mediated GFP-LC3 punctae formation appears to be independent of PI3-kinase activation because treatment with these inhibitors had no effect on the ability of VopQ to induce punctae formation **(Figure 21B)**. Based on our molecular microbiology studies with the POR3*ΔvopQ* deletion strain and our cell biology studies with purified recombinant protein, we propose that VopQ is both necessary and sufficient to induce autophagy during *V. parahaemolyticus* infection.

VopQ Induces Autophagy Independent of PI3-kinases

Incubation of GFP-LC3 HeLa cells with the PI3-kinase inhibitors 3-MA or wortmannin prior to microinjection does not abrogate punctae formation **(Figure 21B)**. In addition, despite the fact that treatment of GFP-LC3 cells with wortmannin during infection abrogates GFP-LC3 punctae

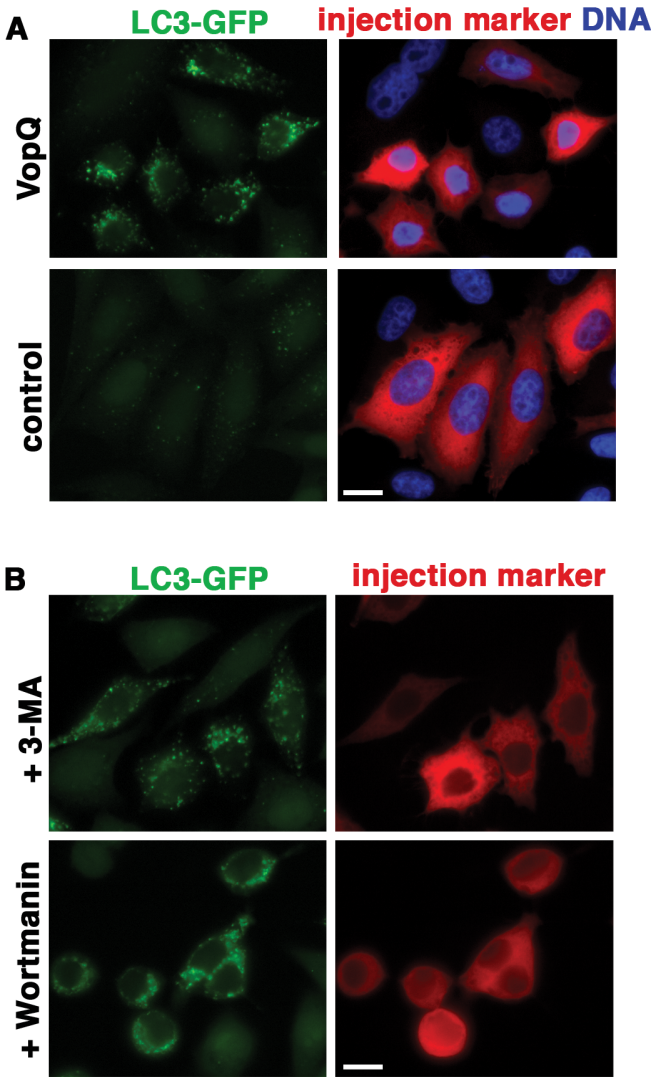

Figure 21. VopQ is sufficient for T3SS1-mediated induction of autophagy. GFP-LC3 HeLa cells were microinjected with either recombinant 0.5 mg/ml GST (control) or rHis$_6$-VopQ (VopQ) along with Texas-Red dextran as an injection marker. Cells were either left untreated **(A)** or preincubated with PI3-kinase inhibitors 3-MA (10mM) and wortmannin (10μM) for 30 minutes prior to injection and throughout the duration of the experiment **(B)**. Cells were fixed at 30 minutes post injection and DNA was stained with Hoechst. Red, Texas-Red dextran injection marker; blue, DNA; green, GFP-LC3. Scale bar represents 15 μm.

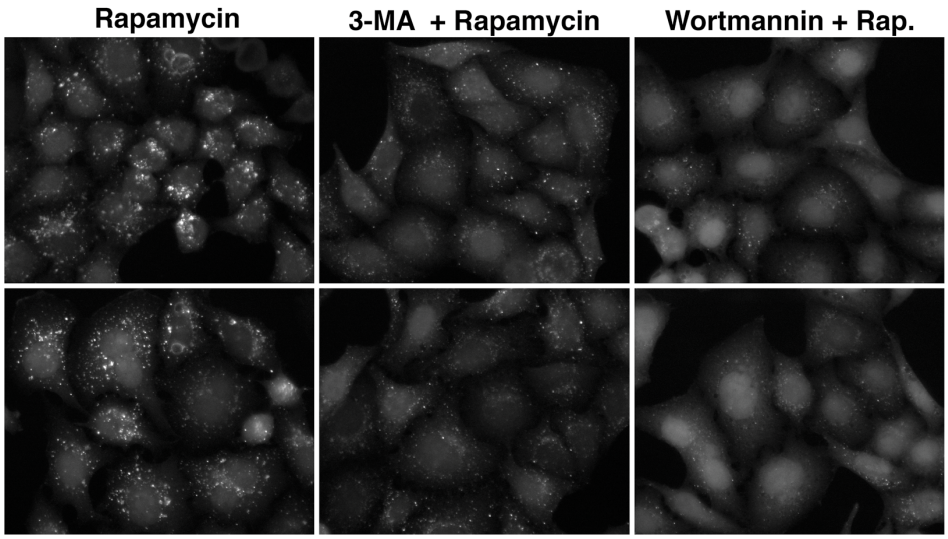

Figure 22 The PI3-kinase pathway in GFP-LC3 HeLa cells is functional. GFP-LC3 HeLa cells were pretreated with the PI3-kinase inhibitors 3-MA (10mM) and wortmannin (10μM) for 30 minutes prior to induction of autophagy for 4 hours with 1μg/ml of rapamycin in the absence or presence of 3-MA (10mM) and wortmannin (10μM). Scale bar represents 20 μm.

formation, some punctae remain. This suggests that during *V. parahaemolyticus* infection, autophagy is proceeding by both a PI3-kinase-dependent (wortmannin-sensitive) and PI3-kinase-independent (wortmannin-insensitive) pathway. We hypothesize that VopQ is inducing autophagy via a PI3-kinase-independent mechanism. To address this, we infected GFP-LC3 HeLa cells with POR3 or POR3*ΔvopQ* in the absence or presence of wortmannin treatment **(Figure 23)**. Wortmannin-treated POR3-infected cells or untreated POR3*ΔvopQ*-infected cells show less punctae accumulation relative to untreated cells and untreated POR3-infected cells consistent with previous data **(Figure 23; A, B, and C)** (Burdette et al., 2008). In contrast, wortmannin treatment combined with infection with POR3*ΔvopQ* strains almost completely abrogates GFP-LC3 punctae formation **(Figure 23A)**. Analysis of GFP-LC3-II conversion by Western blot supports our microscopic observations **(Figure 23; B and C)**. These results are consistent with our hypothesis that VopQ is inducing autophagy independent of PI3-kinases.

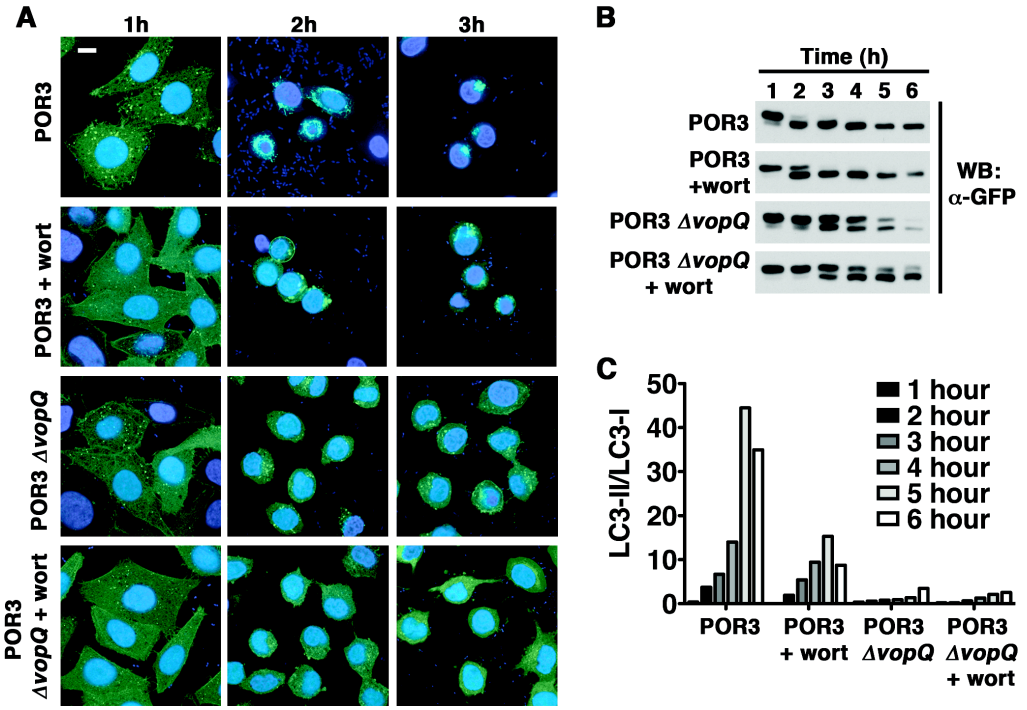

Figure 23. VopQ induces autophagy independent of PI3-kinases**. (A)** GFP-LC3 HeLa cells were pretreated with or without wortmannin (10μM) for 30 minutes and infected with POR3 or POR3*ΔvopQ*, with and without wortmannin (10μM). Scale bar represents 10 μm. **(B)** Samples were processed for Western blot analysis at the indicated timepoints and probed with an anti-GFP antibody. **(C)** Relative LC3-II accumulation was determined as described in Materials and Methods. The data are the means from a representative experiment.

Induction of Autophagy by VopQ Prevents Phagocytosis

We hypothesized that induction of rapid autophagy may be redirecting the cellular machinery essential for phagocytosis. Therefore, we examined POR3 and POR3Δ*vopQ*-infected macrophages for the presence of intracellular bacteria by electron microscopy. POR3-infected macrophages had few, if any, intracellular bacteria at 1 and 3 hours post infection with extracellular bacteria surrounding lysed cells **(Figure 24; A and B)**. In contrast, macrophages infected with the POR3Δ*vopQ* strain show the presence of multiple intracellular bacteria at both 1 and 3 hours post infection. At 3 hours post infection, many of the cells have greater than 4 intracellular bacteria per cell **(Figure 24B)**. These results demonstrate that the presence of the type III effector VopQ attenuates phagocytosis of *V. parahaemolyticus*. during infection.

Discussion

V. parahaemolyticus uses a temporally controlled mechanism to induce cell death that involves autophagy, modulation of the actin cytoskeleton and finally, cell lysis (Burdette et al., 2008). In this manuscript, we characterize the type III effector VopQ as a key mediator

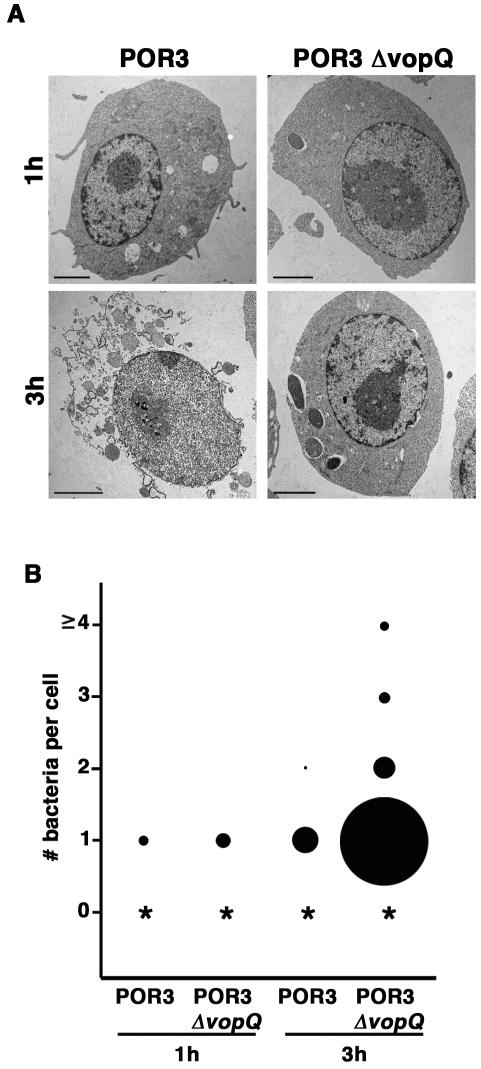

Figure 24. Induction of autophagy prevents phagocytosis. **(A)** RAW 264.7 macrophages were infected with POR3 or POR3*ΔvopQ.* At the indicated timepoints, cells were fixed and processed for electron microscopy as described in Materials and Methods. Scale bars represent 2μm. **(B)** Cells were scored for the presence of intracellular bacteria and the number of bacteria per cell is reflected as described in Materials and Methods. An asterisk represents greater than >90% of bacteria counted did not have intracellular bacteria.

of autophagy and cell lysis. Our results show that VopQ is a type III secreted effector and *V. parahaemolyticus* strains lacking VopQ are attenuated in their ability to induce cytotoxicity in a tissue culture model of infection. Cells infected with the POR3*ΔvopQ* strain did not round up as fast as cells infected with wild type *V. parahaemolyticus* **(Figure 17; compare all panels at the 2 hour time point)**. In addition, cells infected with POR3 release cellular contents by 3 hours post infection while cells infected with the POR3*ΔvopQ* strain are intact up to 5 hours post infection. This demonstrates that VopQ is a key virulence factor in T3SS1-mediated cytotoxicity.

Autophagy is a highly regulated process by which cells degrade bulk cytoplasmic contents for the purpose of generating nutrients under starvation conditions (Levine & Yuan, 2005). While apoptosis is known as type I programmed cell death, autophagy has been referred to as type II programmed cell death. However, autophagy has a historical role in cell survival, differentiation and remodeling (Cecconi & Levine, 2008, Penaloza *et al.*, 2008). *V. parahaemolyticus* can be counted among the intracellular bacterial and viral pathogens that hijack the autophagy pathway for their own benefit (Colombo, 2007). Herein, we showed that the *V. parahaemolyticus* T3SS1 effector VopQ is essential for autophagy during

infection because the POR3Δ*vopQ* strain is attenuated in its ability to induce autophagy as measured by GFP-LC3-II conversion and GFP-LC3 punctae formation. Furthermore, we have shown that VopQ is sufficient for the induction of autophagy by microinjection of recombinant VopQ into cells. This system is analogous to the type III secretion system, except that the amounts of protein and refolding requirements are distinct.

In previous studies, we were able to reduce the number of punctae observed in POR3-infected cells with the PI3-kinase inhibitor wortmannin (an inhibitor of class I and class III PI3-kinases) (Powis et al., 1994, Burdette et al., 2008). We were unable to use the PI3-kinase inhibitor 3-MA (an inhibitor specific for class III PI3-kinase) during infection as 3-MA is toxic to *V. parahaemolyticus* (data not shown) (Seglen & Gordon, 1982). Interestingly, when we pretreated cells with either inhibitor, we were unable to prevent GFP-LC3 punctae formation in cells microinjected with recombinant VopQ. These observations support the hypothesis that VopQ is inducing autophagy in a PI3-kinase-independent manner. Our analysis of GFP-LC3 cells infected with various POR3 strains in the presence or absence of wortmannin support this hypothesis. While there are far fewer GFP-LC3 punctae and more cytoplasmic (soluble) GFP-LC3 in the POR3-infected cells, the POR3Δ*vopQ*-infected cells treated with wortmannin

have almost no punctae and all of the GFP-LC3 appears to be cytoplasmic. The migration of GFP-LC3 by Western blot supports these findings. We are currently pursuing the nature of the PI3-kinase-independent VopQ-dependent mechanism of autophagy.

What are the roles of autophagy during infection? Induction of autophagy may be the bacteria's way of forcing the cell to provide nutrients for the bacteria in a readily usable form. By inducing autophagy, the bacteria manipulate the host cell into degrading intracellular proteins and organelles, generating essential amino acids and cofactors. Upon lysis, these degraded components are liberated for consumption by the pathogen. In addition, we speculate that induction of autophagy may be a way to prevent phagocytosis of an extracellular pathogen. We examined POR3 infected cells for the presence of intracellular bacteria and found that although electron microscopic images of *V. parahaemolyticus* infected cells showed the appearance of early autophagosomal structures, these cells lacked intracellular bacteria. Images of cells infected with the POR3*ΔvopQ* strain lacked signs of autophagosomal structures, yet an overwhelming number of cells contained intracellular bacteria. We propose that induction of autophagy sequesters the necessary membrane components that are required for phagocytosis. In fact, many of the

cellular factors involved in autophagic vesicle nucleation and transport are also required for generating sufficient membranes to engulf bacteria during phagocytosis (Fader & Colombo, 2009, Xie & Klionsky, 2007, Yoshimori & Noda, 2008). These cellular factors can include PI3-kinase signaling and the actin cytoskeleton (Reggiori *et al.*, 2005, Monastyrska *et al.*, 2008, Stephens *et al.*, 2002). Furthermore, proteins required for trafficking of multivesicular bodies (MVB) (Rab5, Rab7, and ESCRT complexes) are also found on autophagosomal membranes and are involved in phagocytosis (Deretic & Fratti, 1999, Rusten & Simonsen, 2008). Herein, we present a novel mechanism used by the type III effector VopQ from the extracellular pathogen *V. parahaemolyticus* to manipulate the host's cellular response to infection. Further research will not only aid in our understanding of the pathogen but also identify critical cellular factors that govern the host cells' decision between life and death.

Chapter 6

Utilization of the Yeast *Saccharomyces cerevisiae* as a Model System to Study the Molecular Mechanism of the *V. parahaemolyticus* T3SS1-encoded Effector VopQ

Introduction:

V. parahaemolyticus harbors two type-III secretion systems required for pathogenesis (Park et al., 2004b). Encoded within the T3SS on chromosome 1 are three type III effectors; *vopQ*, *vopR*, and *vopS* (Ono et al., 2006). We have shown that during infection, *V. parahaemolyticus* induces autophagy, a collapse of the actin cytoskeleton and cell death (Burdette et al., 2008). VopS, an AMPylator of Rho-GTPases, is the effector that serves to cripple the actin cytoskeleton leading to rounding and VopR remains uncharacterized (Yarbrough et al., 2009). VopQ has been shown to be responsible for the induction of autophagy by a PI3-kinase independent mechanism. In addition, VopQ is a key contributor to T3SS1-mediated cytotoxicity during infection (Burdette et al., Submitted March 2009). Despite what is known about VopQ, the molecular target is unknown and its mechanism of action remains unclear. In an effort to

identify the target and delineate the mechanism, we turned to *S. cerevisiae*; a genetically tractable model system of eukaryotic biology.

There is considerable precedence for the use of *S. cerevisiae* as a model organism to study the mechanism of type III effectors. Yeast systems have been used to characterize T3SS effectors from *Yersinia* spp., *Pseudomonas*, and *Salmonella* (Rohde *et al*., 2007, Rabin & Hauser, 2003, Yoon *et al*., 2003). Central to the dogma of a T3SS effector is that it mimics or captures an essential eukaryotic function. Typically, these functions are basic evolutionarily conserved molecular mechanisms throughout eukaryota. Using *S. cerevisiae*, one can study the effector's actions in an inexpensive and easily manipulated system. In this chapter, we show that ectopic expression of VopQ is cytotoxic to yeast. This cytotoxicity is reversible, as yeast expressing VopQ under control of a galactose inducible promoter, can recover upon promoter repression. This phenotype was exploited in an un-biased genetic screen of the yeast haploid deletion library that aimed to identify genes required for VopQ-mediated growth inhibition. Finally, in an effort to understand VopQ-mediated autophagy, we demonstrated VopQ's ability to induce autophagy in this model organism and used a biased approach to screen known genes required for autophagy in yeast. The results of the latter supported

our hypothesis that VopQ induces autophagy by an unknown, PI3-kinase-independent mechanism. Ultimately, the work presented in this chapter did not identify an essential genetic component, molecular target or mechanism but these studies provide insight for further studies on the mechanism of VopQ and its contribution to *V. parahaemolyticus* pathogenicity.

Results:

VopQ Targets an Evolutionarily Conserved Mechanism to Induce Cytotoxicity: Ectopic Expression of VopQ in HeLa cells and *Saccharomyces cerevisiae*

V. parahaemolyticus uses two T3SS to cause disease during infection (Park et al., 2004b). T3SS1 induces autophagy, cellular rounding and cell lysis through the coordinated action of T3SS effectors including but not limited to VopQ, VopR, and VopS (Ono et al., 2006). Previous work has attributed the induction of autophagy to the effector VopQ. In addition, VopQ also partially contributes to cytotoxicity and cell lysis (Burdette et al., Submitted March 2009). These *in vitro* tissue culture studies identified VopQ as a critical mediator of *V. parahaemolyticus*

pathogenesis. In an effort to gain a deeper understanding of the molecular mechanisms used by VopQ to induce autophagy and cell death, we co-transfected HeLa cells with a plasmid expressing VopQ and a plasmid expressing GFP. Cells transfected with GFP alone appeared healthy and expressed high amounts of GFP **(Figure 25)**. However, in cells co-transfected with VopQ and GFP, as early as 6 hours post-transfection, the GFP-positive cells were rounded and by 24 hours post transfection, these cells were completely round, dying, and floating off the plate **(Figure 25)**. These results demonstrate that VopQ is cytotoxic *in vitro*. The severe cytotoxicity seen during these transfections with VopQ may limit potential biochemical assays due to loss of cells and protein content. As a result, we pursued other methods of examining VopQ-mediated cytotoxicity.

In this aim, we turned to the budding yeast *S. cerevisiae*. We ectopically expressed VopQ with a FLAG-tag under a galactose inducible promoter in wild-type *S. cerevisiae* (BY4741). Yeast harboring an empty vector (control) grew well when streaked on media with either glucose or galactose/raffinose as the carbon source **(Figure 26A)**. However, while a yeast harboring the plasmid encoding VopQ grew well on media containing glucose, this strains did not grow well on media containing

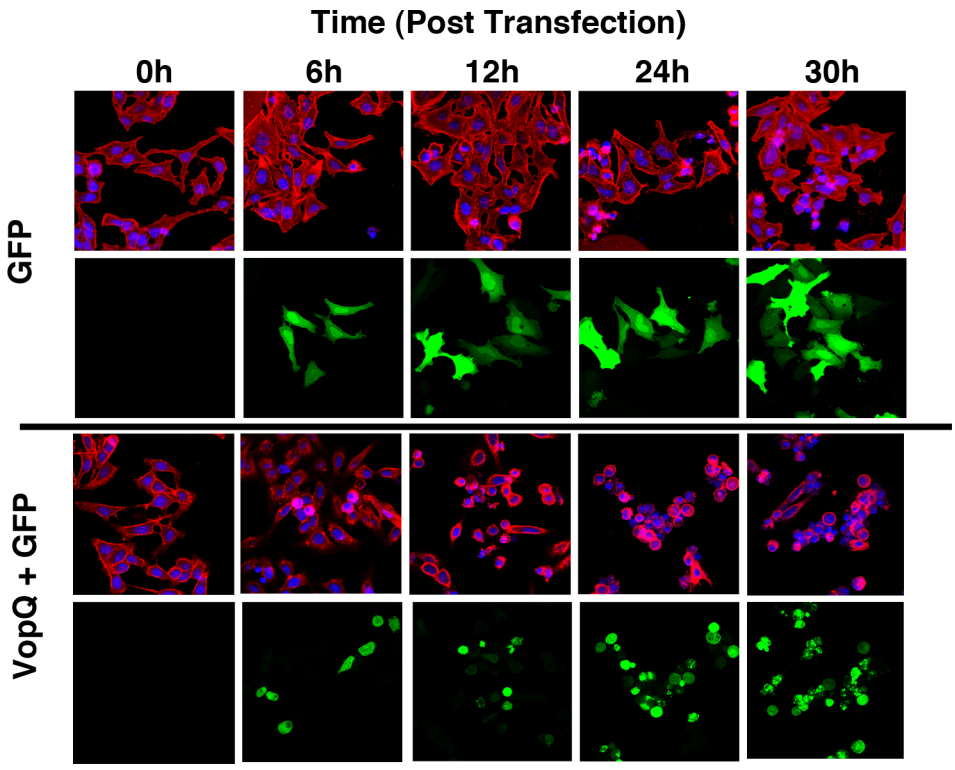

Figure 25. Transfection of VopQ induces cytotoxicity. Plasmids expressing GFP or VopQ and GFP were transfected into HeLa cells. At the indicated time points, cells were fixed and stained for actin (red) and DNA (blue) and visualized using confocal microscopy.

galactose/raffinose. **(Figure 26A)**. This effect is also seen in liquid cultures. Yeast were grown in liquid culture overnight and diluted back into media containing galactose/raffinose. While control yeast grew well, yeast expressing VopQ failed to enter logarithmic growth or reach stationary phase **(Figure 26B)**. Furthermore, this effect can be reversed by returning yeast expressing VopQ to glucose plates, thus repressing transcription of the VopQ gene **(Figure 26A)**. At each time point, yeast were harvested for Western blot analysis and probed with anti-FLAG antibodies. A 54kDa band corresponding to VopQ-FLAG was detected in yeast expressing VopQ and not in control yeast. The yeast lysates were reprobed with anti-porin antibodies as a control for protein extraction **(Figure 26C)**. These data demonstrate that VopQ is also cytotoxic when expressed in *S. cerevisiae* and are consistent with our results observed with tissue culture cells **(Figure 25)**. We can conclude that the type III effector VopQ is targeting an evolutionarily conserved mechanism to induce cytotoxicity during infection.

In an effort to determine the nature of VopQ's growth arrest, we performed growth curve analysis on synchronized yeast cultures. Yeast were synchronized using alpha factor, which arrests yeast at the G1/S

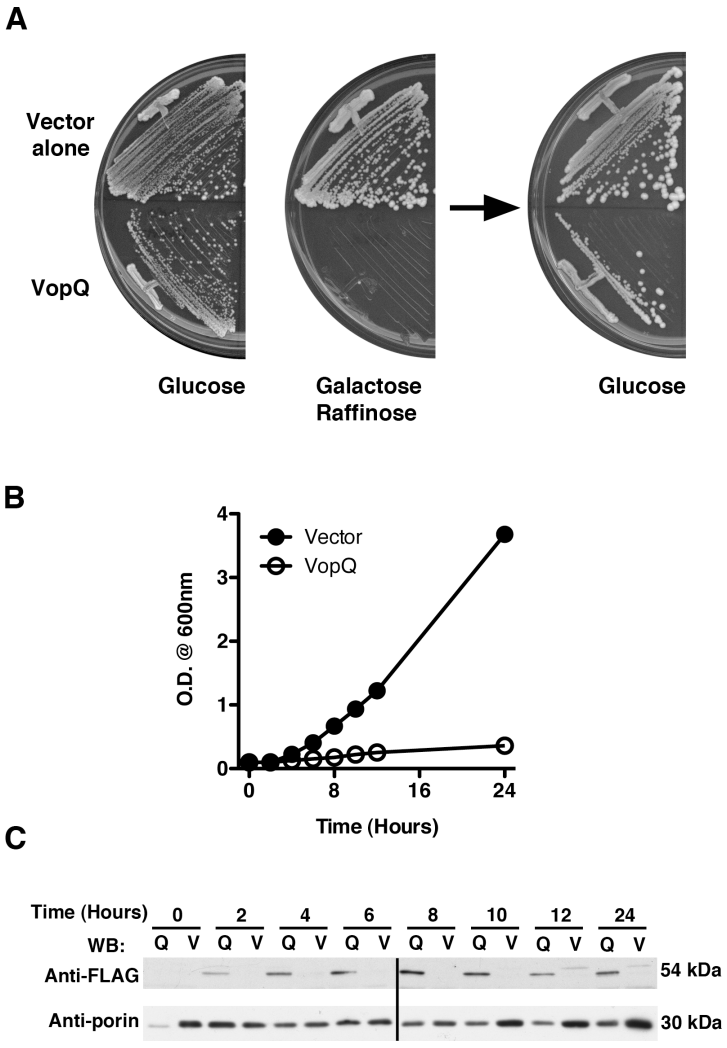

Figure 26. VopQ is cytotoxic to yeast. **(A)** Yeast expressing vector and VopQ were streaked on media containing glucose and galactose/raffinose. Following growth for 3 days at 30°C, the yeast growing on galactose/raffinose were streaked onto glucose. **(B)** Overnight cultures of yeast expressing vector alone (●) and VopQ (❍) were diluted into media containing galactose/raffinose and monitored for growth. **(C)** At the indicated time points, protein was harvested, separated by SDS-PAGE and probed with anti-FLAG antibody for the presence of VopQ and anti-porin antibody to confirm equal loading.

transition step of the cell cycle (Breeden, 1997). Upon removal of alpha factor, we can watch yeast bud and grow simultaneously. Synchronized control yeast grew well over time however, synchronized yeast expressing VopQ showed growth defects **(Figure 27A)**. Synchronized yeast proceed normally through the first rounds of cell division together. To visualize this process, yeast were photographed at each various intervals following release from the G1/S block. Control yeast bud and divide as predicted, however VopQ-expressing yeast have difficulty growing. Initially, VopQ-expressing yeast bud but do not complete the division **(Figure 27B)**. These results demonstrate VopQ targets an evolutionarily conserved mechanism to induce cytotoxicity.

Use of a Genetic Screen to Identify Genes Required for VopQ-mediated Cytotoxicity in *S. cerevisiae*

In an effort to identify genetic targets required for VopQ-mediated cytotoxicity, we screened the haploid yeast deletion library. This library is a systematic deletion of all 4850 non-essential yeast genes in the *S. cerevisiae* genome (Winzeler *et al.*, 1999, Schneider *et al.*, 2004). Positive hits would be genes whose absence permitted the growth of yeast in the

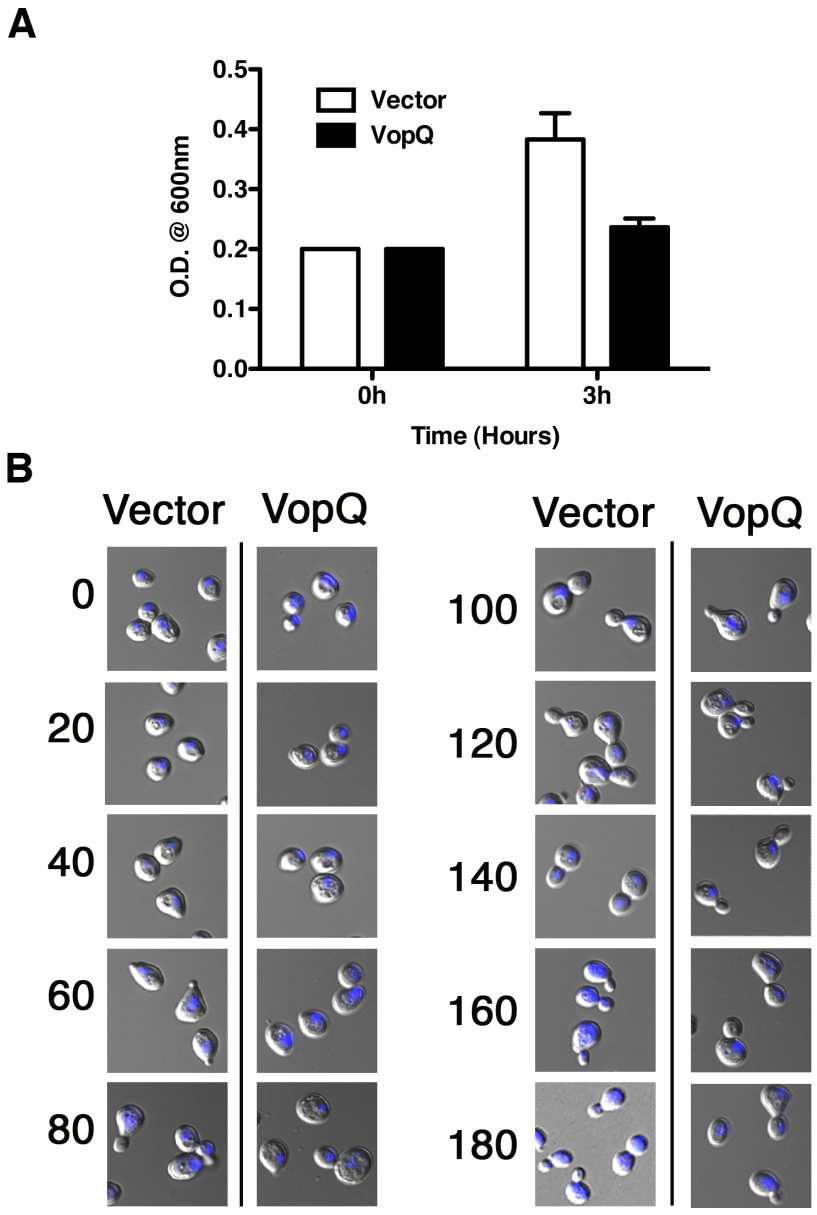

Figure 27. VopQ induces growth arrest in synchronized cultures. Overnight cultures of yeast expressing vector and VopQ were diluted and synchronized using alpha factor, then released from cell cycle block in media containing galactose/raffinose. **(A)** Growth of yeast at the end of the experiment. **(B)** Yeast were fixed and stained with Hoechst (DNA, blue) and photographed at the indicated time points.

presence of VopQ. The 4850 yeast deletions were screened in a 96-well format. Yeast were transformed with a plasmid expressing VopQ under a galactose-inducible promoter. Transformants selected for 3 days after which yeast were plated onto glucose as a control and galactose/raffinose to induce expression of VopQ. From over 50 96-well plates, 251 yeast strains grew in the presence of VopQ. These 251 positives were pulled from the original YPAD plates and re-arrayed into a 96-well format and retransformed with vector and vector expressing VopQ. This step eliminated all but 89 positives that were organized into functional groups **(Figure 28)**. Each positive was streaked onto selective media and scored for a degree of fitness; 0 for poor growth and 3 for good growth. Of the 89 positives, 15 scored a 3. These 15 were pulled from the freezer stock and retransformed with vector and VopQ **(Figure 28)**. Of these strains, only 3 strains grew in the presence of VopQ. Strain YOR360C was confirmed by PCR as scPde2 but despite rigorous evaluation at each step, scPde2 proved to be a false positive. The other two were not pursued. These false positives might result from mutations acquired by the yeast to accommodate toxic proteins such as VopQ.

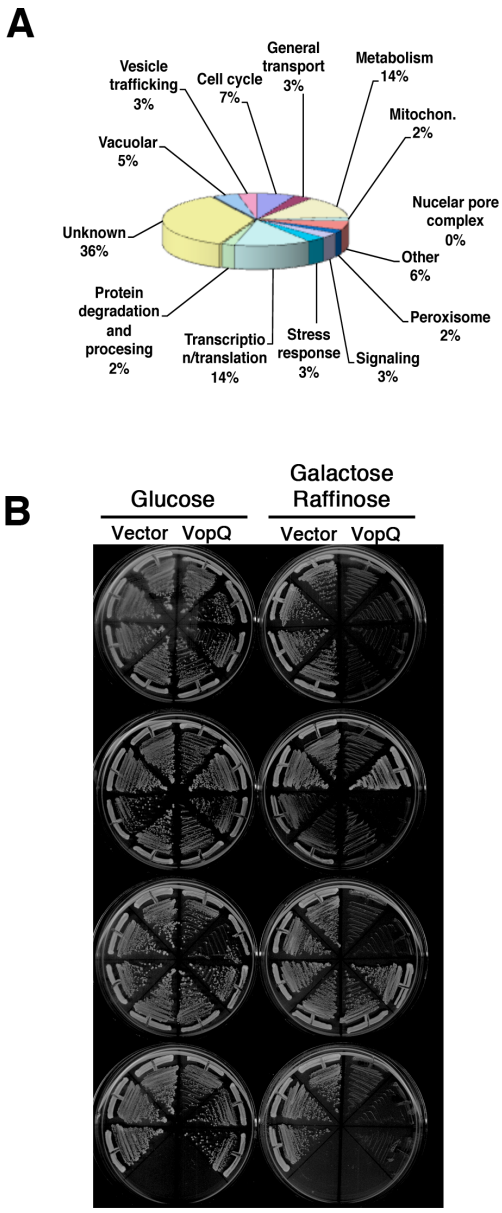

Figure 28. Yeast Deletion Library Results. **(A)** Distribution of positives from the initial deletion library screen shown as percent of total 251 positives. **(B)** Screen of the final 13 positives on glucose and galactose/raffinose.

VopQ Induces Autophagy in *S. cerevisiae*

Autophagy in *S. cerevisiae* is very well characterized (Klionsky et al., 2007). Similar to the eukaryotic system, many biochemical assays exist to ascertain if autophagy is occurring. In yeast, Apg8p is the homologue of mammalian LC3. Like LC3, Apg8p is required for autophagy and colocalizes to forming autophagosomes through a PE conjugation. However, its role in this process is unknown (Lang et al., 1998). Apg8p expression is upregulated at the transcriptional level during autophagy and therefore expression of Apg8p in yeast is an indicator of autophagy versus LC3, which uses a ratio of cytosolic (LC3-I) to membrane bound form (LC3-II) (Kirisako et al., 1999). Expression of VopQ in yeast corroborates the phenotypes we see during infection with *V. parahaemolyticus* POR3 strains, in transfections with VopQ expressing plasmids, and with microinjections of recombinant VopQ. We examined *S. cerevisiae* strains expressing VopQ for the induction of Apg8p expression. Overnight cultures of yeast expressing vector or VopQ-FLAG were diluted back into media containing galactose/raffinose and harvested at the indicated time points. In yeast expressing vector alone, Apg8p is not produced, however in yeast expressing VopQ-FLAG, Apg8 accumulates within one hour of induction and corresponds to VopQ-FLAG expression **(Figure 29A)**.

Induction of Apg8p in yeast expressing VopQ-FLAG supports our previous data that VopQ is sufficient for the induction of autophagy.

Autophagy can also be monitored in *S. cerevisiae* using an alkaline phosphatase assay. The yeast gene *pho8* encodes for alkaline phosphatase. It has an amino terminal domain that targets it to the endoplasmic reticulum. From there, Pho8 moves through the secretory pathway to the acidic environment of the lysosome where it is activated. Deleting 60 amino acids from the amino terminus (Pho8Δ60) renders it strictly cytoplasmic. The only way it can reach the lysosome is through autophagy (Klionsky et al., 2007). We expressed VopQ in the Pho8Δ60 strain and saw that expression of VopQ induces 6-fold greater alkaline phosphatase activity than yeast expressing vector alone **(Figure 29B)**. These data further suggests that VopQ is inducing autophagy in yeast.

Yeast Autophagy Genes are not Required for VopQ-mediated Cytotoxicity or Autophagy

In 1993, the genes for autophagy were identified in yeast (Tsukada & Ohsumi, 1993). Since then, over 30 yeast autophagy (atg) genes have been characterized in *S. cerevisiae* **(Table 1)**. In an attempt to identify the

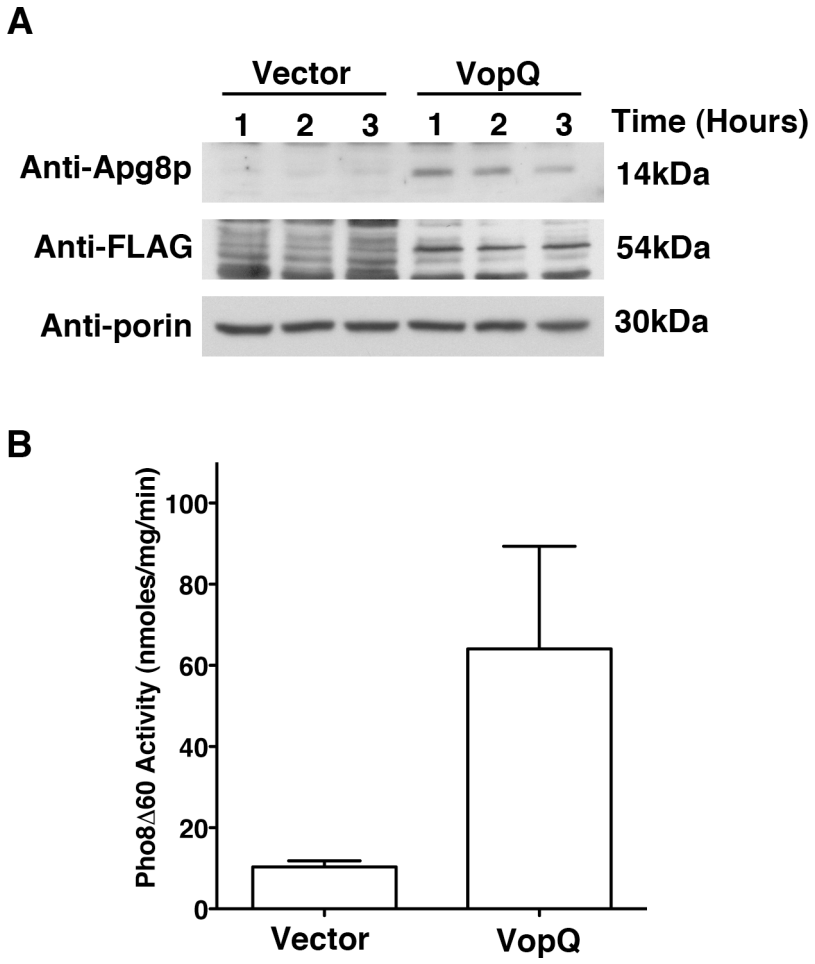

Figure 29. VopQ induces autophagy in yeast. Yeast expressing vector alone of VopQ were diluted into nutrient rich media. **(A)** At the indicated timepoints, yeast were harvested for protein extraction and lysates were separated via SDS-PAGE and probed with anti-Apg8p, anti-FLAG, and anti-porin antibodies. **(B)** Yeast at 3 hours post induction were harvested and processed for alkaline phosphatase activity as described.

mechanism of VopQ-mediated autophagy, we expressed VopQ-FLAG under a galactose-inducible promoter in several gene deletion strains. The deletion mutants tested herein include *atg* and *vps* genes involved in the regulation of induction (*atg1*, *atg11*, and *atg17*), cargo packaging (*atg8* and *atg11*), vesicle nucleation (*atg6*, *vps34*, and *vps15*), expansion (*atg3*, *atg5*) and completion of autophagy (*atg3*, *atg5*, *atg7*, and *atg8*) (Levine & Klionsky, 2004). In yeast, *vps34* is the PI3-kinase involved in the induction of autophagy, and in complex with *vps15* and *atg6*, mediates vesicle nucleation in response to autophagy stimuli. Each yeast deletion was transformed with vector or vector expressing VopQ. The yeast were plated by serial dilution onto media containing glucose or galactose/raffinose. Yeast harboring vector alone grew well on media containing glucose and media containing galactose/raffinose. However, yeast expressing VopQ-FLAG grew well on media containing glucose, but not on media containing galactose/raffinose. Within each dilution, there were fewer yeast than with vector alone, and those that did grow were very small in size **(Figure 30)**. Therefore, the autophagy genes tested herein are not required for VopQ-mediated cytotoxicity.

In order to examine the effect of VopQ on autophagy in these

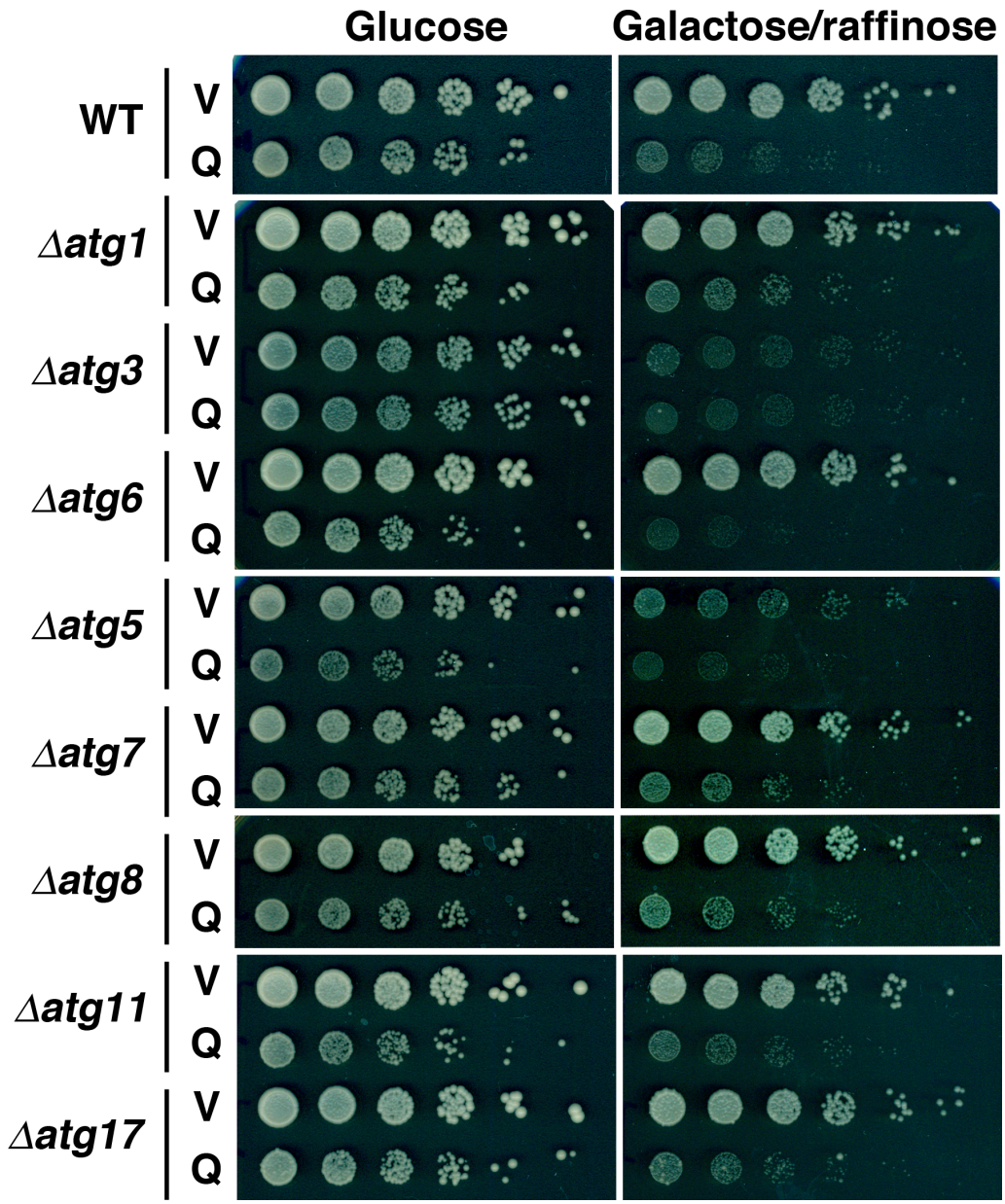

Figure 30. VopQ-mediated cytotoxicity is independent of genes required for autophagy. Overnight cultures of yeast expressing vector alone or VopQ were diluted to a final dilution of 0.1OD/mL and 5 1:5 serial dilutions were made from that in phosphate buffered saline. Each dilution was plated on glucose or galactose/raffinose.

strains, yeast expressing vector alone or VopQ-FLAG were examined for Apg8p production. Expression of VopQ-FLAG induced Apg8 expression in each *atg* deletion strain except for the *Δatg8* strain, which served as a negative control **(Figure 31)**. Interestingly, VopQ is also able to induce autophagy in the *Δvps34* strain. These results support our hypothesis that VopQ is inducing autophagy in a PI3-kinase-independent manner.

Discussion:

V. parahaemolyticus induces cell death that first involves the induction of autophagy, followed by cell rounding and ultimately, cell death (Burdette et al., 2008). We have attributed the induction of autophagy to VopQ, a type III effector encoded on T3SS1. VopQ induces autophagy in a PI3-kinase independent manner. In addition, VopQ plays a role in the induction of host cellular toxicity during infection. However, the molecular mechanism of VopQ's actions during infection remains unknown. In an effort to elucidate these mechanisms, we used the model organism *S. cerevisiae* as a tool in this aim.

Our initial studies on VopQ initiated in a tissue culture model of infection, however cellular toxicity made using eukaryotic systems difficult

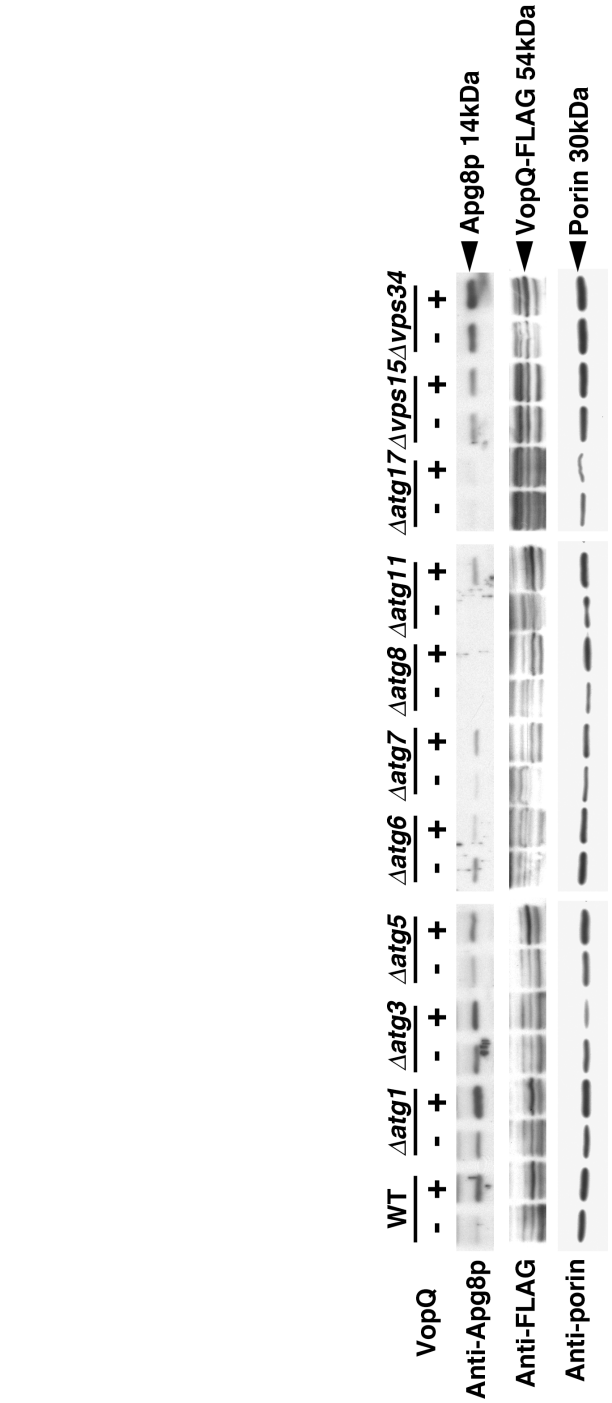
VopQ
WT
Δatg1
Δatg3
Δatg5
Δatg6
Δatg7
Δatg8
Δatg11
Δatg17
Δvps15
Δvps34
- + - + - + - + - + - + - + - +
Anti-Apg8p
Anti-FLAG
Anti-porin
Apg8p 14kDa
VopQ-FLAG 54kDa
Porin 30kDa

Figure 31. VopQ is able to induce autophagy in *atg* yeast deletion strains. Yeast expressing vector alone of VopQ were diluted into media containing galactose/raffinose and grown for 2 hours at 30°C. At the indicated timepoints, yeast were harvested for protein extraction and lysates were separated via SDS-PAGE and probed with anti-Apg8p, anti-FLAG, and anti-porin antibodies.

(Figure 25). Studies using tissue culture models to understand the mechanism of VopQ are presented in following chapters. Expression of VopQ in yeast is cytotoxic indicating VopQ is targeting an evolutionarily conserved mechanism. The mechanism is reversible as shutting of VopQ expression restores growth **(Figure 26)**. Viewing yeast expressing VopQ by microscopy did not reveal any drastic physiological abnormalities. Therefore we synchronized yeast at the G1/S transition using the mating pheromone alpha factor. Using synchronized cells, we were then able to watch VopQ expressing yeast as they progress through cell division. Yeast expressing VopQ bud and begin to divide synchronously, however this process does not proceed to completion **(Figure 27)**. Some cells finish cell division, whereas some do not. If VopQ affected a regulated step in cell division, we would have expected to see a uniform effect following release from alpha factor arrest. This was not the case.

We next utilized the haploid yeast deletion library in an effort to indentify genes required for VopQ-mediated cytotoxicity **(Figure 28)**. However, we were unable to identify any genes using this technique. Ultimately, we hypothesized that VopQ's mechanism might target an essential protein or pathway. Crucial to the haploid deletion library is that all included mutations are non-essential genes. Therefore, if VopQ targets

an essential protein or signaling pathway, this screen is not designed to detect such interactions. Additional genetic screens in yeast to elucidated the mechanism of VopQ will include a multicopy suppressor screens, which would not eliminate essential genes, or focus on more biased approaches.

This chapter also demonstrates and supports the previous conclusion that VopQ is necessary and sufficient to induce autophagy in a PI3-kinase independent manner (Burdette et al., Submitted March 2009). We show that in yeast, expression of VopQ induces Apg8p expression and alkaline phosphatase activity **(Figure 29A, B and C)**. We tested a panel of deletions strains for yeast autophagy genes in order to indentify critical factors required for VopQ-mediated autophagy. Using these strains, we show that VopQ induces autophagy in yeast in a PI3-kinase independent manner **(Figure 30)**. Again, this is consistent with our infection studies done in the presence of wortmannin. We show that infection with POR3 in the presence of wortmannin significantly reduces GFP-LC3 punctae and LC3-II conversion. Deletion of *vopQ* is able to abrogate this effect almost to completion, however in both cases, some punctae remain. Therefore, we believe VopQ is targeting a PI3-kinase independent mechanism. *V. parahaemolyticus* may also be signaling

through a VopQ-independent mechanism to activate classical autophagy that is inhibited by PI3-kinase inhibitors (Burdette et al., Submitted March 2009). Finally, we return to our tissue culture model of infection and show that T3SS1-mediated autophagy does not require the TOR signaling pathway that is induced in response to nutrient deprivation **(Figure 31)**. These studies presented herein support the conclusion that VopQ is inducing cytotoxicity and autophagy in an evolutionarily conserved manner. This genetic system remains as a relevant tool to understand the mechanism of VopQ-mediated functions.

Chapter 7

Contributions to the Understanding of T3SS1-mediated Cell Death and the Mechanism of the T3SS1-effector VopQ

Introduction:

V. parahaemolyticus is the causative agent of gastroenteritis associated with the consumption of raw or undercooked shellfish. Endemic in Southeast Asia, *V. parahaemolyticus* has also been isolated from waters along the eastern and western seaboards of the United States (Yeung & Boor, 2004). The TDH is the most well studied virulence factor, however *V. parahaemolyticus* also harbors two T3SS, one on each chromosome (Park et al., 2004b). Previous research has attributed cytotoxicity in a tissue culture model of infection to the T3SS on chromosome 1 and enterotoxicity in the ligated rabbit ileal loop model to the T3SS on chromosome 2 (Liverman et al., 2007, Park et al., 2004a). We have shown that the mechanism of T3SS1-mediated cell death initiates with autophagy, followed by cell rounding, and culminates in cellular lysis and death (Burdette et al., 2008). Induction of autophagy during infection requires the type III effector VopQ, encoded with T3SS1.

Furthermore, VopQ is required for full T3SS1-mediated virulence in the tissue culture model of infection. VopQ induces autophagy independent of class III PI3-kinase as demonstrated in yeast, however the exact nature of its actions remain unknown (Burdette et al., Submitted March 2009).

This chapter focuses on experiments performed in an effort to understand the mechanism of action of VopQ. In this aim, we present data that culminates in a deeper understanding of the role VopQ plays during infection. This information sets the stage for further studies on VopQ and *V. parahaemolyticus*. Herein, we demonstrate the kinetics of VopQ expression in *V. parahaemolyticus*, expression and secretion of VopQ in T3SS1 effector mutant strains, and the use of a heterologous system in *Yersinia pseudotuberculosis* (*Y. pseudotuberculosis*) to study effector function. Furthermore, we present and test the hypothesis that VopQ is a phospholipase. In addition, using deletion analysis, we attempt to identify critical domains required for VopQ function and localization.

Results:

Secretion of VopQ in *Vibrio parahaemolyticus*

VopQ is a type III secreted effector secreted from T3SS1 of *V. parahaemolyticus* however it is not known to what extent VopQ is

produced and secreted over the duration of infection in the strains used in this dissertation (Ono et al., 2006). In order to understand these kinetics, *V. parahaemolyticus* strains POR1 (*Δtdh*, *Δtrh*), POR2 (POR1 *ΔT3SS1*), and POR3 (POR1 *ΔT3SS2*) were grown in calcium chelating media at 37°C to induce secretion. At one hour time points for 16 hours, bacteria were harvested to assess the total amount of VopQ produced in each strain. In addition, culture supernatants were filtered and TCA precipitated to test for the amount of VopQ secreted into the media. VopQ is not produced or secreted in bacteria from the overnight cultures grown at 30°C **(Figure 32; lane 1 in A-F)**. However, VopQ protein is produced within one hour of growth in secretion inducing media in all strains **(Figure 32; A, B, and C)**. In POR1 and POR3 strains, VopQ continues to be produced for up to 10 hours post induction. However, VopQ production is rapidly shutoff in the POR2 strain following the shift to T3SS inducing conditions **(Figure 32B)**. Production of VopQ in POR1 and POR3 corresponds to secretion into the media. Secretion of VopQ occurs for approximately 5-7 hours in both POR1 and POR3 strains **(Figure 32; D and F)**. However, secretion of VopQ into the media was not detected in TCA precipitated culture supernatants from POR2 at any time

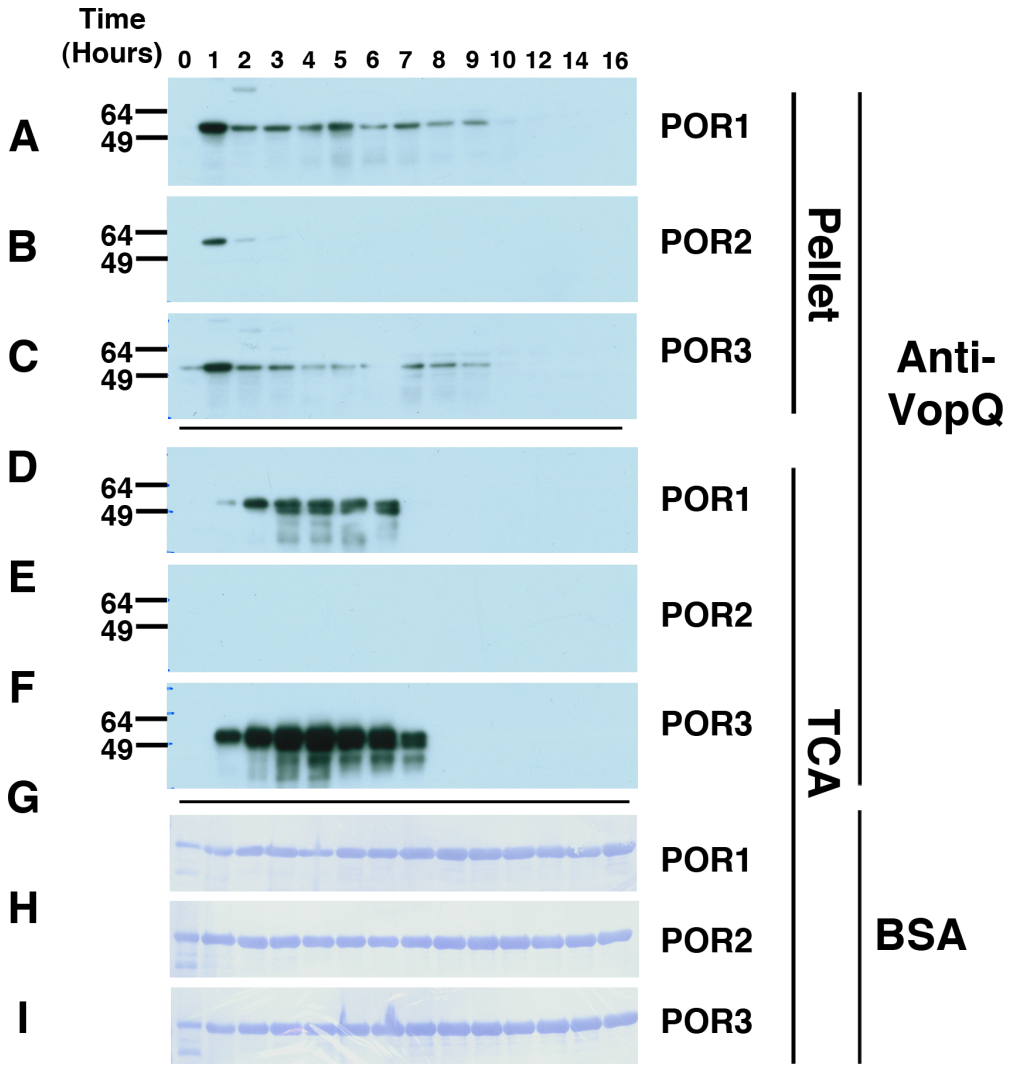

Figure 32. VopQ is secreted in the early phase of secretion induction in *V. parahaemolyticus*. Overnight cultures of strains POR1 **(A, D, and G)**, POR2 **(B, E, and H)** and POR3 **(C, F, and I)** were inoculated into secretion inducing media. At each time point, bacteria were harvested to look for production of VopQ **(A-C; pellet)** or culture supernatants were filtered and TCA-precipitated for the presence of secreted VopQ **(D-F; TCA)**. The membrane from the TCA samples was coomassie stained to detect BSA that was added to the culture media as a precipitation control **(G-I; BSA)**.

point **(Figure 32E)**. These results confirm VopQ is an effector protein secreted specifically from T3SS1 during the initial hours of induction.

Many bacterial pathogens utilize a panel of type III effectors during infection in order to manipulate the host cell response to infection. However, recent evidence supports the notion that effectors secreted from the same system are not secreted equally in order to coordinate the most ideal environment for the bacterium during infection. In fact, the order, duration, and quantity of effector secretion is coordinated by the pathogen in a precise fashion. This is the case for *Salmonella*, which uses two T3SS during infection. The type III effector SopE is a guanine nucleotide exchange factor (GEF) activating Cdc42 and Rac1 resulting in membrane ruffling and bacterial uptake. Later during infection, SptP acts as a G-protein activating protein (GAP) on Cdc42 and Rac1 to inhibit the modulation of the actin cytoskeleton in order to prevent fusion of bacterial containing vacuoles with the lysosome. Effector half-life is also highly regulated. Again, in the case of *Salmonella*, SopE is degraded rapidly by the proteaseome whereas SptP degradation is far slower (Kubori & Galan, 2003). This complex hierarchy ultimately aims to benefit the pathogen during infection. It seeks to reason then that deletion of effectors within a locus can affect the secretion of other effectors through the same

apparatus. In addition to VopQ, *V. parahaemolyticus* T3SS1 encodes for at least two additional effectors, VopR and VopS, however it is not known the rate or order with which these proteins are secreted during infection. We examined *V. parahaemolyticus* effector mutant strains for the secretion of other effectors encoded within T3SS1. As expected, *V. parahaemolyticus* strains POR1 and POR3 secrete the type III effectors VopQ and VopS **(Figure 33; lanes 1 and 3)**, however, secretion of neither protein is detected in TCA precipitated culture supernatants from POR2 strains **(Figure 33; lanes 2, 5, and 8)**. VopQ is not detected in the TCA precipitated culture supernatants of *ΔvopQ* strains, however it is secreted in *ΔvopS* strains **(Figure 33; lanes 7 and 9)**. Conversely, VopS is not detected in the TCA precipitated culture supernatants of *ΔvopS* strains but is secreted in *ΔvopQ* strains **(Figure 33; lanes 4 and 6)**. Therefore, deletion of a T3SS effector encoded with T3SS1 does not have an appreciable effect on the secretion of other T3SS1 effectors.

Using *Yersinia pseudotuberculosis* as a Heterologous System to Study the Mechanism of VopQ

V. parahaemolyticus induces autophagy and cell lysis during

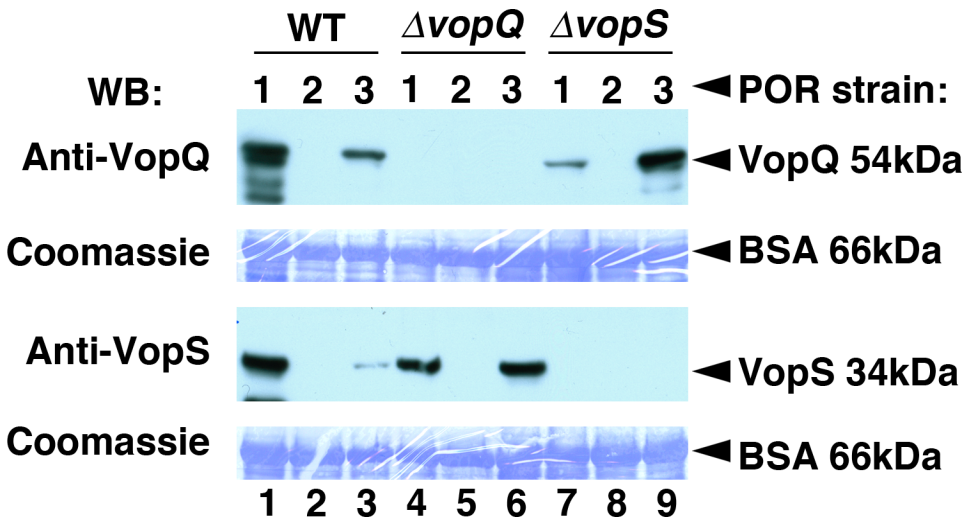

Figure 33. *V. parahaemolyticus* T3SS1 effector mutant strains are not compromised in their ability to secrete other T3SS1 effectors. *V. parahaemolyticus* wild-type, *ΔvopQ*, or *ΔvopS* strains were examined for the secretion of VopQ and VopS following an *in vitro* secretion assay as described in Materials and Methods. Membranes were stained with coomassie to detect the presence of BSA added the culture media as a precipitation control.

infection (Burdette et al., 2008). Autophagy and in part, cell death, have been attributed to the type III effector VopQ, as POR3*ΔvopQ* strains are attenuated in their ability to induce autophagy and cell lysis. These results demonstrated that VopQ is necessary for autophagy and full virulence (Burdette et al., Submitted March 2009). We took advantage of a heterologous expression system in *Y. pseudotuberculosis* that would allow us to study VopQ in the absence of other T3SS effectors. This system has been widely used in the study of T3SS effectors from a variety of pathogens (Frithz-Lindsten et al., 1998). We cloned *vopQ-FLAG* into an IPTG-inducible expression vector and conjugated this plasmid into several *Y. pseudotuberculosis* strains. The genotypes of each strain used can be found in Table 2 in Chapter 3. Briefly, we utilized YP27 (*ΔyopEHJ*) and YP37 (*ΔyopEHJOMK*); two *Y. pseudotuberculosis* strains that lack effectors responsible for virulence. In addition, we used strains YP44 and YP71 as negative controls. YP44 (*ΔyopEHJOMKB*) can secrete into the media but is unable to translocate into host cells. YP71 (*Δysc*) cannot secrete or translocate. *Y. pseudotuberculosis* strains harboring the plasmid expressing VopQ-FLAG were able to efficiently produce VopQ in response to IPTG induction, however no VopQ was detected in TCA-precipitated culture supernatants **(Figure 34)**.

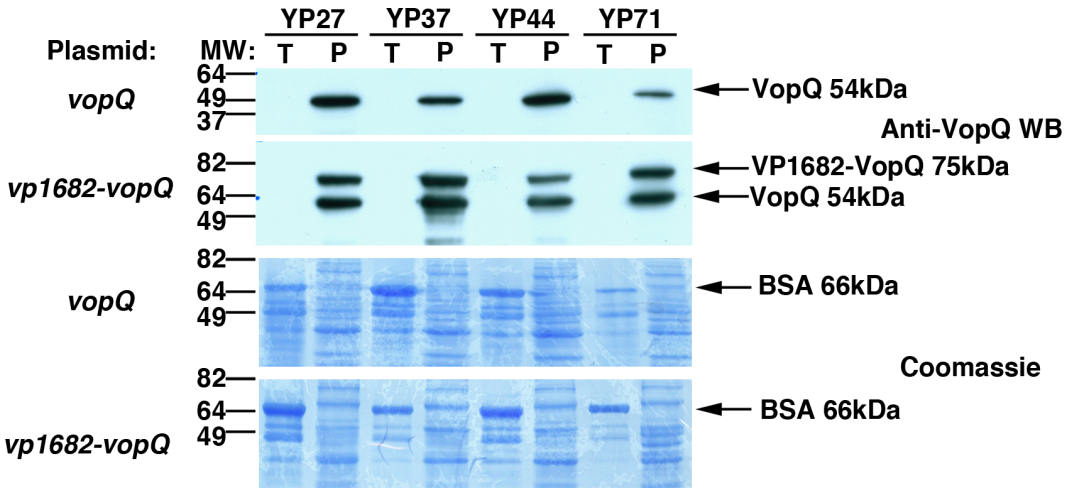

Figure 34. *In vitro* secretion assay using *Y. pseudotuberculosis* as a heterologous expression system. *Y. pseudotuberculosis* strains expressing either *vopQ* alone or *vp1682-vopQ* were evaluated for the production (P) and secretion into the culture supernatant (T) of VopQ.

Others have shown that the chaperone is require for secretion in a heterologous system (Feldman & Cornelis, 2003). We hypothesized that the lack of secretion may result from the lack of a suitable chaperone for VopQ in *Y. pseudotuberculosis*. The gene encoding *vp1682* is immediately upstream and in frame of the gene for *vopQ*. Genomic DNA upstream of *vp1682* encodes putative -35 and -10 promoter elements. In addition, there is a Shine-Dalgarno sequence upstream of *vp1682*, between *vp1682* and *vopQ*. This suggests that *vp1682* and *vopQ* are transcribed in the same operon, however we have not shown this experimentally. We cloned the genomic region encoding both *vopQ* and its putative chaperone *vp1682*, into the heterologous expression system. While *Y. pseudotuberculosis* strains harboring this construct were able to produce VopQ, they were unable to secrete VopQ **(Figure 34)**. Interestingly, the induction from this larger construct produced a band corresponding the predicted size of a VP1682-VopQ fusion protein **(Figure 34)**. The addition of the chaperone did not enhance VopQ secretion in this system.

VopQ is a not a Phospholipase

Previous research has identified VopQ as a key mediator in T3SS1-mediated cell death (Burdette et al., Submitted March 2009). Transfection

of VopQ into HeLa cells results in cell rounding, cytotoxicity, and cell death and following 18 hours of transfection, few cells remain on the plate. Co-transfection experiments with VopQ and GFP show that, at the onset of GFP expression at four to six hours post transfection, cells are already rounded and dying suggesting the VopQ phenotype is extremely potent **(Chapter 6, Figure 25)**. Furthermore, the mechanism of VopQ is evolutionarily conserved, as expression of VopQ in yeast is also cytotoxic **(Chapter 6, Figure 26)**. These phenomena are reminiscent of ExoU, a potent type III effector from *Pseudomonas aeruginosa*. ExoU is a phospholipase and a major contributor to cytotoxicity and virulence during infection (Sato & Frank, 2004). It is a member of the cytosolic phospholipase A_2 ($cPLA_2$) family and requires a catalytic dyad of a serine residue (GXSXG) and an aspartic acid residue (DXG) for enzymatic action. In addition, phospholipases like ExoU also contains a glycine rich region (GXGXXG) upstream required for nucleotide binding (Winstead et al., 2000). Members of the $cPLA_2$ family hydrolyze the sn-2 ester of glycerophospholipids producing fatty acid and lysophospholipid. In eukaryotic cells, membrane phospholipids are the substrate and hydrolysis generates arachadonic acid, a mediator in inflammation

(Balsinde et al., 2002). In the case of ExoU, the exact phospholipid substrate is unknown.

VopQ was examined for the presence of these conserved residues. In an alignment with ExoU and other cPLA$_2$ family phospholipases, VopQ was shown to contain the glycine rich sequence, a serine residue (GIISGG) and the aspartic acid residue **(Figure 35** and (Sato & Frank, 2004)**)**. We generated serine (S288A) and aspartic acid mutants (D433A) in constructs expressing VopQ-FLAG and VopQ-GFP and tested these constructs in transfection of HeLa cells. Transfection of wild-type VopQ induces rounding and cell death, and the S288A mutation does not abrogate this affect. In contrast, the D433A mutation in the VopQ-GFP construct significantly abrogates the phenotype, however VopQ-FLAG D433A is still somewhat active **(Figure 36A)**. Western blot analysis of lysates from transfected cells revealed equal levels of expression from all constructs **(Figure 36B)**. In order to test to role of VopQ as a phospholipase during infection, we infected HeLa cells with POR3 in the absence or presence of two different phospholipase inhibitors, methylarachandonylfluorophosphonate (MAFP) and bromoenolactone (BEL). Both MAFP and BEL are irreversible and selective phospholipase

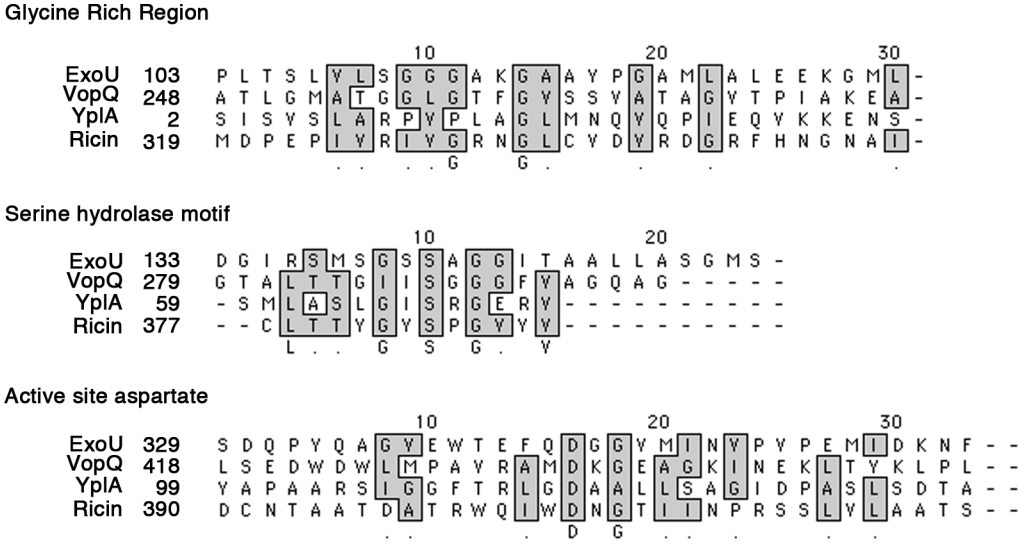

Figure 35. Alignment of VopQ with ExoU family phospholipases. VopQ is aligned with each family member showing the conserved residues in each domain. ExoU 687 amino acids (AAC16023), YplA 324 amino acids (AAC31479), Ricin precursor 576 amino acids (P02879) (Sato & Frank, 2004).

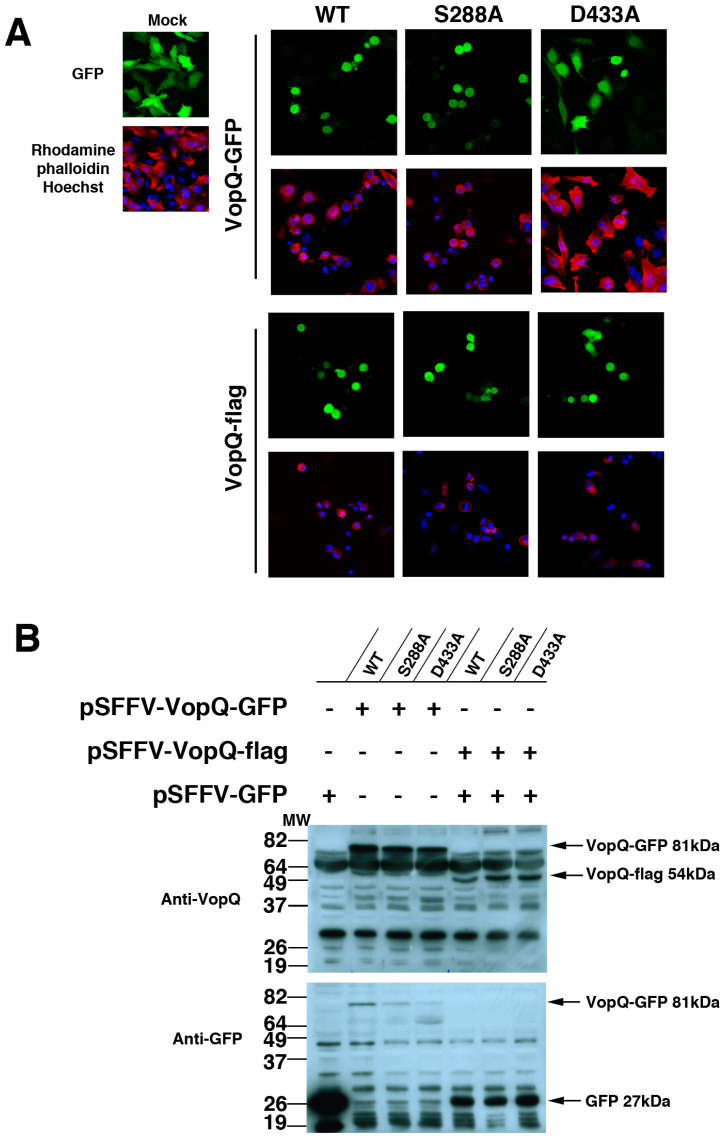

Figure 36. Mutation of putative residues required for phospholipase activity does not abrogate VopQ-mediated cytotoxicity. Serine 288 and aspartic acid 433 were mutated to alanine on plasmids pSFFV VopQ-GFP or pSFFV VopQ-FLAG and then transfected into HeLa cells. **(A)** Cells were fixed and stained for actin (red) and the nuclei (blue) as described. **(B)** Cells were lysed in SDS sample buffer and processed for Western blot analysis. Samples were probed with anti-VopQ and anti-GFP antibodies.

inhibitors (Balsinde et al., 1999). MAFP inhibits both $cPLA_2$ and calcium independent PLA_2 ($iPLA_2$) family members whereas BEL is most specific for $iPLA_2$ family members (Lio *et al.*, 1996, Ackermann *et al.*, 1995). Both inhibitors are effective against ExoU (Phillips et al., 2003). The phospholipase activity of ExoU contributes greatly to the ability of *P. aeruginosa* to induce LDH release during infection of tissue culture cells. Therefore, HeLa cells were monitored for cytotoxicity as measured by LDH release during infection with *V. parahaemolyticus*. Neither MAFP nor BEL significantly reduced the ability of POR3 to induce cell lysis **(Figure 37; A and B)**. These results demonstrate that VopQ is not a phospholipase and that the mechanism T3SS1-mediated cell does not involve phospholipase activity.

VopQ Deletion Construct Mutational Analysis

In an effort to understand the function of VopQ, we sought to identify the existence of eukaryotic homologues. The amino acid sequence of the coding region was subjected to BLAST analysis that ultimately, did not reveal any clear homologues or eukaryotic domains. We used other protein characterization programs such as hydrophilicity plots to predict

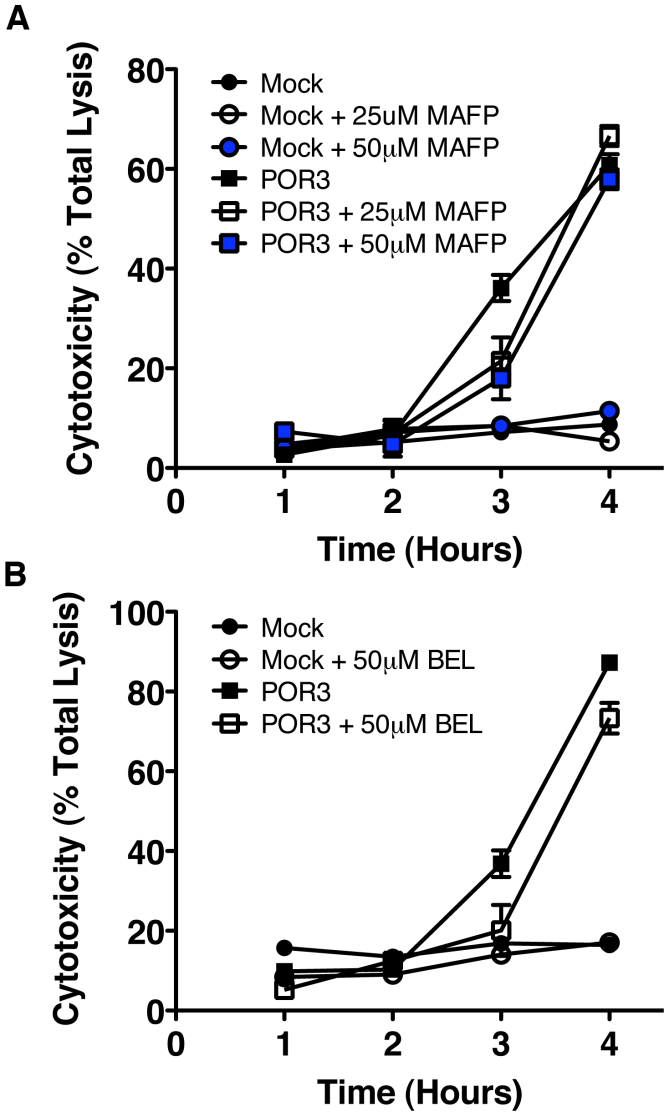

Figure 37. Phospholipase inhibitors do not inhibit POR3 induced LDH release. HeLa cells were pretreated with **(A)** MAFP (25μM and 50μM) or **(B)** BEL (50μM) for 30 minutes and then mock-infected or infected with POR3. Inhibitors were maintained throughout the duration of the experiment. At the indicated time points, cytotoxicity was measured by LDH release as described. Cytotoxicity is reflected as percent of total lysis in 1% Triton X-100.

unique features of VopQ. We subjected the VopQ amino acid sequence to the Kyte Doolittle algorithm to predict hydrophobic segments (Kyte & Doolittle, 1982). This analysis predicted a 60 amino acid hydrophobic segment in the middle of the VopQ amino acid sequence **(Figure 38)**. We predicted this hydrophobic region may aid in targeting VopQ to subcellular compartments in a cell such as the ER, mitochondria, lysosome, or Golgi. We constructed deletion mutants to determine the contribution of this region to VopQ function and localization. Co-transfection of GFP with full length VopQ into HeLa cells induced the characteristic phenotype of rounded and dying cells **(Figure 39A)**. However, none of the deletion constructs induced cell rounding **(Figure 39A)**. We confirmed the expression of each construct by probing lysates from transfected HeLa cells with anti-FLAG antibody **(Figure 39B)**.

We hypothesized that the hydrophobic nature of this segment may mediate VopQ membrane binding following T3SS secretion into the host cell. In order to test this, we created a construct fusing GFP in frame with the full length VopQ coding sequence. The pattern of GFP expression following transfection of VopQ-GFP into HeLa cells is predominantly cytoplasmic with strong GFP positive punctate dots appearing in some

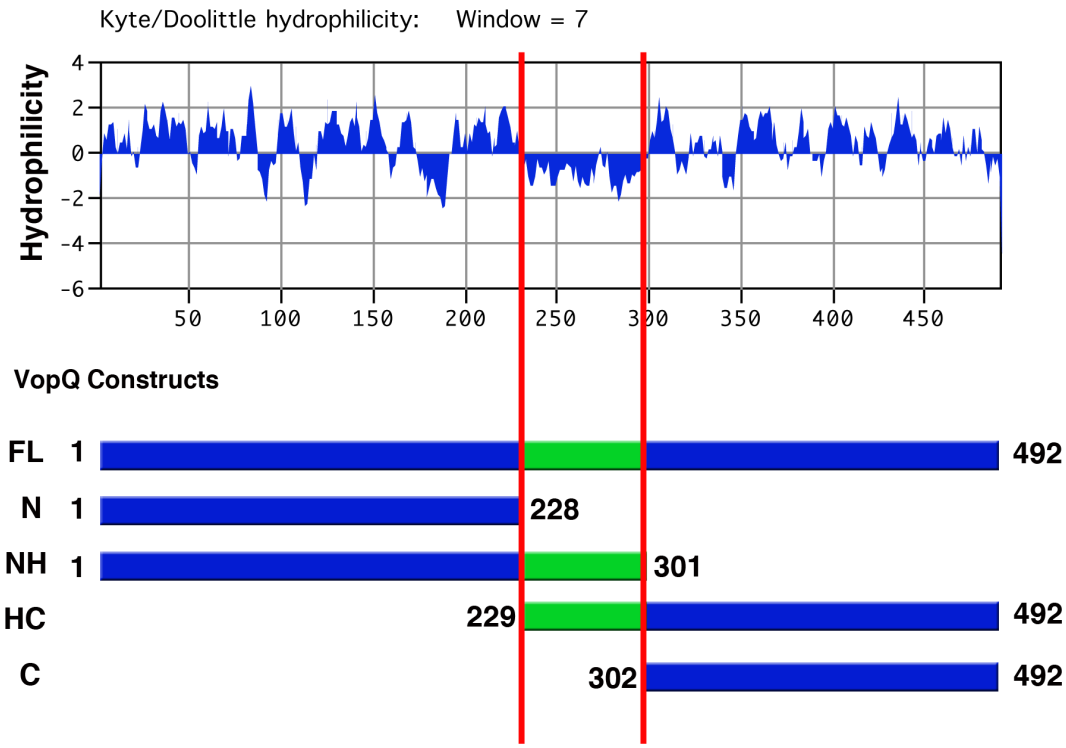

Figure 38. VopQ contains a hydrophobic domain. Kyte Doolittle plot of hydrophilicity shows a hydrophobic domain in VopQ. Graphical depiction of VopQ amino acid sequence and the deletion constructs generated to understand the function of the predicted hydrophobic amino acid segment.

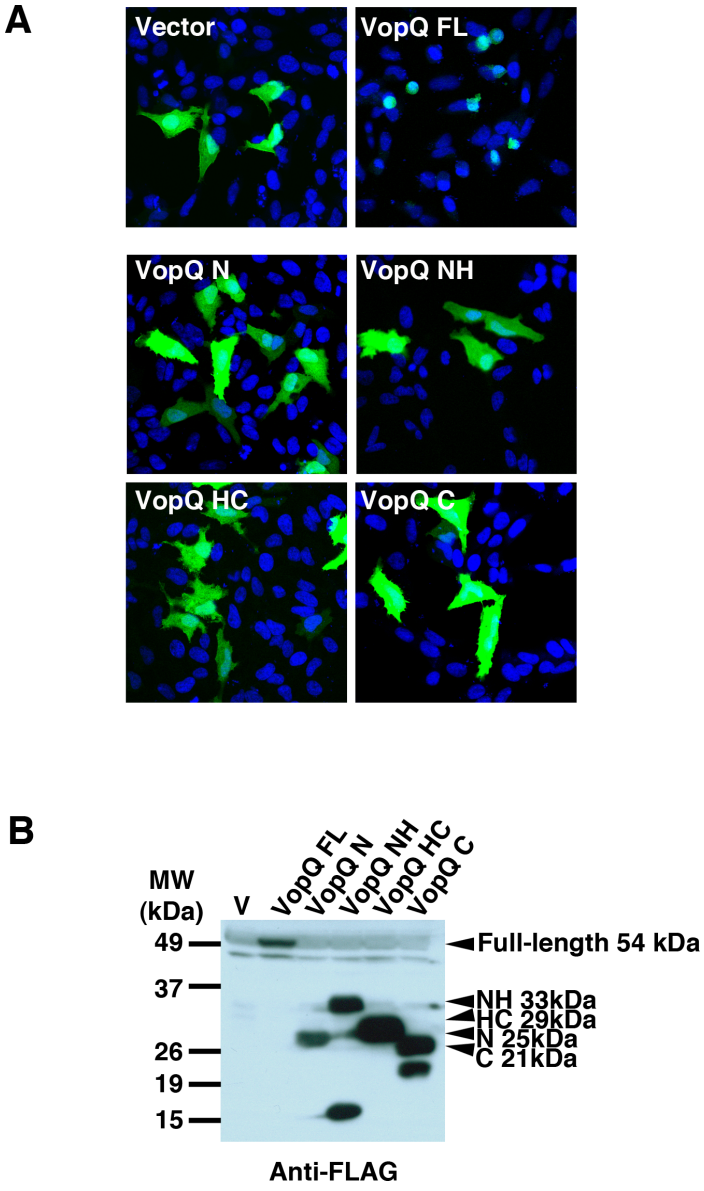

Figure 39. VopQ requires a full-length protein for function. Deletion constructs were cotransfected with GFP into HeLa cells for 18 hours. Cells were fixed and stained with Hoechst (nuclei, blue) and visualized by confocal microscopy **(A)** or identical samples were processed for Western blot analysis with anti-FLAG antibodies **(B)**.

cells compared to transfection with GFP alone **(Figure 40; A, B, C, and D, bottom left panels in each)**. To determine if VopQ is localizing to any subcellular compartments, we utilized fluorescent markers for the endoplasmic reticulum (ER Tracker Red, **Figure 40A**), the lysosome (Lyso Tracker Red, **Figure 40B**), the mitochondria (Mito Tracker Red, **Figure 40C**), and the Golgi (Anti-golgin97; **Figure 40D**). Transfection with GFP alone confirms that each fluorescent marker is properly staining its appropriate compartment **(Figure 40; A, B, C, and D, top panels)**. In VopQ-GFP transfected cells incubated with ER Tracker Red, we notice GFP expression partially coincides with ER staining **(Figure 40A)**. However, VopQ-GFP expression does not overlap with the other fluorescent markers for the lysosome, mitochondria, or Golgi apparatus **(Figure 40B, 40C and 40D)**.

To confirm this localization, we performed biochemical subcellular fractionation of cells expressing VopQ. A purification schematic is shown in **Figure 41A**. This describes the separation of the nuclei (P1), organelles (P10), plasma membrane (P100), and the soluble lysate (S100). The integrity of each fraction is confirmed using antibodies against lamin for the nuclei, calnexin for the P10 fraction, and aldolase for the soluble lysate

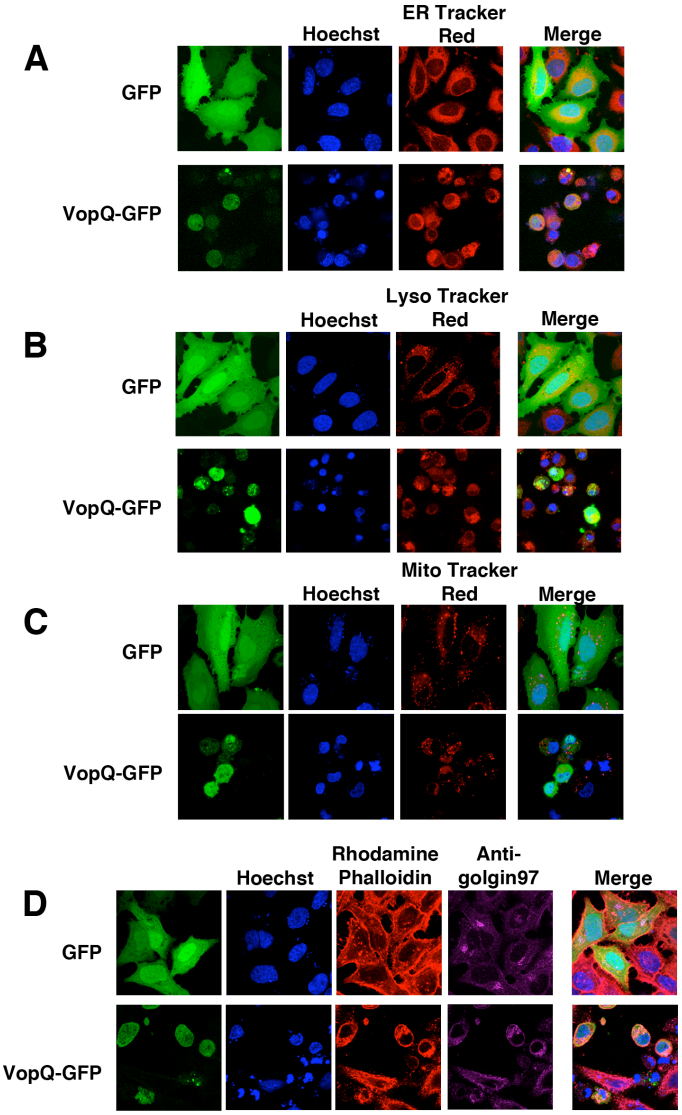

Figure 40. VopQ may localize to the endoplasmic reticulum. GFP or VopQ -GFP was transfected into HeLa cells. At 18 hours post-transfection, cells were incubated with ER Tracker Red **(A)**, Lyso Tracker Red **(B)** or Mito Tracker Red **(C)** with Hoechst (nuclei, blue) for 30 minutes at 37°C. Cells were fixed and visualized by confocal microscopy. In **(D)**, cells were fixed at 18 hours post-transfection and processed for immunofluorescence with anti-golgin97 antibodies (pink). Cells were stained for actin (red) and the nuclei (blue).

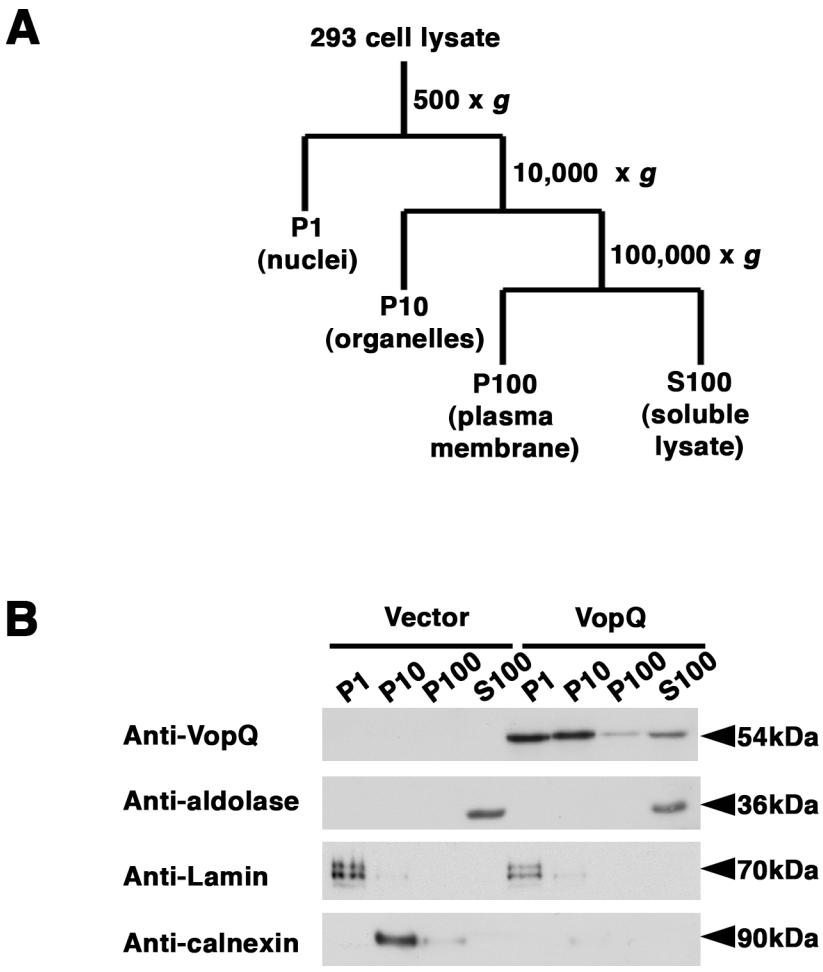

Figure 41. VopQ may localize to the endoplasmic reticulum. **(A)** Schematic depicting centrifugation steps isolating subcellular organelles. **(B)** 293 cells were transfected with vector or VopQ and subjected to the centrifugation steps in **(A)**. Samples were processed for Western blot analysis and membranes were probed with anti-VopQ, anti-aldolase (soluble lysate), anti-Lamin (nuclei), and anti-calnexin (endoplasmic reticulum) antibodies.

via Western blot analysis. HEK293 cells were transfected with vector alone or vector expressing VopQ. Lysates were harvested and subjected to the centrifugation steps described in **Figure 41A**. In cells transfected with vector alone, the integrity of each fraction was confirmed using anti-lamin, anti-calnexin and anti-aldolase antibodies. This demonstrated that the purification scheme used efficiently separated each fraction without contaminating others. In VopQ-transfected cells, VopQ is found predominantly in the P10 fraction that contains subcellular organelles such as the endoplasmic reticulum **(Figure 41B)**. Interestingly, the amount of calnexin in VopQ transfected cells is reduced compared to vector alone transfected cells. However, the integrity of other compartments remained intact as indicated by markers of the nuclei (Lamin) and cytoplasm (aldolase) **(Figure 41B)**. These results characterize a putative membrane localization domain encoded within VopQ and imply VopQ may localize to a subcellular compartment, potentially the endoplasmic reticulum.

Discussion:

VopQ is a type III effector secreted from the T3SS on chromosome 1 of *V. parahaemolyticus* (Ono et al., 2006). We have determined *V. parahaemolyticus* induces a temporally controlled series of events that

begins with the induction of autophagy, followed by cell rounding, and then lysis that is caspase independent (Burdette et al., 2008). We attribute the induction of autophagy and a component of cellular lysis to the type III effector VopQ (Burdette et al., Submitted March 2009). In this chapter, we describe experiments aimed in the effort to understand the molecular mechanism of VopQ-mediated cytotoxicity and autophagy.

Previous research on *V. parahaemolyticus* demonstrated T3SS1 was required for cytotoxicity in a tissue culture model of infection and secreted 4 T3SS effectors (VopQ, VopS, VP1656, and VPA450) (Ono et al., 2006). T3SS2 has been shown to be responsible for enterotoxicity and secretes the effectors VopA, VopC, VopL and VopT (Trosky et al., 2007, Liverman et al., 2007, Kodama et al., 2007). Many Gram-negative bacterial pathogens that utilize multiple type III secretion systems, coordinately regulate them. For instance, the Salmonella SPI1 and SPI2 secretion systems regulate seemingly disparate events during infection by modulating effector expression, secretion and degradation within each system (Kubori & Galan, 2003). We wanted to understand the kinetics of VopQ expression and secretion by *V. parahaemolyticus* in an *in vitro* secretion assay. We demonstrate that immediately following shift to higher temperatures and low calcium conditions, VopQ is rapidly produced and

secreted into the tissue culture media in both POR1 and POR3 strains. Expectedly, we did not see secretion in POR2, since it lacks a functional T3SS1 **(Figure 32)**. This secretion profile is different from another effector, VopL, encoded on T3SS2, which requires different conditions for induction of secretion (Liverman et al., 2007). We hypothesize this difference reflects a mechanism of control of each T3SS by *V. parahaemolyticus*. We also show that secretion of other effectors encoded with T3SS1 are, for the most part, not affected by deletion of another effector within this locus **(Figure 33)**. Therefore, it is likely that in the case of *V. parahaemolyticus* T3SS1, the regulation of effectors may occur within the host cell.

We attempted to utilize *Y. pseudotuberculosis* as a heterologous expression system to study the molecular mechanism of VopQ. We were unable to use this system as *Y. pseudotuberculosis* did not secrete VopQ protein into the culture media. We attempted to express VP1682, the putative chaperone, in frame of VopQ but this did not result in VopQ secretion **(Figure 34)**. This plasmid used the coding sequence corresponding to *vp1682* and *vopQ* but it did not include any of the upstream sequences that would include the *V. parahaemolyticus* promoter since expression depended on an IPTG-inducible promoter. Interestingly, complementation of the *ΔvopQ* deletion in *V. parahaemolyticus* required

almost 1000bp upstream of *vopQ*, a region that includes *vp1682* and the putative promoter. Future efforts at using *Y. pseudotuberculosis* will refine the genetic region used to include more upstream sequences.

VopQ is extremely cytotoxic when transfected into tissue culture cells or expressed in yeast (Chapter 6). The VopQ phenotype is reminiscent of a type III effector from *P. aeruginosa*, ExoU. Like VopQ, ExoU is a highly potent and cytotoxic enzyme and we asked if, on a sequence level, they shared any conservation. ExoU is a phospholipase and harbors a nucleotide binding region and conserved serine and aspartic acids residues essential for catalysis. While VopQ harbored nearly all of these residues, neither mutation of the conserved serine nor aspartic acids residue appreciably inhibited VopQ cytotoxicity. In addition, Infection of HeLa cells with *V. parahaemolyticus* POR3 in the presence of two different phospholipase inhibitors MAFP and BEL did not abrogate cytotoxicity. Thus, we concluded VopQ is not a phospholipase.

Finally, using a Kyte Doolittle hydrophilicity plot, we identified a hydrophobic segment in the middle of VopQ. This hydrophobic domain may comprise a segment of VopQ that mediates membrane insertion. In addition, it divided VopQ into two segments. We generated deletion constructs to understand the role, if any, of each segment. Unfortunately,

neither amino or carboxyl terminal segments with or without the hydrophobic region recapitulated the phenotype seen with full-length VopQ (Figure 36 and 37). Interestingly, microscopic and biochemical localization studies do somewhat support the localization of VopQ to fractions containing subcellular organelles (Figure 38 and 39). Sucrose gradient centrifugation is the necessary next step to delineate the true subcellular localization of VopQ in host cells. Since the inception of this project in 2004, full length and truncated amino acid sequences for VopQ have been subjected to repeated BLAST analysis. The only results have been closely related orthologues in *V. alginolyticus* and *V. harveyi*. We hypothesize that the function of VopQ, once understood, will reveal conservation in tertiary amino acid structure. This is common for guanine nucleotide exchange factors that have limited primary amino acid sequence homology but share similarities in fold (Schlumberger et al., 2003). Ultimately, the work presented herein sets the stage for future experiments on the type III effector VopQ.

Chapter 8

Characterizing the Role of Autophagy During Infection

Introduction:

Autophagy is the process by which cells degrade long-lived proteins and remove damaged organelles via lysosomal proteases. The importance of autophagy in cellular growth, differentiation and development is without question, yet its role in cellular death is still being defined. In contrast to apoptosis, which requires activation of caspases, autophagy is primarily a caspase-independent process that requires a distinct set of autophagy genes (Lockshin & Zakeri, 2002). Furthermore, some research suggests that these pathways are mutually exclusive or that there is a balance between them. Thus, the decision between apoptosis and autophagy or even other cell death mechanisms is a critical step in determining cellular fate; however, the mechanisms that govern this decision are not well understood. In many instances, cells unable to undergo autophagy either by genetic mutation or chemical inhibition default to apoptosis. Conversely, cells under the influence of apoptotic inhibitors that are exposed to various types of stress are capable of

activating autophagic machinery (Maiuri et al., 2007). Recently, research from our lab revealed that *V. parahaemolyticus* induces a proinflammatory, multifaceted mechanism that rapidly kills host cells (Burdette et al., 2008). Initially, infected cells induce acute autophagy, followed by cell rounding and then cell lysis. Death of the host cell is caspase-independent. These events are all temporally coordinated by T3SS1, one of the two type III secretions systems of *V. parahaemolyticus* (Makino et al., 2003). These results raise several questions about the role of autophagy during infection: What is the evolutionary reason for the induction of autophagy by *V. parahaemolyticus*? Does the induction of autophagy antagonize the induction of apoptosis in infected cells? Are there cellular stresses responsible for the induction of autophagy and cellular lysis? This chapter presents data that sought to answer these questions and others about the nature of T3SS1-dependent autophagy and cell death.

Results:

T3SS1 Induces Autophagy by a Unique Mechanism

V. parahaemolyticus uses the T3SS encoded on chromosome 1 to induce autophagy, cell rounding and ultimately death (Burdette et al.,

2008). We have shown that the induction of autophagy and in part, cell lysis, can be attributed to the action of VopQ, a type III effector encoded within T3SS1. These results demonstrated VopQ induces autophagy in a PI3-kinase-independent manner (Burdette et al., Submitted March 2009). We sought to examine the role of the TOR protein in VopQ-dependent induction of autophagy. TOR was identified in 1994 as the eukaryotic target of the drug rapamycin (Brown et al., 1994). TOR is a serine/threonine kinase that acts in response to nutrient levels to regulate cell growth and survival. During autophagy, signaling through TOR is shut down in response to nutrient starvation (Diaz-Troya et al., 2008). Therefore, we wanted to know if VopQ-dependent autophagy required signaling through TOR. We infected GFP-LC3 HeLa cells with POR3, POR3Δ*vopQ*, POR3Δ*vopS*, and ΔT3SS1/ΔT3SS2 strains and examined cell lysates via Western blot using antibodies against GFP, phospho-TOR, and phospho-p70 S6 kinase (p70S6K), a downstream target of TOR. In mock-infected cells, autophagy is not induced as measured by a lack of LC3 conversion and phosphorylation of TOR and p70S6K **(Figure 42; lane 1)**. In response to starvation, we can see less and LC3-I, TOR is off and not signaling to downstream targets such as p70S6K

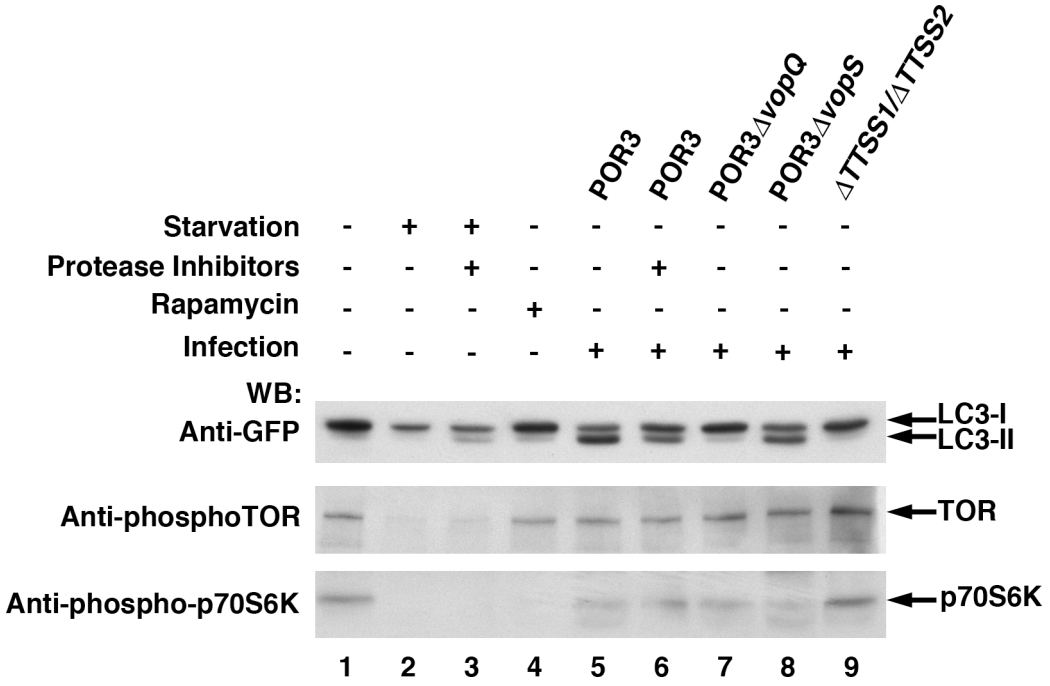

Figure 42. Induction of autophagy during infection is independent of TOR signaling. GFP-LC3 HeLa cells were either starved with HBSS or treated with 1μg/mL rapamycin for 4 hours. Cells were also mock infected or infected with the indicated strains for 2 hours. Protease inhibitors pepstatin A (10μg/mL) and E64-d (10μg/mL) were used for 4 hours (starved) or 2 hours (POR3). Cells were lysed and processed for Western blot analysis. Membranes were probed with anti-GFP, anti-phosphoTOR and anti-phosphop70S6K antibodies.

(Figure 42; lane 2). Starvation in the presence of protease inhibitors pepstatin A and E64-d inhibits lysosomal proteases thus stabilizing the LC3-II form **(Figure 42; lane 3)**. Furthermore, rapamycin also inhibits TOR as its downstream target p70S6K is not phosphorylated **(Figure 42; lane 4)**. During *V. parahaemolyticus* infection, POR3 induces robust LC3-II conversion **(Figure 42; lane 5)**. This phenomenon is not enhanced in the presence of protease inhibitors that stabilized LC3-II **(Figure 42; lane 6)**. LC3-II conversion is abrogated in infection with POR3*ΔvopQ and* ΔT3SS1/ΔT3SS2 but not with POR3*ΔvopS* **(Figure 42; lanes 7, 8, and 9 respectively)**. However, we see no change in TOR phosphorylation or p70S6K phosphorylation during infection with these *V. parahaemolyticus* strains **(Figure 42; lanes 5-9)**. These results indicate T3SS1-mediated induction of autophagy does not proceed through the TOR pathway.

Our data suggest VopQ induces autophagy by a novel mechanism and this is supported by our yeast results that demonstrate the lack of requirement for classic autophagy genes for VopQ mediated autophagy. Therefore, we sought to examine the role of other cellular factors required for autophagy. Forming autophagosomes require microtubules to traffic to and fuse with lysosomes. Disruption of microtubules with the microtubule depolymerizing agent nocodazole significantly lowers the number of

autophagic vesicles in the cell (Fass et al., 2006). Therefore, we examined the role of microtubules during T3SS1-mediated autophagy. GFP-LC3 HeLa cells were untreated or pretreated with nocodazole and then mock infected, starved, or infected with POR3. Following infection, cells fixed and processed for immunofluorescence using anti-tubulin antibodies, in untreated, mock-infected cells, tubulin forms a peri-nuclear net-like structure. After incubation with nocodazole, tubulin is diffuse and no longer organized into tubules. In untreated and treated starved cells, we see GFP-LC3 punctae indicating the cell is undergoing autophagy. In untreated POR3 infected cells, we see the characteristic accumulation of GFP-LC3 punctae however, treatment with nocodazole does not abrogate punctae formation **(Figure 43)**. These results demonstrate T3SS1-mediated autophagy does not require microtubules as GFP-LC3 punctae formation still occurs despite microtubule depolymerization. We also asked if transport from the Golgi apparatus was required for T3SS1-mediated induction of autophagy using brefeldin A. Brefeldin A treatment causes the golgi to collapse onto the endoplasmic reticulum, golgi protein dispersal and inhibition of transport from the golgi (Helms & Rothman, 1992, Kaufman, 1999, Breckenridge *et al.*, 2003). GFP-LC3 HeLa cells were

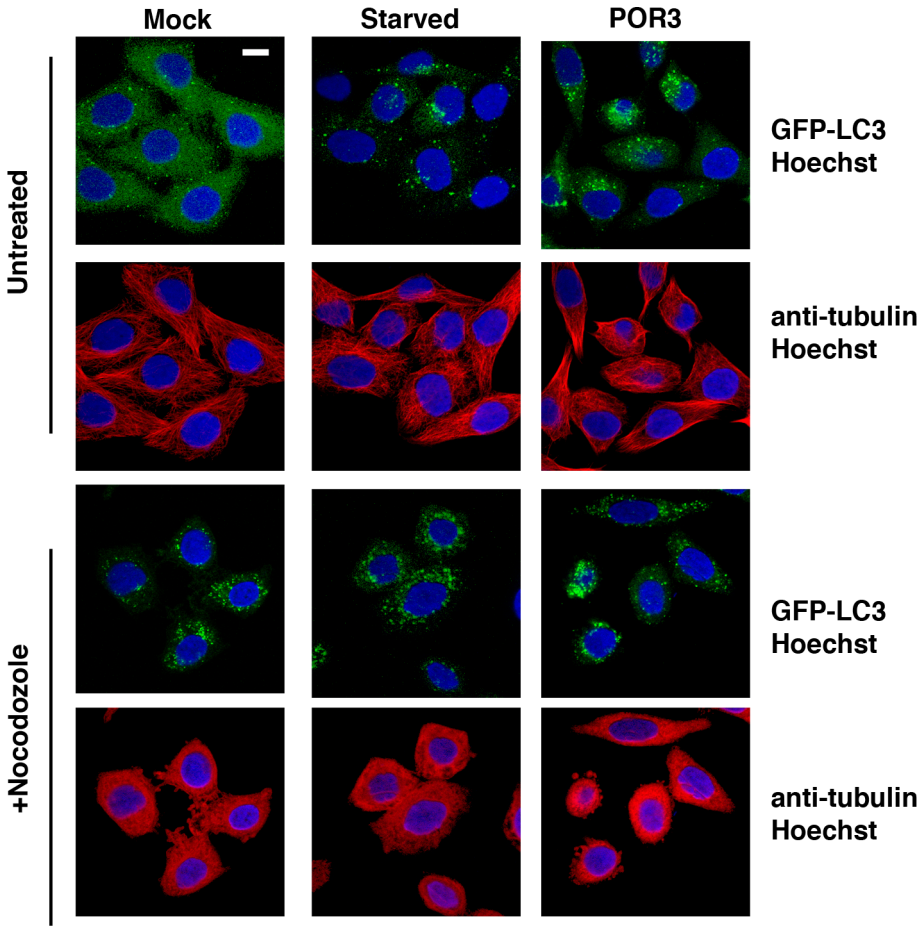

Figure 43. Induction of autophagy does not require microtubules. GFP-LC3 HeLa cells were either mock infected, starved for four hours, or infected with POR3 for 2 hours. Cells were fixed and processed for immunofluorescence using anti-tubulin antibodies and Hoechst to stain for nuclei.

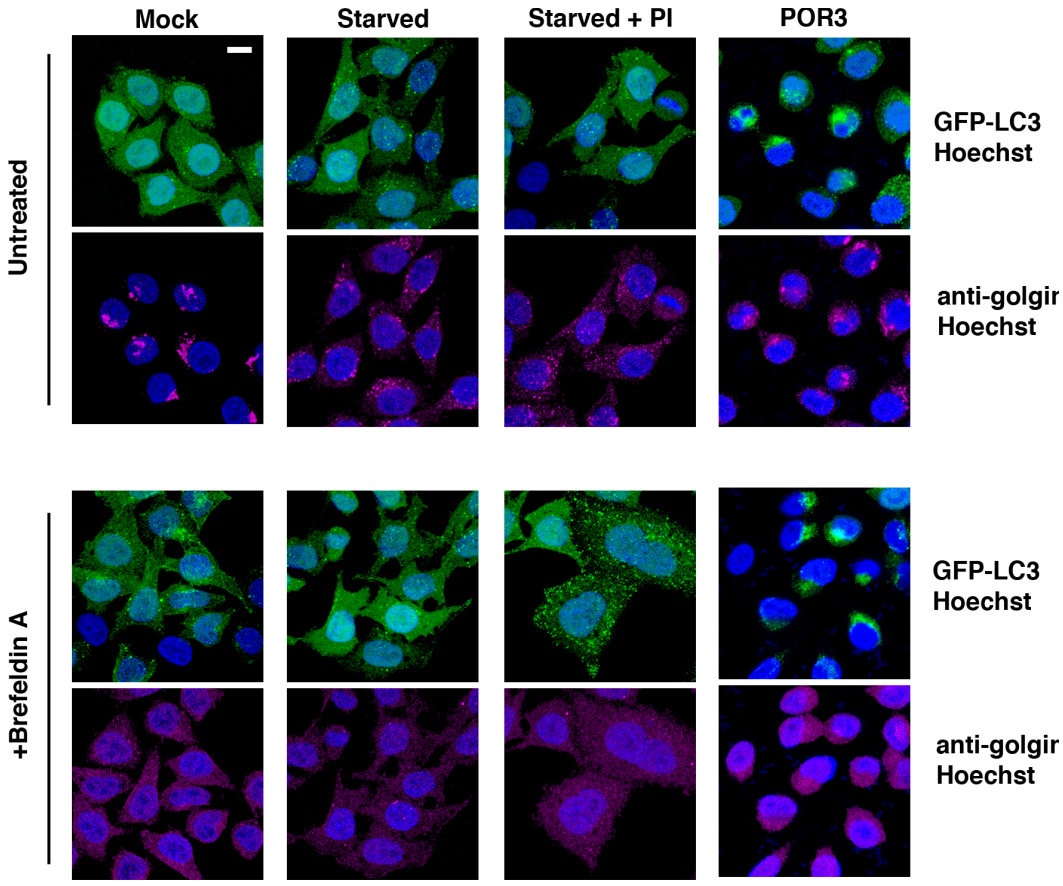

Figure 44. POR3-induced autophagy does not require transport from the Golgi. GFP-LC3 HeLa cells were either mock infected, starved in the absence or presence of protease inhibitors for four hours or infected with POR3 for two hours. Cells were fixed and processed for immunofluorescence using anti-golgin97 antibodies and Hoechst to stain for nuclei.

infected as above and processed for immunofluorescence using an anti-golgin97 antibody that recognizes golgin97, a Golgi resident protein. In mock-infected cells, we can see the characteristic pattern of golgi staining, however upon brefeldin A treatment, we no longer see anit-golgin97 immunofluorescence. In POR3 infected cells, disruption of the Golgi has no effect on the induction of autophagy during infection as shown by GFP-LC3 punctae accumulation **(Figure 44)**. Therefore, we can conclude from these data that neither microtubules nor the Golgi apparatus is required for induction of autophagy during infection.

Induction of Autophagy and Nutrient Scavenging

We entertained the possibility that *V. parahaemolyticus* may be utilizing autophagy to gain access to essential nutrients. In order to demonstrate this, we employed the long-lived protein degradation assay. Short-lived cellular proteins are degraded by the ubiquitin:proteasome system, however autophagy degrades long-lived proteins in the cell (Mortimore & Mondon, 1970, Seglen *et al.*, 1980). The degradation of long-lived proteins can be used as a tool to monitor the process of autophagy. First, we label the cell with ^{14}C-valine, which gets incorporated into proteins during protein synthesis. The radioactivity is chased with cold

valine for a short period of time to allow for the degradation of short-lived proteins. Then, autophagy is induced in the presence of cold valine and the cell free supernatant is analyzed for the presence of radioactivity as a sign of autophagy-specific protein degradation. In order to distinguish radioactive proteins from 14C-valine released as a result of degradation, the proteins in the supernatant are precipitated with TCA. The degraded ^{14}C-valine remains in the acid soluble portion. During starvation, a 1-2% increase in the acid soluble radioactivity is a significant for the induction of autophagy (Tamai *et al.*, 2007, Klionsky et al., 2007). We evaluated mock, starved and POR3 infected cells for the induction of autophagy using this long-lived protein degradation assay. While mock infected cells show an increase over time of approximately 0.5% per hour, starved cells show a 1.5% increase per hour in the acid-soluble radioactivity indicating long-lived proteins are being degraded by autophagy. POR3-infected cells are able to induce a 1% increase in the release of acid-soluble radioactivity between 1 and 2 hours, however there is no significant increase in acid-soluble radioactivity in later time points **(Figure 45A)**. These results demonstrate that we are able to quantitate autophagy during starvation and infection, albeit at early time points.

At 3 hours post-infection with POR3, we begin to see LDH release into the supernatant corresponding to cellular lysis (Burdette et al., 2008). We hypothesized that we are unable to see the change in acid-soluble radioactivity at later time points during infection because *V. parahaemolyticus* is rapidly consuming the ^{14}C-valine made available by autophagy. If this were the case, we should see an increase in the amount of radioactivity associated with the bacteria. To address this, we infected ^{14}C-valine labeled cells as above with POR3. At various time points, culture supernatant was harvested and the infected cells were washed to remove all the bacteria associated with the cells. The bacteria were isolated by centrifugation from the supernatant and subsequent washes and counted in a scintillation counter for the presence of radioactivity. In this assay, we saw an increase in the amount of bacterial associated radioactivity over time **(Figure 45B)**. This result supports our hypothesis that the bacteria are consuming the valine degraded in response to autophagy.

V. parahaemolyticus may be inducing autophagy to gain access to specific nutrients. During infection pathogenic bacteria have an absolute requirement for iron and have developed multiple iron scavenging

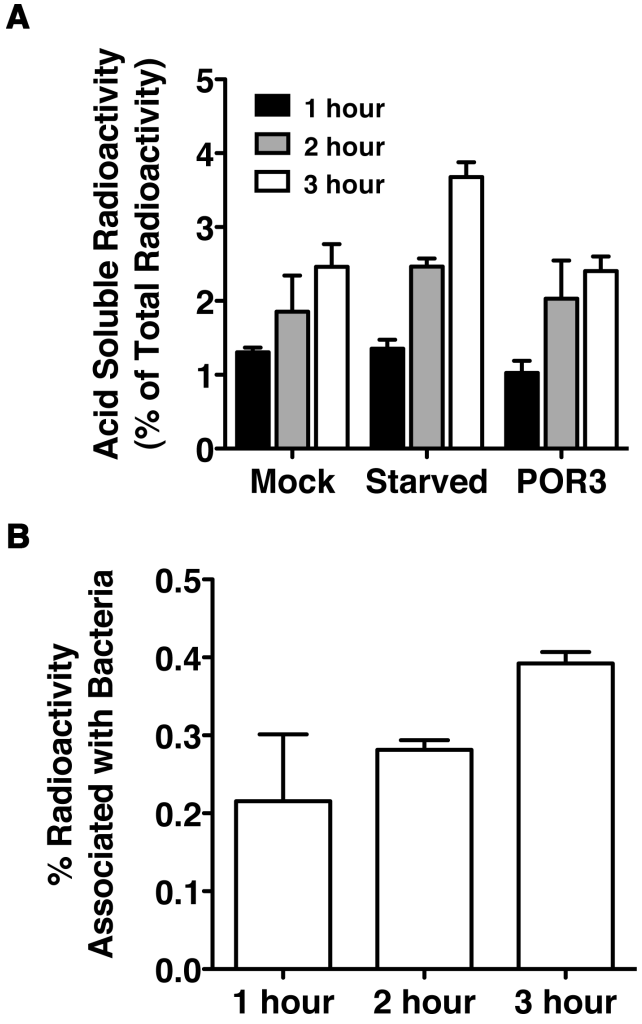

Figure 45. Measurement of nutrient release and uptake during *V. parahaemolyticus* infection. HeLa cells were pulsed with ^{14}C-labeled valine and chased to eliminate radiolabeled short-lived proteins. Following the chase, cells were either mock infected, starved, or infected with POR3. **(A)** At the indicated time points, cell culture supernatant was collected and TCA-precipitated. The supernatant after this precipitation is the acid-soluble fraction and contains radioactivity released as a result of long-lived protein degradation. Results are shown as percent of the total cellular radioactivity. **(B)** HeLa cells are labeled as in **(A)** and infected with POR3. At the indicated time points, bacteria were measured for the amount of acquired radioactivity reflected as the percent of total cellular radioactivity.

mechanisms (Schaible & Kaufmann, 2004). We hypothesized that induction of autophagy by *V. parahaemolyticus* may also allow access to iron sequestered in iron-containing proteins. Iron-starved *V. parahaemolyticus* would induce autophagy during infection and the nutrients obtained as a result would allow for the bacteria to proliferate. In contrast, iron-starved *V. parahaemolyticus* unable to induce autophagy would be unable to proliferate during infection. In this aim, we first titrated the iron chelator 2'2'-bipyridyl (BP) and established the ideal concentration that efficiently chelated iron but did not kill the bacteria **(Figure 46A)**. Iron chelation with BP efficiently inhibited growth and that adding exogenous iron to the cultures restored growth **(Figure 46B)**. We infected HeLa cells with POR3, BP-treated POR3, *ΔT3SS1/ΔT3SS2*, and BP-treated *ΔT3SS1/ΔT3SS2* strains and assayed for proliferation using a viable cell count assay. We did not see a significant difference between POR3 and ΔT3SS1/ΔT3SS2 strains in their ability to proliferate during infection. In addition, iron-chelation did not affect the ability of either strain to proliferate during infection **(Figure 47)**. These results show that the bacteria are able to proliferate during infection independently of their ability to scavenge nutrients or induce cytotoxicity.

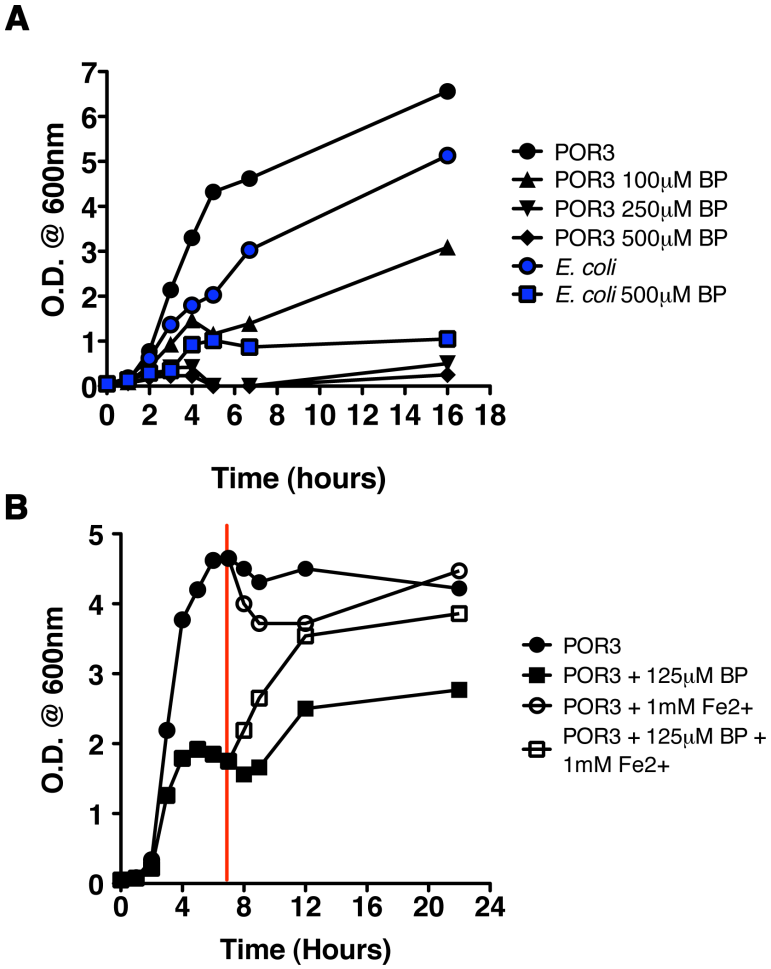

Figure 46. Iron chelation inhibits *V. parahaemolyticus* growth. **(A)** Overnight cultures of *V. parahaemolyticus* POR3 and *E. coli* K12 were diluted back into media containing various concentrations of the iron chelator 2'2'-bipyridyl and monitored for growth over time using optical density at 600nm. **(B)** Overnight cultures of *V. parahaemolyticus* were diluted back into media containing 125μM 2'2'-bipyridyl and monitored for growth over time by optical density at 600nm. At 7 hours post-inoculation (red line), 1mM iron sulfate (Fe^{2+}) was added to the culture media.

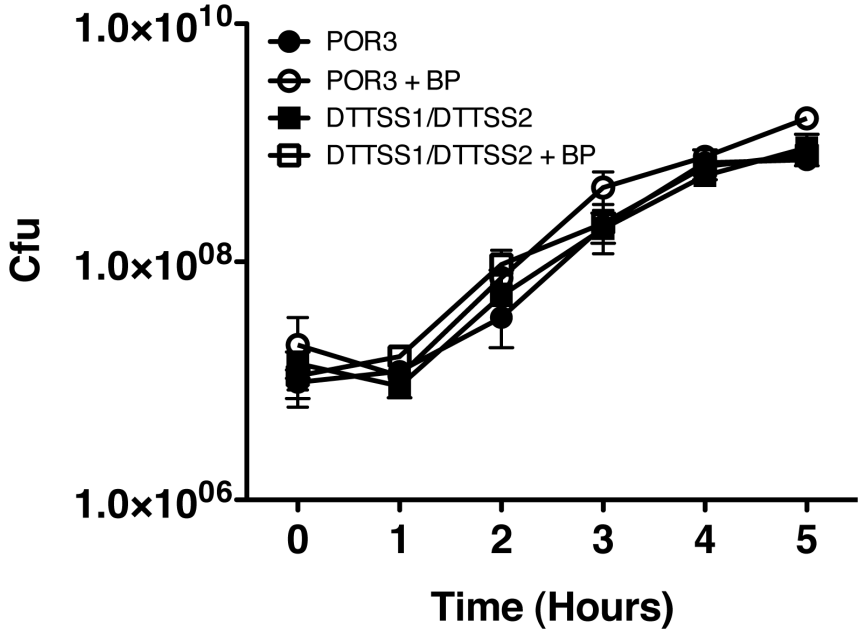

Figure 47. Iron chelation does not enhance *V. parahaemolyticus*' potential to obtain cellular nutrients. *V. parahaemolyticus* strains POR3 or ΔT3SS1/ΔT3SS2 left untreated or treated with 2'2'-bipyridyl to chelate iron were used to infect HeLa cells. At the indicated time points, media was removed and diluted serially onto MMM + gal and grown for two days at 30°C after which time, colony forming units were counted.

Understanding *V. parahaemolyticus* Induced Cell Death

We demonstrate *V. parahaemolyticus* infection results in induction of autophagy, cell rounding and inflammatory cell lysis. This process proceeds independently of apoptosis as we do not see caspase activation during infection (Burdette et al., 2008). However, other caspases mediate cell death processes distinct from apoptosis. Caspase 1 is part of an intracellular protein complex called the inflammasome that mediates a form of cell death called pyroptosis that involves cell lysis and activation and release of IL-1β. Bacteria such as *Salmonella enterica, Legionella pneumophila*, and *Shigella flexneri* induce caspase 1 mediated cell death during infection (Suzuki *et al.*, 2007, Amer *et al.*, 2006, Fink & Cookson, 2006). We hypothesized that *V. parahaemolyticus* induced cell death involves caspase 1 and the inflammasome since T3SS1-mediated cell death is also highly inflammatory. To test this, we infected immortalized B6 caspase 1-/- macrophages with POR3 and assayed for the ability of these bacteria to induce LDH release. Compared to immortalized wild-type B6 macrophages, we did not see a significant difference in the ability of POR3 to induce cell lysis in the absence of caspase 1 **(Figure 48)**. These results show that caspase 1 is not required for T3SS1-dependent cell death.

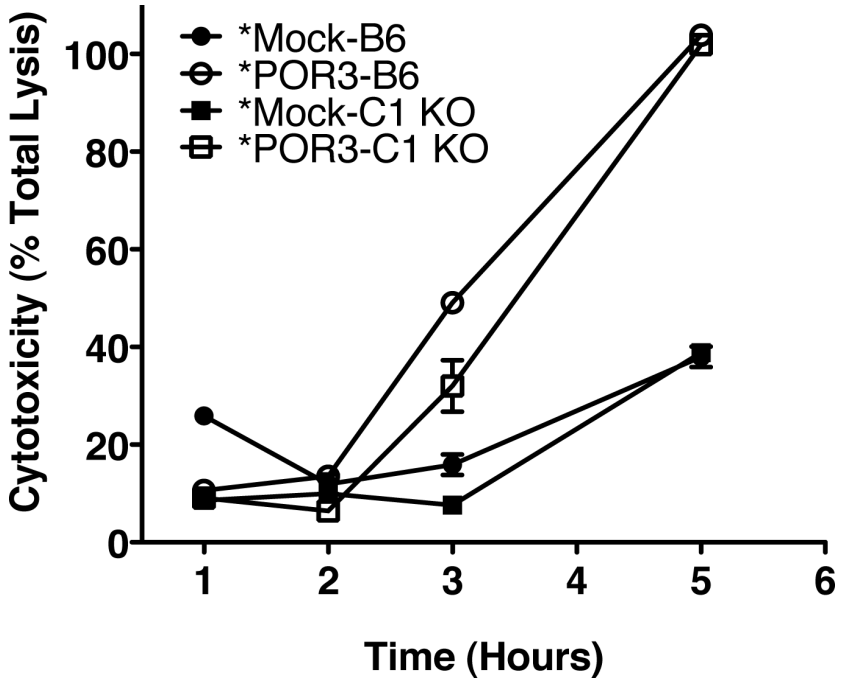

Figure 48. T3SS1-mediated cell death does not require caspase 1. Immortalized wild type or caspase 1-/- macrophages were either mock infected or infected with POR3. At the indicated time points, At the indicated time points, cytotoxicity was measured by LDH release as described. Cytotoxicity is reflected as percent of total lysis in 1% Triton X-100.

Inflammatory cell death can also occur as a result of pore-forming toxins that physically disrupt host cell membranes causing cellular lysis. The cytotoxicity seen during T3SS1-mediated cell death may be the result of one of the T3SS1-encoded effectors functioning as a pore-forming toxin. The amino acid glycine has been shown to act as a cytoprotectant, inhibiting the release of cytoplasmic contents as a result of pore-formation (Fink & Cookson, 2005, Mejia *et al.*, 2008). We hypothesized that an effector encoded on T3SS1 acts as a pore-forming toxin following secretion into host cells. In order to test this, we infected HeLa cells with induced and uninduced POR3 in the absence and presence of 5mM and 10mM glycine. Neither 5mM nor 10mM glycine had an effect on the ability of POR3 to induce cytotoxicity **(Figure 49)**. This demonstrates that T3SS1-mediated cytotoxicity does not occur as a result of pore-formation in the host cell membrane.

The ER is an organelle involved in protein synthesis. In addition, it functions as an intracellular calcium storage unit. Inhibition of protein synthesis or deregulation of the calcium gradient can induce ER stress that can result in necrosis leading to cell lysis and death. ER stress can be induced through induction of an unfolded protein response or deregulation

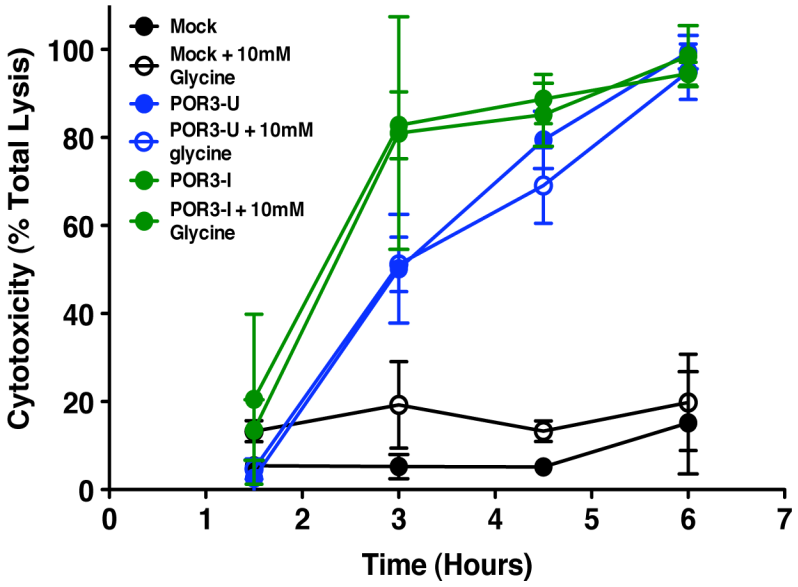

Figure 49. *V. parahaemolyticus* does not induce pyroptosis. HeLa cells were pretreated with 5mM or 10mM glycine for 30 minutes prior to infection with POR3. Glycine was maintained throughout the duration of the infection. At the indicated time points, cytotoxicity was measured by LDH release as described. Cytotoxicity is reflected as percent of total lysis in 1% Triton X-100.

of inositol phosphate 3 (IP_3) receptors leading to inappropriate calcium release. Salubrinal (SAL) is an inhibitor of phosphates that dephosphorylate eukaryotic initiation factor 2 subunit α (eIF2α) and protects against ER-stress induced cell death (Boyce et al., 2005). Xestospongin C (XeC) blocks IP_3-mediate calcium release (Gafni et al., 1997). In order to address the role of ER stress in T3SS1-mediated cell death, we treated HeLa cells with inhibitors of ER stress during infection with POR3. Treatment of HeLa cells with either salubrinal or xestospongin C did not block LDH release during infection **(Figure 50)**. This suggests the mechanism of cytotoxicity proceeds independently of the generation of ER stress through the unfolded protein response or deregulation of calcium stores.

The production of reactive oxygen species (ROS) can be damaging to a eukaryotic cell. Their high reactivity can damage cell structures including organelles and lipids that can reduce function and survival. We have evolved mechanisms to counteract the negative effects or ROS through redox pathways, superoxide dismutase and catalase, all which function to maintain ROS levels in the cell at a tolerable level. Yu and colleagues have demonstrated that degradation of catalase by autophagy

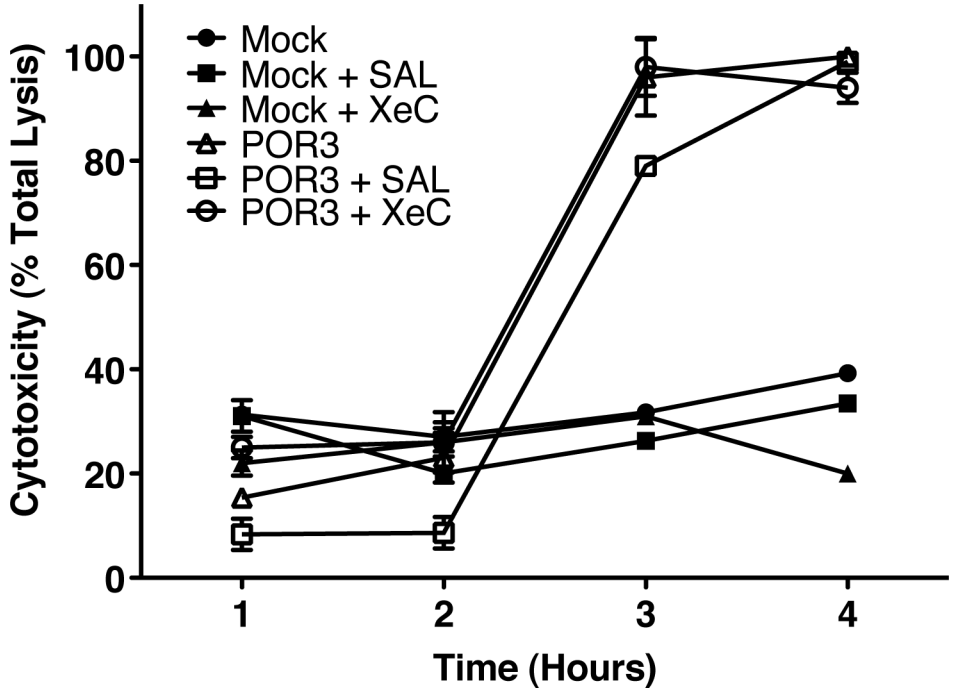

Figure 50. Inhibitors of ER stress do not prevent LDH release during *V. parahaemolyticus* infection. HeLa cells were treated with 20μM Salubrinal and 1μM Xestospongin C and either left uninfected or infected with POR3. At the indicated time points, cytotoxicity was measured by LDH release as described. Cytotoxicity is reflected as percent of total lysis in 1% Triton X-100.

results in the accumulation of reactive oxygen species that ultimately result in the death of the cell (Yu et al., 2006). We hypothesized that T3SS1-mediated cell death may involve the production of toxic ROS. In order to test this, we used an inhibitor of ROS, butylated hydroxyanisole (BHA). BHA does not have an impact on *V. parahaemolyticus* growth **(Figure 51A)**. Therefore we assessed its impact of the ability of POR3 to induce LDH release. Treatment with BHA significantly abrogated POR3-induced cell death during the early stages of infection as measured by LDH release **(Figure 51B)**. These results indicate ROS production may be a key mediator of T3SS1-dependent inflammatory cell death.

Discussion:

In this chapter, we attempt to understand the function of POR3-induced autophagy and its role during infection. First, we assessed the role of the TOR pathway during infection. Interestingly, we did not see a change in TOR phosphorylation or in TOR's ability to phosphorylate a downstream target. Although the mechanism is unknown, PI3-kinase signaling is upstream of the TOR pathway. Therefore, these results support our yeast data suggesting VopQ (via T3SS1) is inducing

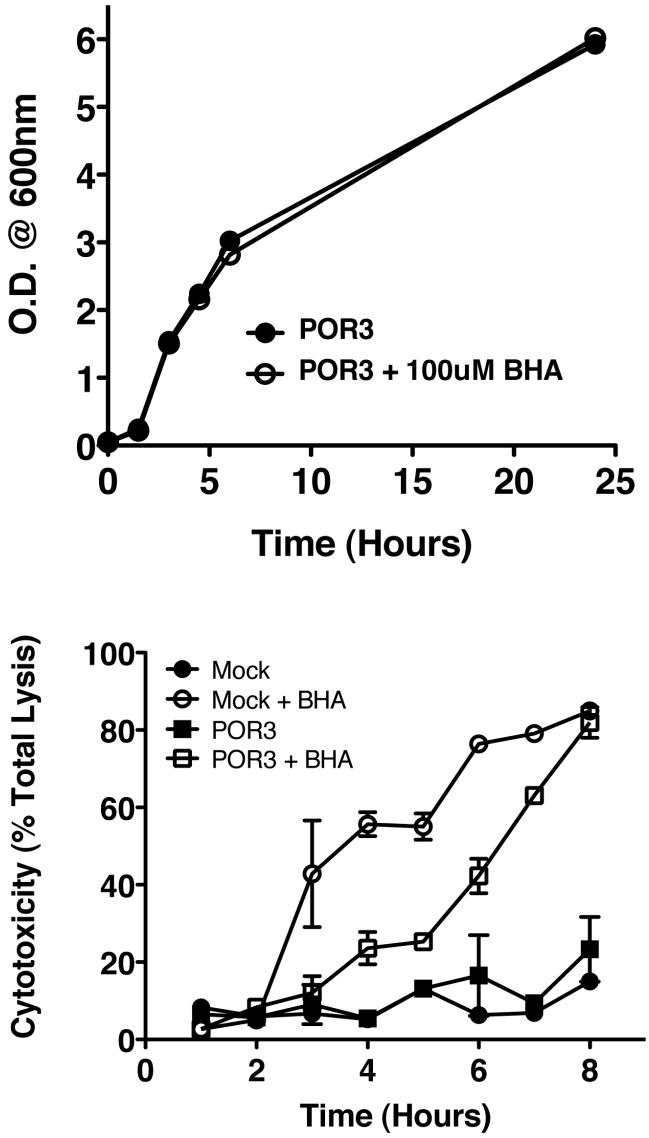

Figure 51. The antioxidant BHA protects against T3SS1-mediated cell death. **(A)** Overnight cultures of POR3 were diluted into fresh media alone or media containing 100μM BHA and monitored for growth over time. **(B)** HeLa cells were incubated with 100μM BHA for 30 minutes and then infected with POR3 in the presence of 100μM BHA. At the indicated time points, cytotoxicity was measured by LDH release as described. Cytotoxicity is reflected as percent of total lysis in 1% Triton X-100.

autophagy in a PI3-kinase independent manner. Why might *V. parahaemolyticus* induce autophagy at such an accelerated rate during the initial stages of infection? One possibility is that *V. parahaemolyticus* may be utilizing autophagy to gain access to essential nutrients. By inducing autophagy, the bacteria force the cell to do the work for them. The end result is an increased pool of amino acids in a readily usable form, perhaps the first example of bacterial fast food. As a gastrointestinal pathogen, these bacteria have evolved mechanisms to rapidly access nutrients, before being expelled from the host. We attempted to address this issue using a long-lived protein degradation assay, however this assay was complicated by the extremely cytotoxic nature of *V. parahaemolyticus*. As a result we were unable to conclusively demonstrate specific nutrient release and bacterial consumption. After removing the bacteria as described above, we noticed that many bacteria remained on the plate. In addition, we began to see an increase in the amount of bacteria associated radioactivity at exactly the same time we begin to see LDH release (Burdette et al., 2008). We are unable to distinguish between ^{14}C-valine released by the cell as a result of autophagy-mediated degradation and ^{14}C-valine released as a result of POR3-mediated cytotoxicity.

The degradation of intracellular organelles might also provide access to an important and essential metal, iron. *V. parahaemolyticus* is poised to scavenge iron and is known to contain complex regulatory mechanisms for this purpose (Lemos & Osorio, 2007). However, in our assay, we were unable to see a difference in proliferation between *V. parahaemolyticus* strains capable of inducing autophagy and those unable to do so, or a difference between chelated and non-chelated bacteria. Given the limitations in experimental design, it remains to be seen if *V. parahaemolyticus* induces autophagy for a nutrient benefit.

We show in this chapter that *V. parahaemolyticus* induced cell death occurs independently of caspase 1. However, there is an inflammatory cell death that does not involve caspase 1 but requires other components of the inflammasome such as ASC (apoptosis-associated speck-like protein containing a caspase recruitment domain), NLRP3 (the NOD (nucleoside oligimerization domain)-like receptor protein 3), Cryopyrin, and CIAS1 (cold-induced autoinflammatory syndrome 1). This process has been called programmed necrosis and is a hallmark of *Shigella* and *Klebsiella* pathogenesis. Programmed necrosis leads to high mobility group box 1 (HMGB1) release from the cell and ROS production. During infection of NLRP3 knockout cells, *Shigella* survive within host cells and there is no

necrotic cell death (Willingham et al., 2007). This is similar to what we see during infection with the POR3*DvopQ* strain: reduced cytotoxicity and an increase in intracellular bacteria. Therefore, future research should be focused on the role of other inflammasome components such as ASC, NLRP3, cryopyrin, or CIAS1 in *V. parahaemolyticus* induced cell death.

Another feature of programmed necrosis is the production of ROS that irreversibly damage the host cell leading to death. Indeed, ROS may activate inflammasome components leading to a pro-inflammatory cell death (Franchi et al., 2009). Therefore, it is interesting that T3SS1-mediated cell death results from the production of ROS and does not require caspase 1. It is tempting to speculate that a single T3SS1-encoded effector is responsible for the accumulation of ROS, autophagy and cell lysis. Interestingly, the kinetics of LDH release during infection with POR3*ΔvopQ* resembles the LDH release profile or POR3 infection in the presence of BHA. The role of VopQ in the generation of reactive oxygen species will be pursued for future studies.

Chapter 9

Conclusions and Recommendations

Discussion of Research Findings

V. parahaemolyticus is a major causative agent of gastroenteritis associated with the consumption of raw or undercooked shellfish (Daniels et al., 2000). Virulence has been associated with the presence of thermolysins that cause hemolysis on Wagatsuma agar (Park et al., 2004a). This bacterium also harbors two T3SS, one on each chromosome that have been shown to contribute to virulence in both tissue culture and animal models of infection. This dissertation has focused on the T3SS on chromosome 1 that has been shown to be associated with both clinical and environmental *V. parahaemolyticus* strains (Park et al., 2004b). Previous research has attributed the cytotoxicity seen during infection to apoptosis, however we demonstrate that *V. parahaemolyticus* induces a temporally controlled series events that first involves the induction of autophagy, followed by cell rounding, and culminating in release of cellular contents and death (Burdette et al., 2008, Ono et al., 2006). Interestingly, we demonstrate that *V. parahaemolyticus* induced autophagy does not

contribute to cell lysis as inhibition of autophagy with the PI3-kinase inhibitor wortmannin does not abrogate cytotoxicity (Burdette et al., 2008). In addition, others have shown T3SS1-mediated cell death can be abrogated by the addition of cytoprotectants and therefore attributed cell death due to oncosis. In this study, they used strain NY-4, which is different from the sequenced RIMD2210633 strain used in this dissertation (Zhou et al., 2009).

We focused our analysis on the effectors encoded within T3SS1 in order to gain a better understanding of autophagy induction, cell rounding and cell lysis. To date, T3SS1 has been shown to secrete four effectors, VopQ, VopR, VopS and VPA450, however it is likely that all have not been identified yet (Panina et al., 2005). Research from our lab has attributed the cellular rounding phenotype to the T3SS effector VopS, which AMPylates Rho GTPases, leading to actin depolymerization (Yarbrough et al., 2009). This thesis focuses on the T3SS effector VopQ. We demonstrate VopQ is a type III secreted effector that is required for full virulence in a tissue culture model of infection. Furthermore, we show that VopQ is necessary and sufficient for the induction of autophagy during *V. parahaemolyticus* infection. In addition, VopQ-dependent induction of autophagy does not require PI3-kinases. Finally, induction of autophagy

prevents the cell from efficiently engulfing bacteria as macrophages infected with POR3Δ*vopQ* strains have more intracellular bacteria than macrophages infected with POR3 strains. We hypothesize VopQ mediated induction of autophagy redirects the cellular machinery away from phagocytosis towards autophagy (Burdette et al., Submitted March 2009).

This dissertation also seeks to highlight work done in characterizing the molecular mechanism of VopQ. While the molecular mechanism of VopQ is still unknown, the data presented in Chapters 6, 7, and 8 culminate in a deeper understanding of VopQ. We show that VopQ targets an evolutionarily conserved mechanism to induce both cytotoxicity and autophagy. Furthermore, the work done in *S. cerevisiae* confirmed that VopQ-mediated induction of autophagy is PI3-kinase-independent process and likely occurs through a novel mechanism. In addition, we describe several experiments that were designed to assess the putative function of VopQ. For instance, VopQ shares some distant homology with ExoU, a type III effector from *P. aeruginosa*, ExoU is a phospholipase that contributes to cytotoxicity during infection, much like VopQ. However, mutation of the catalytic residues did not abolish VopQ function and phospholipase inhibitors did not alter the kinetics of LDH release during *V.*

parahaemolyticus infection confirming VopQ is not a phospholipase. Therefore, the mechanism of VopQ is distinct from ExoU.

Furthermore, we identified a hydrophobic domain within VopQ that may potentially mediate membrane binding. Biochemical fractionation studies demonstrate that VopQ does predominantly localize to fractions that contain subcellular organelles such as the mitochondria, endoplasmic reticulum, and Golgi apparatus. Using confocal microscopy and dyes specific for several subcellular organelles, we show that VopQ-GFP colocalizes with compounds that specifically stain the ER.

The final chapter summarizes work done in efforts to understand POR3-mediated autophagy and its role during infection. We demonstrate the induction of autophagy during infection does not require the TOR signaling pathway. Our infection data using the PI3-kinase inhibitor wortmannin supports this conclusion. Experiments using yeast autophagy mutants further support a PI3-kinase independent induction of autophagy. In an effort to identify other cellular factors required for POR3-mediated autophagy, we inhibited transport from the Golgi, using brefeldin A. Brefeldin A selectively disrupted the Golgi but did not have an affect on the ability of POR3 to induce autophagy. This suggested POR3-induced autophagy does not require Golgi membranes. We also used nocodazole

to depolymerize microtubules. Trafficking of autophagic vesicles to the lysosomes has been shown to require an intact microtubule network. Loss of the microtubule network did not affect the ability of POR3 to induce autophagy.

We attempted to delineate the function of *V. parahaemolyticus* induced autophagy. We hypothesized that such rapid and acute induction of autophagy would induce the host cell to generate nutrients for *V. parahaemolyticus*. We attempted to show uptake of essential nutrients by *V. parahaemolyticus* during infection using a radio-labeled long-lived protein degradation assay, but were unable to conclusively show specific uptake. Next, we reasoned that access to these nutrients, such as iron, might provide a specific growth advantage to those bacteria capable of inducing autophagy. We showed that T3SS1-dependent induction of autophagy did not provide a significant growth advantage during infection.

Finally, we examined other factors that have been demonstrated to contribute to inflammatory death of host cells during infection. Many Gram-negative bacteria that induce a highly inflammatory cell death such as *Salmonella* and *Shigella*, activate caspase 1 and the inflammasome. In this aim, we used caspase 1 deficient macrophages to analyze the contribution of the inflammasome to T3SS1 mediated cytotoxicity, but

were unable to see a reduction in the severity of cytotoxicity. We also explored other cellular factors that might be manipulated by the bacteria and result in severe cytotoxicity during infection. In combination with data generated in Chapter 7, in which we show VopQ may be targeting the endoplasmic reticulum, we hypothesized that disruptions in ER integrity could independently lead to cytotoxicity and autophagy. ER stress can result from a loss in the calcium gradient or inhibition of protein synthesis. Therefore, we tested two different inhibitors of ER stress that target the IP3 receptor (XeC) and protein translation machinery (SAL). However, neither inhibitor was able to prevent POR3-dependent cytotoxicity. Finally, we investigated the role of toxic ROS during infection and demonstrated that inhibition of ROS can abrogate T3SS1-mediated cytotoxicity.

Main Contributions to the Field

Research summarized herein has provided an extensive study on the cell death mechanisms utilized by the Gram-negative pathogen *V. parahaemolyticus*. Prior to our understanding of T3SS1-mediated cell death, others have attributed host cell death in the tissue culture model of infection to apoptosis. We have discovered that in contrast to previous reports, *V. parahaemolyticus* induces a multi-faceted host cell death that

initiates with the induction of autophagy, followed by host cell rounding and culminates in the lysis of the host cell. Inhibition of autophagy does not prevent T3SS1-mediated cell lysis. The method by which *V. parahaemolyticus* induces autophagy and cell death represents a new paradigm in acute cell death. Our studies have contributed greatly to the understanding of the role of T3SS1 during infection.

In order to understand the molecular basis underlying T3SS1-dependent mediated cell death, we focused our attention on type III effectors encoded within T3SS1. Specifically, this dissertation focuses on the T3SS1-encoded effector, VopQ. We demonstrate VopQ is necessary and sufficient for the induction of autophagy during *V. parahaemolyticus* infection. This is the first example of the usurpation of autophagy by a type III effector from an extracellular pathogen. Furthermore, the induction of autophagy is independent of PI3-kinase. Very little is known about the signaling pathways downstream of nutrient sensing that mediate the first steps of autophagy. VopQ is novel tool for understanding this mysterious step in the initiation of autophagy.

Future Directions

The experiments presented herein set the stage for future work on T3SS1 of *V. parahaemolyticus* and its T3SS1-encoded effector, VopQ. We demonstrate that induction of autophagy may benefit the bacteria by redirecting cellular machinery away from the plasma membrane. This renders the host cell incapable of engulfing extracellular bacteria. This is confirmed in POR3*ΔvopQ* strains in which we see a significant amount of extracellular bacteria at 3 hours post infection compared to cells infected with POR3. Future efforts will focus on understanding the nature of this phenomenon. To address this, we will examine intracellular vesicular trafficking pathways. We know from data presented in chapters 7 and 8 that VopQ may localize to the ER. We will examine transport pathways that originate from the ER and analyze contributions made to the induction of autophagy and phagocytosis. In addition, we will pursue *in vivo* experiments in the germ-free mouse model.

In order to understand the mechanism of VopQ-mediated autophagy and its contribution to cytotoxicity, it is imperative to elucidate its molecular mechanism. To delineate the molecular mechanism, we propose additional studies using the yeast system. The initial studies presented in Chapter 6 demonstrate VopQ targets an evolutionarily

conserved mechanism however, screens to identify genes required for VopQ cytotoxicity were not successful. The yeast deletion library is a systematic deletion of all non-essential genes, however the very nature of VopQ's action suggests it is targeting a crucial regulatory pathway. We propose performing a multicopy suppressor screen in search of genes required for VopQ function. This screen includes all yeast genes, essential and non-essential and may also identify genes responsible for VopQ-mediated induction of autophagy.

Chapter 8 presents data showing inhibition of ROS abrogates T3SS1-mediated cytotoxicity. The generation of ROS during infection is a common hallmark of necrotic cell death, however recent studies have demonstrated ROS production may also be a component of caspase 1-independent inflammasome-dependent cell death. In the case of *Shigella*, inflammatory cell death does not require caspase 1 but does require other inflammasome components (Willingham et al., 2007). Regulation and function of the inflammasome is not well understood. Therefore, identifying inflammasome components required for T3SS1-mediated cell death may not only establish the mechanism of *V. parahaemolyticus* cell death but also deepen our understanding of inflammatory cell death mechanisms.

Bibliography

Abeliovich, H. & D. J. Klionsky, (2001) Autophagy in yeast: mechanistic insights and physiological function. *Microbiol Mol Biol Rev* **65**: 463-479, table of contents.

Ackermann, E. J., K. Conde-Frieboes & E. A. Dennis, (1995) Inhibition of macrophage Ca(2+)-independent phospholipase A2 by bromoenol lactone and trifluoromethyl ketones. *J Biol Chem* **270**: 445-450.

Akeda, Y. & J. E. Galan, (2005) Chaperone release and unfolding of substrates in type III secretion. *Nature* **437**: 911-915.

Alfano, J. R. & A. Collmer, (2004) Type III secretion system effector proteins: double agents in bacterial disease and plant defense. *Annu Rev Phytopathol* **42**: 385-414.

Amer, A., L. Franchi, T. D. Kanneganti, M. Body-Malapel, N. Ozoren, G. Brady, S. Meshinchi, R. Jagirdar, A. Gewirtz, S. Akira & G. Nunez, (2006) Regulation of Legionella phagosome maturation and infection through flagellin and host Ipaf. *J Biol Chem* **281**: 35217-35223.

Andersson, K., N. Carballeira, K. E. Magnusson, C. Persson, O. Stendahl, H. Wolf-Watz & M. Fallman, (1996) YopH of Yersinia pseudotuberculosis interrupts early phosphotyrosine signalling associated with phagocytosis. *Mol Microbiol* **20**: 1057-1069.

Anglade, P., S. Vyas, F. Javoy-Agid, M. T. Herrero, P. P. Michel, J. Marquez, A. Mouatt-Prigent, M. Ruberg, E. C. Hirsch & Y. Agid, (1997) Apoptosis and autophagy in nigral neurons of patients with Parkinson's disease. *Histol Histopathol* **12**: 25-31.

Baker-Austin, C., J. V. McArthur, A. H. Lindell, M. S. Wright, R. C. Tuckfield, J. Gooch, L. Warner, J. Oliver & R. Stepanauskas, (2009) Multi-site analysis reveals widespread antibiotic resistance in the marine pathogen Vibrio vulnificus. *Microb Ecol* **57**: 151-159.

Balsinde, J., M. A. Balboa, P. A. Insel & E. A. Dennis, (1999) Regulation and inhibition of phospholipase A2. *Annu Rev Pharmacol Toxicol* **39**: 175-189.

Balsinde, J., M. V. Winstead & E. A. Dennis, (2002) Phospholipase A(2) regulation of arachidonic acid mobilization. *FEBS Lett* **531**: 2-6.

Bartz, R., L. P. Sun, B. Bisel, J. H. Wei & J. Seemann, (2008) Spatial separation of Golgi and ER during mitosis protects SREBP from unregulated activation. *EMBO J* **27**: 948-955.

Bergamini, E., G. Cavallini, A. Donati & Z. Gori, (2003) The anti-ageing effects of caloric restriction may involve stimulation of macroautophagy and lysosomal degradation, and can be intensified pharmacologically. *Biomed Pharmacother* **57**: 203-208.

Bergsbaken, T., S. L. Fink & B. T. Cookson, (2009) Pyroptosis: host cell death and inflammation. *Nat Rev Microbiol* **7**: 99-109.

Bhattacharjee, R. N., K. S. Park, Y. Kumagai, K. Okada, M. Yamamoto, S. Uematsu, K. Matsui, H. Kumar, T. Kawai, T. Iida, T. Honda, O. Takeuchi & S. Akira, (2006) VP1686, a Vibrio type III secretion protein, induces toll-like receptor-independent apoptosis in macrophage through NF-kappaB inhibition. *J Biol Chem* **281**: 36897-36904.

Blocker, A., K. Komoriya & S. Aizawa, (2003) Type III secretion systems and bacterial flagella: insights into their function from structural similarities. *Proc Natl Acad Sci U S A* **100**: 3027-3030.

Boles, B. R. & L. L. McCarter, (2000) Insertional inactivation of genes encoding components of the sodium-type flagellar motor and switch of Vibrio parahaemolyticus. *J Bacteriol* **182**: 1035-1045.

Bolin, I., L. Norlander & H. Wolf-Watz, (1982) Temperature-inducible outer membrane protein of Yersinia pseudotuberculosis and Yersinia enterocolitica is associated with the virulence plasmid. *Infect Immun* **37**: 506-512.

Bolin, I. & H. Wolf-Watz, (1984) Molecular cloning of the temperature-inducible outer membrane protein 1 of Yersinia pseudotuberculosis. *Infect Immun* **43**: 72-78.

Boyce, M., K. F. Bryant, C. Jousse, K. Long, H. P. Harding, D. Scheuner, R. J. Kaufman, D. Ma, D. M. Coen, D. Ron & J. Yuan, (2005) A

selective inhibitor of eIF2alpha dephosphorylation protects cells from ER stress. *Science* **307**: 935-939.

Breckenridge, D. G., M. Germain, J. P. Mathai, M. Nguyen & G. C. Shore, (2003) Regulation of apoptosis by endoplasmic reticulum pathways. *Oncogene* **22**: 8608-8618.

Breeden, L. L., (1997) Alpha-factor synchronization of budding yeast. *Methods Enzymol* **283**: 332-341.

Brennan, M. A. & B. T. Cookson, (2000) Salmonella induces macrophage death by caspase-1-dependent necrosis. *Mol Microbiol* **38**: 31-40.

Brown, E. J., M. W. Albers, T. B. Shin, K. Ichikawa, C. T. Keith, W. S. Lane & S. L. Schreiber, (1994) A mammalian protein targeted by G1-arresting rapamycin-receptor complex. *Nature* **369**: 756-758.

Burdette, D. L., J. Seemann & K. Orth, (Submitted March 2009) Vibrio VopQ induces PI3 kinase independent autophagy and prevents phagocytosis. *Mol Microbiol*.

Burdette, D. L., M. L. Yarbrough, A. Orvedahl, C. J. Gilpin & K. Orth, (2008) Vibrio parahaemolyticus orchestrates a multifaceted host cell infection by induction of autophagy, cell rounding, and then cell lysis. *Proc Natl Acad Sci U S A* **105**: 12497-12502.

Buttner, D. & U. Bonas, (2002) Port of entry--the type III secretion translocon. *Trends Microbiol* **10**: 186-192.

Cao, Y. & D. J. Klionsky, (2007) Atg26 is not involved in autophagy-related pathways in Saccharomyces cerevisiae. *Autophagy* **3**: 17-20.

Cecconi, F. & B. Levine, (2008) The role of autophagy in mammalian development: cell makeover rather than cell death. *Dev Cell* **15**: 344-357.

Chae, Y. K., H. Im, Q. Zhao, J. H. Doelling, R. D. Vierstra & J. L. Markley, (2004) Prevention of aggregation after refolding by balanced stabilization-destabilization: production of the Arabidopsis thaliana protein APG8a (At4g21980) for NMR structure determination. *Protein Expr Purif* **34**: 280-283.

Cheong, H., T. Yorimitsu, F. Reggiori, J. E. Legakis, C. W. Wang & D. J. Klionsky, (2005) Atg17 regulates the magnitude of the autophagic response. *Mol Biol Cell* **16**: 3438-3453.

Colombo, M. I., (2007) Autophagy: a pathogen driven process. *IUBMB Life* **59**: 238-242.

Colwell, R. R., (1973) Genetic and phenetic classification of bacteria. *Adv Appl Microbiol* **16**: 137-175.

Coombes, B. K., B. A. Coburn, A. A. Potter, S. Gomis, K. Mirakhur, Y. Li & B. B. Finlay, (2005) Analysis of the contribution of Salmonella pathogenicity islands 1 and 2 to enteric disease progression using a novel bovine ileal loop model and a murine model of infectious enterocolitis. *Infect Immun* **73**: 7161-7169.

Cornelis, G. R., (2002) Yersinia type III secretion: send in the effectors. *J Cell Biol* **158**: 401-408.

Cornelis, G. R., (2006) The type III secretion injectisome. *Nat Rev Microbiol* **4**: 811-825.

Cornelis, G. R., T. Biot, C. Lambert de Rouvroit, T. Michiels, B. Mulder, C. Sluiters, M. P. Sory, M. Van Bouchaute & J. C. Vanooteghem, (1989) The Yersinia yop regulon. *Mol Microbiol* **3**: 1455-1459.

Cornelis, G. R., A. Boland, A. P. Boyd, C. Geuijen, M. Iriarte, C. Neyt, M. P. Sory & I. Stainier, (1998) The virulence plasmid of Yersinia, an antihost genome. *Microbiol Mol Biol Rev* **62**: 1315-1352.

Daniels, N. A., L. MacKinnon, R. Bishop, S. Altekruse, B. Ray, R. M. Hammond, S. Thompson, S. Wilson, N. H. Bean, P. M. Griffin & L. Slutsker, (2000) Vibrio parahaemolyticus infections in the United States, 1973-1998. *J Infect Dis* **181**: 1661-1666.

Datsenko, K. A. & B. L. Wanner, (2000) One-step inactivation of chromosomal genes in Escherichia coli K-12 using PCR products. *Proc Natl Acad Sci U S A* **97**: 6640-6645.

Delgado, M. A., R. A. Elmaoued, A. S. Davis, G. Kyei & V. Deretic, (2008) Toll-like receptors control autophagy. *EMBO J* **27**: 1110-1121.

Dengjel, J., O. Schoor, R. Fischer, M. Reich, M. Kraus, M. Muller, K. Kreymborg, F. Altenberend, J. Brandenburg, H. Kalbacher, R. Brock, C. Driessen, H. G. Rammensee & S. Stevanovic, (2005) Autophagy promotes MHC class II presentation of peptides from intracellular source proteins. *Proc Natl Acad Sci U S A* **102**: 7922-7927.

DePaola, A., L. H. Hopkins, J. T. Peeler, B. Wentz & R. M. McPhearson, (1990) Incidence of Vibrio parahaemolyticus in U.S. coastal waters and oysters. *Appl Environ Microbiol* **56**: 2299-2302.

Deretic, V. & R. A. Fratti, (1999) Mycobacterium tuberculosis phagosome. *Mol Microbiol* **31**: 1603-1609.

Diaz-Troya, S., M. E. Perez-Perez, F. J. Florencio & J. L. Crespo, (2008) The role of TOR in autophagy regulation from yeast to plants and mammals. *Autophagy* **4**: 851-865.

Ditta, G., S. Stanfield, D. Corbin & D. R. Helinski, (1980) Broad host range DNA cloning system for gram-negative bacteria: construction of a gene bank of Rhizobium meliloti. *Proc Natl Acad Sci U S A* **77**: 7347-7351.

Dong, Z., P. Saikumar, J. M. Weinberg & M. A. Venkatachalam, (1997) Internucleosomal DNA cleavage triggered by plasma membrane damage during necrotic cell death. Involvement of serine but not cysteine proteases. *Am J Pathol* **151**: 1205-1213.

Engel, J. & P. Balachandran, (2009) Role of Pseudomonas aeruginosa type III effectors in disease. *Curr Opin Microbiol*.

Enos-Berlage, J. L., Z. T. Guvener, C. E. Keenan & L. L. McCarter, (2005) Genetic determinants of biofilm development of opaque and translucent Vibrio parahaemolyticus. *Mol Microbiol* **55**: 1160-1182.

Fader, C. M. & M. I. Colombo, (2009) Autophagy and multivesicular bodies: two closely related partners. *Cell Death Differ* **16**: 70-78.

Falcao, J. P., F. Sharp & V. Sperandio, (2004) Cell-to-cell signaling in intestinal pathogens. *Curr Issues Intest Microbiol* **5**: 9-17.

Fan, T. J., L. H. Han, R. S. Cong & J. Liang, (2005) Caspase family proteases and apoptosis. *Acta Biochim Biophys Sin (Shanghai)* **37**: 719-727.

Farre, J. C., R. Manjithaya, R. D. Mathewson & S. Subramani, (2008) PpAtg30 tags peroxisomes for turnover by selective autophagy. *Dev Cell* **14**: 365-376.

Fass, E., E. Shvets, I. Degani, K. Hirschberg & Z. Elazar, (2006) Microtubules support production of starvation-induced autophagosomes but not their targeting and fusion with lysosomes. *J Biol Chem* **281**: 36303-36316.

Feldman, M. F. & G. R. Cornelis, (2003) The multitalented type III chaperones: all you can do with 15 kDa. *FEMS Microbiol Lett* **219**: 151-158.

Festjens, N., T. Vanden Berghe & P. Vandenabeele, (2006) Necrosis, a well-orchestrated form of cell demise: signalling cascades, important mediators and concomitant immune response. *Biochim Biophys Acta* **1757**: 1371-1387.

Fink, S. L. & B. T. Cookson, (2005) Apoptosis, pyroptosis, and necrosis: mechanistic description of dead and dying eukaryotic cells. *Infect Immun* **73**: 1907-1916.

Fink, S. L. & B. T. Cookson, (2006) Caspase-1-dependent pore formation during pyroptosis leads to osmotic lysis of infected host macrophages. *Cell Microbiol* **8**: 1812-1825.

Forsberg, A., A. M. Viitanen, M. Skurnik & H. Wolf-Watz, (1991) The surface-located YopN protein is involved in calcium signal transduction in Yersinia pseudotuberculosis. *Mol Microbiol* **5**: 977-986.

Franchi, L., T. Eigenbrod, R. Munoz-Planillo & G. Nunez, (2009) The inflammasome: a caspase-1-activation platform that regulates immune responses and disease pathogenesis. *Nat Immunol* **10**: 241-247.

Friedman, A. M., S. R. Long, S. E. Brown, W. J. Buikema & F. M. Ausubel, (1982) Construction of a broad host range cosmid cloning vector and its use in the genetic analysis of Rhizobium mutants. *Gene* **18**: 289-296.

Frithz-Lindsten, E., A. Holmstrom, L. Jacobsson, M. Soltani, J. Olsson, R. Rosqvist & A. Forsberg, (1998) Functional conservation of the effector protein translocators PopB/YopB and PopD/YopD of Pseudomonas aeruginosa and Yersinia pseudotuberculosis. *Mol Microbiol* **29**: 1155-1165.

Fujino, T., (1974) Discovery of VIbrio parahaemolyticus. In: International Symposium of Vibrio parahaemolyticus. Saikon, Tokyo, pp. 1-4.

Fukuda, M. & T. Itoh, (2008) Direct link between Atg protein and small GTPase Rab: Atg16L functions as a potential Rab33 effector in mammals. *Autophagy* **4**: 824-826.

Fukui, T., K. Shiraki, D. Hamada, K. Hara, T. Miyata, S. Fujiwara, K. Mayanagi, K. Yanagihara, T. Iida, E. Fukusaki, T. Imanaka, T. Honda & I. Yanagihara, (2005) Thermostable direct hemolysin of Vibrio parahaemolyticus is a bacterial reversible amyloid toxin. *Biochemistry* **44**: 9825-9832.

Furste, J. P., W. Pansegrau, R. Frank, H. Blocker, P. Scholz, M. Bagdasarian & E. Lanka, (1986) Molecular cloning of the plasmid RP4 primase region in a multi-host-range tacP expression vector. *Gene* **48**: 119-131.

Gafni, J., J. A. Munsch, T. H. Lam, M. C. Catlin, L. G. Costa, T. F. Molinski & I. N. Pessah, (1997) Xestospongins: potent membrane permeable blockers of the inositol 1,4,5-trisphosphate receptor. *Neuron* **19**: 723-733.

Garmendia, J., G. Frankel & V. F. Crepin, (2005) Enteropathogenic and enterohemorrhagic Escherichia coli infections: translocation, translocation, translocation. *Infect Immun* **73**: 2573-2585.

Ghosh, P., (2004) Process of protein transport by the type III secretion system. *Microbiol Mol Biol Rev* **68**: 771-795.

Gomez-Gil, B. & A. Roque, (2006) Isolation, Enumeration, and Preservation of the Vibrionaceae. In: The Biology of VIbrios. F. L. Thompson, B. Austin & J. Swings (eds). Washington, D.C.: ASM Press, pp. 15-28.

Gophna, U., E. Z. Ron & D. Graur, (2003) Bacterial type III secretion systems are ancient and evolved by multiple horizontal-transfer events. *Gene* **312**: 151-163.

Gutierrez, M. G., H. A. Saka, I. Chinen, F. C. Zoppino, T. Yoshimori, J. L. Bocco & M. I. Colombo, (2007) Protective role of autophagy against Vibrio cholerae cytolysin, a pore-forming toxin from V. cholerae. *Proc Natl Acad Sci U S A* **104**: 1829-1834.

Guvener, Z. T. & L. L. McCarter, (2003) Multiple regulators control capsular polysaccharide production in Vibrio parahaemolyticus. *J Bacteriol* **185**: 5431-5441.

Hanada, T., N. N. Noda, Y. Satomi, Y. Ichimura, Y. Fujioka, T. Takao, F. Inagaki & Y. Ohsumi, (2007) The Atg12-Atg5 conjugate has a novel E3-like activity for protein lipidation in autophagy. *J Biol Chem* **282**: 37298-37302.

Hanaoka, H., T. Noda, Y. Shirano, T. Kato, H. Hayashi, D. Shibata, S. Tabata & Y. Ohsumi, (2002) Leaf senescence and starvation-induced chlorosis are accelerated by the disruption of an Arabidopsis autophagy gene. *Plant Physiol* **129**: 1181-1193.

Hansen-Wester, I. & M. Hensel, (2001) Salmonella pathogenicity islands encoding type III secretion systems. *Microbes Infect* **3**: 549-559.

Hapfelmeier, S., B. Stecher, M. Barthel, M. Kremer, A. J. Muller, M. Heikenwalder, T. Stallmach, M. Hensel, K. Pfeffer, S. Akira & W. D. Hardt, (2005) The Salmonella pathogenicity island (SPI)-2 and SPI-1 type III secretion systems allow Salmonella serovar typhimurium to trigger colitis via MyD88-dependent and MyD88-independent mechanisms. *J Immunol* **174**: 1675-1685.

Hart, S. P., I. Dransfield & A. G. Rossi, (2008) Phagocytosis of apoptotic cells. *Methods* **44**: 280-285.

Hein, S., E. Arnon, S. Kostin, M. Schonburg, A. Elsasser, V. Polyakova, E. P. Bauer, W. P. Klovekorn & J. Schaper, (2003) Progression from compensated hypertrophy to failure in the pressure-overloaded human heart: structural deterioration and compensatory mechanisms. *Circulation* **107**: 984-991.

Helms, J. B. & J. E. Rothman, (1992) Inhibition by brefeldin A of a Golgi membrane enzyme that catalyses exchange of guanine nucleotide bound to ARF. *Nature* **360**: 352-354.

Hensel, M., J. E. Shea, C. Gleeson, M. D. Jones, E. Dalton & D. W. Holden, (1995) Simultaneous identification of bacterial virulence genes by negative selection. *Science* **269**: 400-403.

Hernandez, L. D., M. Pypaert, R. A. Flavell & J. E. Galan, (2003) A Salmonella protein causes macrophage cell death by inducing autophagy. *J Cell Biol* **163**: 1123-1131.

Higashide, W. & D. Zhou, (2006) The first 45 amino acids of SopA are necessary for InvB binding and SPI-1 secretion. *J Bacteriol* **188**: 2411-2420.

Hirsch, P. R. & J. E. Beringer, (1984) A physical map of pPH1JI and pJB4JI. *Plasmid* **12**: 139-141.

Honda, T., Y. Ni, T. Miwatani, T. Adachi & J. Kim, (1992) The thermostable direct hemolysin of Vibrio parahaemolyticus is a pore-forming toxin. *Can J Microbiol* **38**: 1175-1180.

Hueck, C. J., (1998) Type III protein secretion systems in bacterial pathogens of animals and plants. *Microbiol Mol Biol Rev* **62**: 379-433.

Iguchi, T., S. Kondo & K. Hisatsune, (1995) Vibrio parahaemolyticus O serotypes from O1 to O13 all produce R-type lipopolysaccharide: SDS-PAGE and compositional sugar analysis. *FEMS Microbiol Lett* **130**: 287-292.

Iida, T., (2003) EM image of V. parahaemolyticus. In.: Genome Resources Information Center, pp.

Itakura, E., C. Kishi, K. Inoue & N. Mizushima, (2008) Beclin 1 forms two distinct phosphatidylinositol 3-kinase complexes with mammalian Atg14 and UVRAG. *Mol Biol Cell* **19**: 5360-5372.

Jeffries, T. R., S. K. Dove, R. H. Michell & P. J. Parker, (2004) PtdIns-specific MPR pathway association of a novel WD40 repeat protein, WIPI49. *Mol Biol Cell* **15**: 2652-2663.

Kabeya, Y., Y. Kamada, M. Baba, H. Takikawa, M. Sasaki & Y. Ohsumi, (2005) Atg17 functions in cooperation with Atg1 and Atg13 in yeast autophagy. *Mol Biol Cell* **16**: 2544-2553.

Kabeya, Y., T. Kawamata, K. Suzuki & Y. Ohsumi, (2007) Cis1/Atg31 is required for autophagosome formation in Saccharomyces cerevisiae. *Biochem Biophys Res Commun* **356**: 405-410.

Kabeya, Y., N. Mizushima, T. Ueno, A. Yamamoto, T. Kirisako, T. Noda, E. Kominami, Y. Ohsumi & T. Yoshimori, (2000) LC3, a mammalian homologue of yeast Apg8p, is localized in autophagosome membranes after processing. *EMBO J* **19**: 5720-5728.

Kabeya, Y., N. Mizushima, A. Yamamoto, S. Oshitani-Okamoto, Y. Ohsumi & T. Yoshimori, (2004) LC3, GABARAP and GATE16 localize to autophagosomal membrane depending on form-II formation. *J Cell Sci* **117**: 2805-2812.

Kaneko, T. & R. R. Colwell, (1975) Adsorption of Vibrio parahaemolyticus onto chitin and copepods. *Appl Microbiol* **29**: 269-274.

Kaufman, R. J., (1999) Stress signaling from the lumen of the endoplasmic reticulum: coordination of gene transcriptional and translational controls. *Genes Dev* **13**: 1211-1233.

Kawamata, T., Y. Kamada, K. Suzuki, N. Kuboshima, H. Akimatsu, S. Ota, M. Ohsumi & Y. Ohsumi, (2005) Characterization of a novel autophagy-specific gene, ATG29. *Biochem Biophys Res Commun* **338**: 1884-1889.

Kaysner, C. A., M. M. Wekell & C. Abeyta, Jr., (1990) Enhancement of virulence of two environmental strains of Vibrio vulnificus after passage through mice. *Diagn Microbiol Infect Dis* **13**: 285-288.

Khalfan, W. A. & D. J. Klionsky, (2002) Molecular machinery required for autophagy and the cytoplasm to vacuole targeting (Cvt) pathway in S. cerevisiae. *Curr Opin Cell Biol* **14**: 468-475.

Kirisako, T., M. Baba, N. Ishihara, K. Miyazawa, M. Ohsumi, T. Yoshimori, T. Noda & Y. Ohsumi, (1999) Formation process of autophagosome is traced with Apg8/Aut7p in yeast. *J Cell Biol* **147**: 435-446.

Kirkegaard, K., M. P. Taylor & W. T. Jackson, (2004) Cellular autophagy: surrender, avoidance and subversion by microorganisms. *Nat Rev Microbiol* **2**: 301-314.

Klionsky, D. J., (2007) Monitoring autophagy in yeast: the Pho8Delta60 assay. *Methods Mol Biol* **390**: 363-371.

Klionsky, D. J., A. M. Cuervo & P. O. Seglen, (2007) Methods for monitoring autophagy from yeast to human. *Autophagy* **3**: 181-206.

Kodama, T., M. Rokuda, K. S. Park, V. V. Cantarelli, S. Matsuda, T. Iida & T. Honda, (2007) Identification and characterization of VopT, a novel ADP-ribosyltransferase effector protein secreted via the Vibrio parahaemolyticus type III secretion system 2. *Cell Microbiol* **9**: 2598-2609.

Kostin, S., L. Pool, A. Elsasser, S. Hein, H. C. Drexler, E. Arnon, Y. Hayakawa, R. Zimmermann, E. Bauer, W. P. Klovekorn & J. Schaper, (2003) Myocytes die by multiple mechanisms in failing human hearts. *Circ Res* **92**: 715-724.

Kourtis, N. & N. Tavernarakis, (2009) Autophagy and cell death in model organisms. *Cell Death Differ* **16**: 21-30.

Kubori, T. & J. E. Galan, (2002) Salmonella type III secretion-associated protein InvE controls translocation of effector proteins into host cells. *J Bacteriol* **184**: 4699-4708.

Kubori, T. & J. E. Galan, (2003) Temporal regulation of salmonella virulence effector function by proteasome-dependent protein degradation. *Cell* **115**: 333-342.

Kuma, A., M. Hatano, M. Matsui, A. Yamamoto, H. Nakaya, T. Yoshimori, Y. Ohsumi, T. Tokuhisa & N. Mizushima, (2004) The role of autophagy during the early neonatal starvation period. *Nature* **432**: 1032-1036.

Kyte, J. & R. F. Doolittle, (1982) A simple method for displaying the hydropathic character of a protein. *J Mol Biol* **157**: 105-132.

Lambert de Rouvroit, C., C. Sluiters & G. R. Cornelis, (1992) Role of the transcriptional activator, VirF, and temperature in the expression of the pYV plasmid genes of Yersinia enterocolitica. *Mol Microbiol* **6**: 395-409.

Lang, P. A., S. Kaiser, S. Myssina, C. Birka, C. Weinstock, H. Northoff, T. Wieder, F. Lang & S. M. Huber, (2004) Effect of Vibrio parahaemolyticus haemolysin on human erythrocytes. *Cell Microbiol* **6**: 391-400.

Lang, T., E. Schaeffeler, D. Bernreuther, M. Bredschneider, D. H. Wolf & M. Thumm, (1998) Aut2p and Aut7p, two novel microtubule-associated proteins are essential for delivery of autophagic vesicles to the vacuole. *EMBO J* **17**: 3597-3607.

Lee, S. H. & J. E. Galan, (2004) Salmonella type III secretion-associated chaperones confer secretion-pathway specificity. *Mol Microbiol* **51**: 483-495.

Lemos, M. L. & C. R. Osorio, (2007) Heme, an iron supply for vibrios pathogenic for fish. *Biometals* **20**: 615-626.

Levine, B. & V. Deretic, (2007) Unveiling the roles of autophagy in innate and adaptive immunity. *Nat Rev Immunol* **7**: 767-777.

Levine, B. & D. J. Klionsky, (2004) Development by self-digestion: molecular mechanisms and biological functions of autophagy. *Dev Cell* **6**: 463-477.

Levine, B. & G. Kroemer, (2008) Autophagy in the pathogenesis of disease. *Cell* **132**: 27-42.

Levine, B. & J. Yuan, (2005) Autophagy in cell death: an innocent convict? *J Clin Invest* **115**: 2679-2688.

Liang, X. H., S. Jackson, M. Seaman, K. Brown, B. Kempkes, H. Hibshoosh & B. Levine, (1999) Induction of autophagy and inhibition of tumorigenesis by beclin 1. *Nature* **402**: 672-676.

Liang, X. H., L. K. Kleeman, H. H. Jiang, G. Gordon, J. E. Goldman, G. Berry, B. Herman & B. Levine, (1998) Protection against fatal Sindbis virus encephalitis by beclin, a novel Bcl-2-interacting protein. *J Virol* **72**: 8586-8596.

Liang, X. H., J. Yu, K. Brown & B. Levine, (2001) Beclin 1 contains a leucine-rich nuclear export signal that is required for its autophagy and tumor suppressor function. *Cancer Res* **61**: 3443-3449.

Lio, Y. C., L. J. Reynolds, J. Balsinde & E. A. Dennis, (1996) Irreversible inhibition of Ca(2+)-independent phospholipase A2 by methyl arachidonyl fluorophosphonate. *Biochim Biophys Acta* **1302**: 55-60.

Liu, Y., M. Schiff, K. Czymmek, Z. Talloczy, B. Levine & S. P. Dinesh-Kumar, (2005) Autophagy regulates programmed cell death during the plant innate immune response. *Cell* **121**: 567-577.

Liverman, A. D., H. C. Cheng, J. E. Trosky, D. W. Leung, M. L. Yarbrough, D. L. Burdette, M. K. Rosen & K. Orth, (2007) Arp2/3-independent assembly of actin by Vibrio type III effector VopL. *Proc Natl Acad Sci U S A* **104**: 17117-17122.

Lockshin, R. A. & Z. Zakeri, (2002) Caspase-independent cell deaths. *Curr Opin Cell Biol* **14**: 727-733.

Lockshin, R. A. & Z. Zakeri, (2004) Apoptosis, autophagy, and more. *Int J Biochem Cell Biol* **36**: 2405-2419.

Lynch, T., S. Livingstone, E. Buenaventura, E. Lutter, J. Fedwick, A. G. Buret, D. Graham & R. DeVinney, (2005) Vibrio parahaemolyticus disruption of epithelial cell tight junctions occurs independently of toxin production. *Infect Immun* **73**: 1275-1283.

Ma, J., R. Jin, X. Jia, C. J. Dobry, L. Wang, F. Reggiori, J. Zhu & A. Kumar, (2007) An interrelationship between autophagy and filamentous growth in budding yeast. *Genetics* **177**: 205-214.

Maiuri, M. C., E. Zalckvar, A. Kimchi & G. Kroemer, (2007) Self-eating and self-killing: crosstalk between autophagy and apoptosis. *Nat Rev Mol Cell Biol* **8**: 741-752.

Majno, G. & I. Joris, (1995) Apoptosis, oncosis, and necrosis. An overview of cell death. *Am J Pathol* **146**: 3-15.

Makino, K., K. Oshima, K. Kurokawa, K. Yokoyama, T. Uda, K. Tagomori, Y. Iijima, M. Najima, M. Nakano, A. Yamashita, Y. Kubota, S. Kimura, T. Yasunaga, T. Honda, H. Shinagawa, M. Hattori & T. Iida, (2003) Genome sequence of Vibrio parahaemolyticus: a pathogenic mechanism distinct from that of V cholerae. *Lancet* **361**: 743-749.

Marlovits, T. C., T. Kubori, A. Sukhan, D. R. Thomas, J. E. Galan & V. M. Unger, (2004) Structural insights into the assembly of the type III secretion needle complex. *Science* **306**: 1040-1042.

Matsuura, A., M. Tsukada, Y. Wada & Y. Ohsumi, (1997) Apg1p, a novel protein kinase required for the autophagic process in Saccharomyces cerevisiae. *Gene* **192**: 245-250.

McCarter, L., (1999) The multiple identities of Vibrio parahaemolyticus. *J Mol Microbiol Biotechnol* **1**: 51-57.

McCarter, L. L., (1998) OpaR, a homolog of Vibrio harveyi LuxR, controls opacity of Vibrio parahaemolyticus. *J Bacteriol* **180**: 3166-3173.

McCarter, L. L., (2004) Dual flagellar systems enable motility under different circumstances. *J Mol Microbiol Biotechnol* **7**: 18-29.

McLaughlin, J. B., A. DePaola, C. A. Bopp, K. A. Martinek, N. P. Napolilli, C. G. Allison, S. L. Murray, E. C. Thompson, M. M. Bird & J. P. Middaugh, (2005) Outbreak of Vibrio parahaemolyticus gastroenteritis associated with Alaskan oysters. *N Engl J Med* **353**: 1463-1470.

Meador, C. E., M. M. Parsons, C. A. Bopp, P. Gerner-Smidt, J. A. Painter & G. J. Vora, (2007) Virulence gene- and pandemic group-specific marker profiling of clinical Vibrio parahaemolyticus isolates. *J Clin Microbiol* **45**: 1133-1139.

Meiling-Wesse, K., F. Bratsika & M. Thumm, (2004) ATG23, a novel gene required for maturation of proaminopeptidase I, but not for autophagy. *FEMS Yeast Res* **4**: 459-465.

Mejia, E., J. B. Bliska & G. I. Viboud, (2008) Yersinia controls type III effector delivery into host cells by modulating Rho activity. *PLoS Pathog* **4**: e3.

Melendez, A. & T. P. Neufeld, (2008) The cell biology of autophagy in metazoans: a developing story. *Development* **135**: 2347-2360.

Melendez, A., Z. Talloczy, M. Seaman, E. L. Eskelinen, D. H. Hall & B. Levine, (2003) Autophagy genes are essential for dauer development and life-span extension in C. elegans. *Science* **301**: 1387-1391.

Miyamoto, Y., T. Kato, Y. Obara, S. Akiyama, K. Takizawa & S. Yamai, (1969) In vitro hemolytic characteristic of Vibrio parahaemolyticus: its close correlation with human pathogenicity. *J Bacteriol* **100**: 1147-1149.

Mizushima, N., A. Kuma, Y. Kobayashi, A. Yamamoto, M. Matsubae, T. Takao, T. Natsume, Y. Ohsumi & T. Yoshimori, (2003) Mouse Apg16L, a novel WD-repeat protein, targets to the autophagic isolation membrane with the Apg12-Apg5 conjugate. *J Cell Sci* **116**: 1679-1688.

Mizushima, N., B. Levine, A. M. Cuervo & D. J. Klionsky, (2008) Autophagy fights disease through cellular self-digestion. *Nature* **451**: 1069-1075.

Mizushima, N., T. Yoshimori & Y. Ohsumi, (2002) Mouse Apg10 as an Apg12-conjugating enzyme: analysis by the conjugation-mediated yeast two-hybrid method. *FEBS Lett* **532**: 450-454.

Monack, D. M., J. Mecsas, N. Ghori & S. Falkow, (1997) Yersinia signals macrophages to undergo apoptosis and YopJ is necessary for this cell death. *Proc Natl Acad Sci U S A* **94**: 10385-10390.

Monastyrska, I., C. He, J. Geng, A. D. Hoppe, Z. Li & D. J. Klionsky, (2008) Arp2 links autophagic machinery with the actin cytoskeleton. *Mol Biol Cell* **19**: 1962-1975.

Monastyrska, I., J. A. Kiel, A. M. Krikken, J. A. Komduur, M. Veenhuis & I. J. van der Klei, (2005) The Hansenula polymorpha ATG25 gene encodes a novel coiled-coil protein that is required for macropexophagy. *Autophagy* **1**: 92-100.

Monastyrska, I., T. Shintani, D. J. Klionsky & F. Reggiori, (2006) Atg11 directs autophagosome cargoes to the PAS along actin cables. *Autophagy* **2**: 119-121.

Morris, J. G., Jr., (2003) Cholera and other types of vibriosis: a story of human pandemics and oysters on the half shell. *Clin Infect Dis* **37**: 272-280.

Morris, J. G., Jr. & R. E. Black, (1985) Cholera and other vibrioses in the United States. *N Engl J Med* **312**: 343-350.

Mortimore, G. E. & C. E. Mondon, (1970) Inhibition by insulin of valine turnover in liver. Evidence for a general control of proteolysis. *J Biol Chem* **245**: 2375-2383.

Mukherjee, S., Y. H. Hao & K. Orth, (2007) A newly discovered post-translational modification--the acetylation of serine and threonine residues. *Trends Biochem Sci* **32**: 210-216.

Murata, S., H. Yashiroda & K. Tanaka, (2009) Molecular mechanisms of proteasome assembly. *Nat Rev Mol Cell Biol* **10**: 104-115.

Nair, G. B., T. Ramamurthy, S. K. Bhattacharya, B. Dutta, Y. Takeda & D. A. Sack, (2007) Global dissemination of Vibrio parahaemolyticus serotype O3:K6 and its serovariants. *Clin Microbiol Rev* **20**: 39-48.

Nakasone, N. & M. Iwanaga, (1990) Pili of a Vibrio parahaemolyticus strain as a possible colonization factor. *Infect Immun* **58**: 61-69.

Navarro, L., N. M. Alto & J. E. Dixon, (2005) Functions of the Yersinia effector proteins in inhibiting host immune responses. *Curr Opin Microbiol* **8**: 21-27.

Nixon, R. A., A. M. Cataldo & P. M. Mathews, (2000) The endosomal-lysosomal system of neurons in Alzheimer's disease pathogenesis: a review. *Neurochem Res* **25**: 1161-1172.

Noda, T., A. Matsuura, Y. Wada & Y. Ohsumi, (1995) Novel system for monitoring autophagy in the yeast Saccharomyces cerevisiae. *Biochem Biophys Res Commun* **210**: 126-132.

Obara, K., T. Sekito, K. Niimi & Y. Ohsumi, (2008) The Atg18-Atg2 complex is recruited to autophagic membranes via phosphatidylinositol 3-phosphate and exerts an essential function. *J Biol Chem* **283**: 23972-23980.

Ogawa, M., T. Yoshimori, T. Suzuki, H. Sagara, N. Mizushima & C. Sasakawa, (2005) Escape of intracellular Shigella from autophagy. *Science* **307**: 727-731.

Okada, N., T. Iida, K. S. Park, N. Goto, T. Yasunaga, H. Hiyoshi, S. Matsuda, T. Kodama & T. Honda, (2009) Identification and characterization of a novel type III secretion system in trh-positive Vibrio parahaemolyticus strain TH3996 reveal genetic lineage and diversity of pathogenic machinery beyond the species level. *Infect Immun* **77**: 904-913.

Ono, T., K. S. Park, M. Ueta, T. Iida & T. Honda, (2006) Identification of proteins secreted via Vibrio parahaemolyticus type III secretion system 1. *Infect Immun* **74**: 1032-1042.

Orvedahl, A., D. Alexander, Z. Talloczy, Q. Sun, Y. Wei, W. Zhang, D. Burns, D. A. Leib & B. Levine, (2007) HSV-1 ICP34.5 confers neurovirulence by targeting the Beclin 1 autophagy protein. *Cell Host Microbe* **1**: 23-35.

Orvedahl, A. & B. Levine, (2009) Eating the enemy within: autophagy in infectious diseases. *Cell Death Differ* **16**: 57-69.

Otto, G. P., M. Y. Wu, N. Kazgan, O. R. Anderson & R. H. Kessin, (2003) Macroautophagy is required for multicellular development of the social amoeba Dictyostelium discoideum. *J Biol Chem* **278**: 17636-17645.

Pallen, M. J., R. R. Chaudhuri & I. R. Henderson, (2003) Genomic analysis of secretion systems. *Curr Opin Microbiol* **6**: 519-527.

Palmer, L. E., A. R. Pancetti, S. Greenberg & J. B. Bliska, (1999) YopJ of Yersinia spp. is sufficient to cause downregulation of multiple mitogen-activated protein kinases in eukaryotic cells. *Infect Immun* **67**: 708-716.

Panina, E. M., S. Mattoo, N. Griffith, N. A. Kozak, M. H. Yuk & J. F. Miller, (2005) A genome-wide screen identifies a Bordetella type III secretion effector and candidate effectors in other species. *Mol Microbiol* **58**: 267-279.

Park, K. S., T. Ono, M. Rokuda, M. H. Jang, T. Iida & T. Honda, (2004a) Cytotoxicity and enterotoxicity of the thermostable direct hemolysin-deletion mutants of Vibrio parahaemolyticus. *Microbiol Immunol* **48**: 313-318.

Park, K. S., T. Ono, M. Rokuda, M. H. Jang, K. Okada, T. Iida & T. Honda, (2004b) Functional characterization of two type III secretion systems of Vibrio parahaemolyticus. *Infect Immun* **72**: 6659-6665.

Parsons, Y. N., K. J. Glendinning, V. Thornton, B. A. Hales, C. A. Hart & C. Winstanley, (2001) A putative type III secretion gene cluster is widely distributed in the Burkholderia cepacia complex but absent from genomovar I. *FEMS Microbiol Lett* **203**: 103-108.

Penaloza, C., L. Lin, R. A. Lockshin & Z. Zakeri, (2006) Cell death in development: shaping the embryo. *Histochem Cell Biol* **126**: 149-158.

Penaloza, C., S. Orlanski, Y. Ye, T. Entezari-Zaher, M. Javdan & Z. Zakeri, (2008) Cell death in mammalian development. *Curr Pharm Des* **14**: 184-196.

Petiot, A., E. Ogier-Denis, E. F. Blommaart, A. J. Meijer & P. Codogno, (2000) Distinct classes of phosphatidylinositol 3'-kinases are involved in signaling pathways that control macroautophagy in HT-29 cells. *J Biol Chem* **275**: 992-998.

Pettersson, J., R. Nordfelth, E. Dubinina, T. Bergman, M. Gustafsson, K. E. Magnusson & H. Wolf-Watz, (1996) Modulation of virulence factor expression by pathogen target cell contact. *Science* **273**: 1231-1233.

Phillips, A. R., A. Suttangkakul & R. D. Vierstra, (2008) The ATG12-conjugating enzyme ATG10 Is essential for autophagic vesicle formation in Arabidopsis thaliana. *Genetics* **178**: 1339-1353.

Phillips, R. M., D. A. Six, E. A. Dennis & P. Ghosh, (2003) In vivo phospholipase activity of the Pseudomonas aeruginosa cytotoxin ExoU and protection of mammalian cells with phospholipase A2 inhibitors. *J Biol Chem* **278**: 41326-41332.

Powis, G., R. Bonjouklian, M. M. Berggren, A. Gallegos, R. Abraham, C. Ashendel, L. Zalkow, W. F. Matter, J. Dodge, G. Grindey & et al., (1994) Wortmannin, a potent and selective inhibitor of phosphatidylinositol-3-kinase. *Cancer Res* **54**: 2419-2423.

Qin, Z. H., Y. Wang, K. B. Kegel, A. Kazantsev, B. L. Apostol, L. M. Thompson, J. Yoder, N. Aronin & M. DiFiglia, (2003) Autophagy regulates the processing of amino terminal huntingtin fragments. *Hum Mol Genet* **12**: 3231-3244.

Rabin, S. D. & A. R. Hauser, (2003) Pseudomonas aeruginosa ExoU, a toxin transported by the type III secretion system, kills Saccharomyces cerevisiae. *Infect Immun* **71**: 4144-4150.

Rainbow, L., C. A. Hart & C. Winstanley, (2002) Distribution of type III secretion gene clusters in Burkholderia pseudomallei, B. thailandensis and B. mallei. *J Med Microbiol* **51**: 374-384.

Ravikumar, B., R. Duden & D. C. Rubinsztein, (2002) Aggregate-prone proteins with polyglutamine and polyalanine expansions are degraded by autophagy. *Hum Mol Genet* **11**: 1107-1117.

Reggiori, F., I. Monastyrska, T. Shintani & D. J. Klionsky, (2005) The actin cytoskeleton is required for selective types of autophagy, but not nonspecific autophagy, in the yeast Saccharomyces cerevisiae. *Mol Biol Cell* **16**: 5843-5856.

Robinson, J. S., D. J. Klionsky, L. M. Banta & S. D. Emr, (1988) Protein sorting in Saccharomyces cerevisiae: isolation of mutants defective in the delivery and processing of multiple vacuolar hydrolases. *Mol Cell Biol* **8**: 4936-4948.

Rodrick, G. E., M. A. Hood & N. J. Blake, (1982) Human vibrio gastroenteritis. *Med Clin North Am* **66**: 665-673.

Rohde, J. R., A. Breitkreutz, A. Chenal, P. J. Sansonetti & C. Parsot, (2007) Type III secretion effectors of the IpaH family are E3 ubiquitin ligases. *Cell Host Microbe* **1**: 77-83.

Romano, P. S., M. G. Gutierrez, W. Beron, M. Rabinovitch & M. I. Colombo, (2007) The autophagic pathway is actively modulated by phase II Coxiella burnetii to efficiently replicate in the host cell. *Cell Microbiol* **9**: 891-909.

Russell, D. W. & J. Sambrook, (2001) *Molecular Cloning: A Laboratory Manual*. Cold Spring Harbor Laboratory Press, Cold Spring Harbor, New York.

Rusten, T. E. & A. Simonsen, (2008) ESCRT functions in autophagy and associated disease. *Cell Cycle* **7**: 1166-1172.

Ryndak, M. B., H. Chung, E. London & J. B. Bliska, (2005) Role of predicted transmembrane domains for type III translocation, pore formation, and signaling by the Yersinia pseudotuberculosis YopB protein. *Infect Immun* **73**: 2433-2443.

Sanjuan, M. A., C. P. Dillon, S. W. Tait, S. Moshiach, F. Dorsey, S. Connell, M. Komatsu, K. Tanaka, J. L. Cleveland, S. Withoff & D. R. Green, (2007) Toll-like receptor signalling in macrophages links the autophagy pathway to phagocytosis. *Nature* **450**: 1253-1257.

Saraste, A. & K. Pulkki, (2000) Morphologic and biochemical hallmarks of apoptosis. *Cardiovasc Res* **45**: 528-537.

Sato, H. & D. W. Frank, (2004) ExoU is a potent intracellular phospholipase. *Mol Microbiol* **53**: 1279-1290.

Schaible, U. E. & S. H. Kaufmann, (2004) Iron and microbial infection. *Nat Rev Microbiol* **2**: 946-953.

Schlumberger, M. C., A. Friebel, G. Buchwald, K. Scheffzek, A. Wittinghofer & W. D. Hardt, (2003) Amino acids of the bacterial toxin SopE involved in G nucleotide exchange on Cdc42. *J Biol Chem* **278**: 27149-27159.

Schlumpberger, M., E. Schaeffeler, M. Straub, M. Bredschneider, D. H. Wolf & M. Thumm, (1997) AUT1, a gene essential for autophagocytosis in the yeast Saccharomyces cerevisiae. *J Bacteriol* **179**: 1068-1076.

Schneider, J., J. Dover, M. Johnston & A. Shilatifard, (2004) Global proteomic analysis of S. cerevisiae (GPS) to identify proteins required for histone modifications. *Methods Enzymol* **377**: 227-234.

Schroeder, G. N. & H. Hilbi, (2008) Molecular pathogenesis of Shigella spp.: controlling host cell signaling, invasion, and death by type III secretion. *Clin Microbiol Rev* **21**: 134-156.

Scott, R. C., O. Schuldiner & T. P. Neufeld, (2004) Role and regulation of starvation-induced autophagy in the Drosophila fat body. *Dev Cell* **7**: 167-178.

Scott, S. V., J. Guan, M. U. Hutchins, J. Kim & D. J. Klionsky, (2001) Cvt19 is a receptor for the cytoplasm-to-vacuole targeting pathway. *Mol Cell* **7**: 1131-1141.

Scovassi, A. I. & G. G. Poirier, (1999) Poly(ADP-ribosylation) and apoptosis. *Mol Cell Biochem* **199**: 125-137.

Seglen, P. O. & P. B. Gordon, (1982) 3-Methyladenine: specific inhibitor of autophagic/lysosomal protein degradation in isolated rat hepatocytes. *Proc Natl Acad Sci U S A* **79**: 1889-1892.

Seglen, P. O., P. B. Gordon & A. Poli, (1980) Amino acid inhibition of the autophagic/lysosomal pathway of protein degradation in isolated rat hepatocytes. *Biochim Biophys Acta* **630**: 103-118.

Shao, F., (2008) Biochemical functions of Yersinia type III effectors. *Curr Opin Microbiol* **11**: 21-29.

Shime-Hattori, A., T. Iida, M. Arita, K. S. Park, T. Kodama & T. Honda, (2006) Two type IV pili of Vibrio parahaemolyticus play different roles in biofilm formation. *FEMS Microbiol Lett* **264**: 89-97.

Shintani, T., W. P. Huang, P. E. Stromhaug & D. J. Klionsky, (2002) Mechanism of cargo selection in the cytoplasm to vacuole targeting pathway. *Dev Cell* **3**: 825-837.

Shirai, H., H. Ito, T. Hirayama, Y. Nakamoto, N. Nakabayashi, K. Kumagai, Y. Takeda & M. Nishibuchi, (1990) Molecular epidemiologic evidence for association of thermostable direct hemolysin (TDH) and TDH-related hemolysin of Vibrio parahaemolyticus with gastroenteritis. *Infect Immun* **58**: 3568-3573.

Shope, R., (1991) Global climate change and infectious diseases. *Environ Health Perspect* **96**: 171-174.

Slee, E. A., H. Zhu, S. C. Chow, M. MacFarlane, D. W. Nicholson & G. M. Cohen, (1996) Benzyloxycarbonyl-Val-Ala-Asp (OMe) fluoromethylketone (Z-VAD.FMK) inhibits apoptosis by blocking the processing of CPP32. *Biochem J* **315 (Pt 1)**: 21-24.

Stasyk, O. V., O. G. Stasyk, R. D. Mathewson, J. C. Farre, V. Y. Nazarko, O. S. Krasovska, S. Subramani, J. M. Cregg & A. A. Sibirny, (2006) Atg28, a novel coiled-coil protein involved in autophagic degradation of peroxisomes in the methylotrophic yeast Pichia pastoris. *Autophagy* **2**: 30-38.

Stephens, L., C. Ellson & P. Hawkins, (2002) Roles of PI3Ks in leukocyte chemotaxis and phagocytosis. *Curr Opin Cell Biol* **14**: 203-213.

Stromhaug, P. E., F. Reggiori, J. Guan, C. W. Wang & D. J. Klionsky, (2004) Atg21 is a phosphoinositide binding protein required for efficient lipidation and localization of Atg8 during uptake of

aminopeptidase I by selective autophagy. *Mol Biol Cell* **15**: 3553-3566.

Suzuki, T., L. Franchi, C. Toma, H. Ashida, M. Ogawa, Y. Yoshikawa, H. Mimuro, N. Inohara, C. Sasakawa & G. Nunez, (2007) Differential regulation of caspase-1 activation, pyroptosis, and autophagy via Ipaf and ASC in Shigella-infected macrophages. *PLoS Pathog* **3**: e111.

Takano-Ohmuro, H., M. Mukaida, E. Kominami & K. Morioka, (2000) Autophagy in embryonic erythroid cells: its role in maturation. *Eur J Cell Biol* **79**: 759-764.

Tamai, K., N. Tanaka, A. Nara, A. Yamamoto, I. Nakagawa, T. Yoshimori, Y. Ueno, T. Shimosegawa & K. Sugamura, (2007) Role of Hrs in maturation of autophagosomes in mammalian cells. *Biochem Biophys Res Commun* **360**: 721-727.

Tampakaki, A. P., V. E. Fadouloglou, A. D. Gazi, N. J. Panopoulos & M. Kokkinidis, (2004) Conserved features of type III secretion. *Cell Microbiol* **6**: 805-816.

Tang, F., J. W. Watkins, M. Bermudez, R. Gray, A. Gaban, K. Portie, S. Grace, M. Kleve & G. Craciun, (2008) A life-span extending form of autophagy employs the vacuole-vacuole fusion machinery. *Autophagy* **4**: 874-886.

Tang, X., Y. Xiao & J. M. Zhou, (2006) Regulation of the type III secretion system in phytopathogenic bacteria. *Mol Plant Microbe Interact* **19**: 1159-1166.

Tanida, I., T. Nishitani, T. Nemoto, T. Ueno & E. Kominami, (2002) Mammalian Apg12p, but not the Apg12p.Apg5p conjugate, facilitates LC3 processing. *Biochem Biophys Res Commun* **296**: 1164-1170.

Tanida, I., E. Tanida-Miyake, T. Ueno & E. Kominami, (2001) The human homolog of Saccharomyces cerevisiae Apg7p is a Protein-activating enzyme for multiple substrates including human Apg12p, GATE-16, GABARAP, and MAP-LC3. *J Biol Chem* **276**: 1701-1706.

Tanida, I., T. Ueno & E. Kominami, (2004) Human light chain 3/MAP1LC3B is cleaved at its carboxyl-terminal Met121 to expose Gly120 for lipidation and targeting to autophagosomal membranes. *J Biol Chem* **279**: 47704-47710.

Thorburn, A., (2008) Apoptosis and autophagy: regulatory connections between two supposedly different processes. *Apoptosis* **13**: 1-9.

Trosky, J. E., Y. Li, S. Mukherjee, G. Keitany, H. Ball & K. Orth, (2007) VopA inhibits ATP binding by acetylating the catalytic loop of MAPK kinases. *J Biol Chem* **282**: 34299-34305.

Trosky, J. E., A. D. Liverman & K. Orth, (2008) Yersinia outer proteins: Yops. *Cell Microbiol* **10**: 557-565.

Tsukada, M. & Y. Ohsumi, (1993) Isolation and characterization of autophagy-defective mutants of Saccharomyces cerevisiae. *FEBS Lett* **333**: 169-174.

Tucker, K. A., F. Reggiori, W. A. Dunn, Jr. & D. J. Klionsky, (2003) Atg23 is essential for the cytoplasm to vacuole targeting pathway and efficient autophagy but not pexophagy. *J Biol Chem* **278**: 48445-48452.

van Engeland, M., H. J. Kuijpers, F. C. Ramaekers, C. P. Reutelingsperger & B. Schutte, (1997) Plasma membrane alterations and cytoskeletal changes in apoptosis. *Exp Cell Res* **235**: 421-430.

Viboud, G. I. & J. B. Bliska, (2005) Yersinia outer proteins: role in modulation of host cell signaling responses and pathogenesis. *Annu Rev Microbiol* **59**: 69-89.

Viboud, G. I., S. S. So, M. B. Ryndak & J. B. Bliska, (2003) Proinflammatory signalling stimulated by the type III translocation factor YopB is counteracted by multiple effectors in epithelial cells infected with Yersinia pseudotuberculosis. *Mol Microbiol* **47**: 1305-1315.

Vuddhakul, V., A. Chowdhury, V. Laohaprertthisan, P. Pungrasamee, N. Patararungrong, P. Thianmontri, M. Ishibashi, C. Matsumoto & M.

Nishibuchi, (2000) Isolation of a pandemic O3:K6 clone of a Vibrio parahaemolyticus strain from environmental and clinical sources in Thailand. *Appl Environ Microbiol* **66**: 2685-2689.

Waterman, S. R. & D. W. Holden, (2003) Functions and effectors of the Salmonella pathogenicity island 2 type III secretion system. *Cell Microbiol* **5**: 501-511.

Willingham, S. B., D. T. Bergstralh, W. O'Connor, A. C. Morrison, D. J. Taxman, J. A. Duncan, S. Barnoy, M. M. Venkatesan, R. A. Flavell, M. Deshmukh, H. M. Hoffman & J. P. Ting, (2007) Microbial pathogen-induced necrotic cell death mediated by the inflammasome components CIAS1/cryopyrin/NLRP3 and ASC. *Cell Host Microbe* **2**: 147-159.

Winstanley, C., B. A. Hales & C. A. Hart, (1999) Evidence for the presence in Burkholderia pseudomallei of a type III secretion system-associated gene cluster. *J Med Microbiol* **48**: 649-656.

Winstead, M. V., J. Balsinde & E. A. Dennis, (2000) Calcium-independent phospholipase A(2): structure and function. *Biochim Biophys Acta* **1488**: 28-39.

Winzeler, E. A., D. D. Shoemaker, A. Astromoff, H. Liang, K. Anderson, B. Andre, R. Bangham, R. Benito, J. D. Boeke, H. Bussey, A. M. Chu, C. Connelly, K. Davis, F. Dietrich, S. W. Dow, M. El Bakkoury, F. Foury, S. H. Friend, E. Gentalen, G. Giaever, J. H. Hegemann, T. Jones, M. Laub, H. Liao, N. Liebundguth, D. J. Lockhart, A. Lucau-Danila, M. Lussier, N. M'Rabet, P. Menard, M. Mittmann, C. Pai, C. Rebischung, J. L. Revuelta, L. Riles, C. J. Roberts, P. Ross-MacDonald, B. Scherens, M. Snyder, S. Sookhai-Mahadeo, R. K. Storms, S. Veronneau, M. Voet, G. Volckaert, T. R. Ward, R. Wysocki, G. S. Yen, K. Yu, K. Zimmermann, P. Philippsen, M. Johnston & R. W. Davis, (1999) Functional characterization of the S. cerevisiae genome by gene deletion and parallel analysis. *Science* **285**: 901-906.

Xie, Z. & D. J. Klionsky, (2007) Autophagosome formation: core machinery and adaptations. *Nat Cell Biol* **9**: 1102-1109.

Yamamoto, S., N. Okujo, S. Miyoshi, S. Shinoda & S. Narimatsu, (1999) Siderophore production of Vibrio parahaemolyticus strains from different sources. *Microbiol Immunol* **43**: 909-912.

Yang, Z., J. Huang, J. Geng, U. Nair & D. J. Klionsky, (2006) Atg22 recycles amino acids to link the degradative and recycling functions of autophagy. *Mol Biol Cell* **17**: 5094-5104.

Yarbrough, M. L., Y. Li, L. N. Kinch, N. V. Grishin, H. L. Ball & K. Orth, (2009) AMPylation of Rho GTPases by Vibrio VopS disrupts effector binding and downstream signaling. *Science* **323**: 269-272.

Yen, W. L., J. E. Legakis, U. Nair & D. J. Klionsky, (2007) Atg27 is required for autophagy-dependent cycling of Atg9. *Mol Biol Cell* **18**: 581-593.

Yeung, P. S. & K. J. Boor, (2004) Epidemiology, pathogenesis, and prevention of foodborne Vibrio parahaemolyticus infections. *Foodborne Pathog Dis* **1**: 74-88.

Yoon, S., Z. Liu, Y. Eyobo & K. Orth, (2003) Yersinia effector YopJ inhibits yeast MAPK signaling pathways by an evolutionarily conserved mechanism. *J Biol Chem* **278**: 2131-2135.

Yorimitsu, T. & D. J. Klionsky, (2005) Atg11 links cargo to the vesicle-forming machinery in the cytoplasm to vacuole targeting pathway. *Mol Biol Cell* **16**: 1593-1605.

Yoshimori, T. & T. Noda, (2008) Toward unraveling membrane biogenesis in mammalian autophagy. *Curr Opin Cell Biol* **20**: 401-407.

Yoshimura, K., M. Shibata, M. Koike, K. Gotoh, M. Fukaya, M. Watanabe & Y. Uchiyama, (2006) Effects of RNA interference of Atg4B on the limited proteolysis of LC3 in PC12 cells and expression of Atg4B in various rat tissues. *Autophagy* **2**: 200-208.

Yu, L., L. Strandberg & M. J. Lenardo, (2008) The selectivity of autophagy and its role in cell death and survival. *Autophagy* **4**: 567-573.

Yu, L., F. Wan, S. Dutta, S. Welsh, Z. Liu, E. Freundt, E. H. Baehrecke & M. Lenardo, (2006) Autophagic programmed cell death by selective catalase degradation. *Proc Natl Acad Sci U S A* **103**: 4952-4957.

Yuk, M. H., E. T. Harvill & J. F. Miller, (1998) The BvgAS virulence control system regulates type III secretion in Bordetella bronchiseptica. *Mol Microbiol* **28**: 945-959.

Zhang, X. H. & B. Austin, (2005) Haemolysins in Vibrio species. *J Appl Microbiol* **98**: 1011-1019.

Zhang, Y., A. T. Ting, K. B. Marcu & J. B. Bliska, (2005) Inhibition of MAPK and NF-kappa B pathways is necessary for rapid apoptosis in macrophages infected with Yersinia. *J Immunol* **174**: 7939-7949.

Zhou, X., M. E. Konkel & D. R. Call, (2009) Type III secretion system 1 of Vibrio parahaemolyticus induces oncosis in both epithelial and monocytic cell lines. *Microbiology* **155**: 837-851.